TRANSVERSE TRANSPORT OF SUSPENDED SEDIMENT ACROSS THE MAIN CHANNEL – FLOODPLAIN SHEAR BOUNDARY

By

Frank Denys

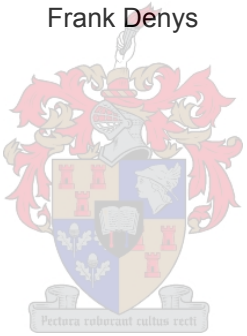

Thesis presented in fulfilment of the requirements for the degree
of *Master of Science in Engineering (Civil)* at the Faculty of Engineering
at the University of Stellenbosch.

Prof GR Basson

Thesis advisor

December 2006

DECLARATION

I, the undersigned, hereby declare that the work contained in this thesis is my own original work and I have not previously in its entirety or in part submitted it at any university for a degree.

_____
FJM Denys

_____
Date

EXECUTIVE SUMMARY

The floodplain of a river forms a close relationship with the stream that created it. Not only does the river influence the characteristics of the floodplain, the floodplain can also very easily influence its river, as is evidenced by examples such as the Huang He River in China and the Columbia River in Canada. These two cases clearly indicate that suspended sediment has a pronounced influence on the floodplain. This thesis investigates the processes which cause sediment to move onto the floodplain.

As observed in many rivers worldwide suspended sediment on the floodplain has a tendency to settle near but not directly next to the main river channel. This gap between the river channel and the location of highest sedimentation rate stems from the fact that there is a zone of relatively higher turbulence at the boundaries of the floodplain. Close to this zone flow on the floodplain is increased in velocity whilst the flow velocity in the main channel is decreased as can be seen in the figure below:

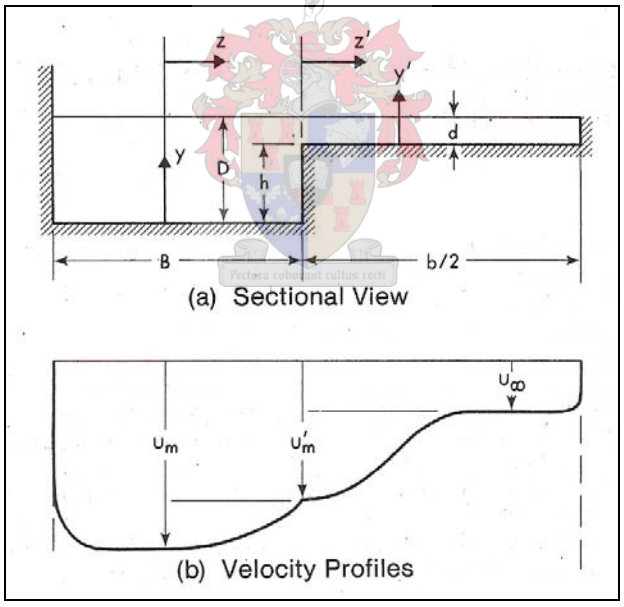

The existence of this turbulent zone or shear layer is also responsible for the establishment of secondary flow patters as can be seen in the following figure. It is these vertical secondary currents that have the largest role to play in determining the behaviour of suspended sediment as it moves onto the floodplain.

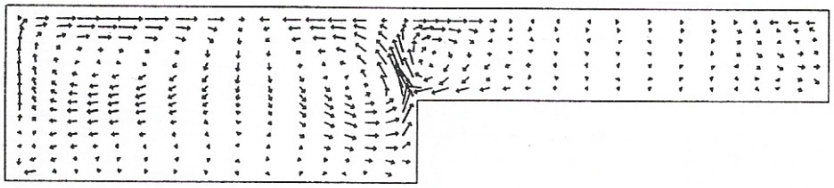

These secondary currents and the effect they have on transverse transport of suspended sediment can be described mathematically but only in a fully three dimensional environment. Though it is possible to emulate them in a two dimensional environment using specially formulated dispersion factors, not every two dimensional model has these dispersion factors built in.

A physical model was set up to measure the spread of suspended sediment onto a floodplain. The suspended sediment concentration data so collected was subsequently used to determine if a chosen mathematical model, namely CCHE2D, was capable of simulating observed phenomena. It was concluded that though the model could predict the broad pattern of movement (if the model time steps were small enough), it was not equipped with the proper modules to be able to simulate the pseudo three dimensional flow field required for cross shear boundary suspended sediment transport.

OPSOMMING

Die vloedvlakte van ‘n rivier toon ‘n sterk verband met die stroom wat dit gegenereer het. Die rivier beinvloed nie net die vloedvlakte nie maar die vloedvlakte seelf kan ook sy rivier beinvloed. Twee goeie voorbeelde van hierdie konsep is die Huang He Rivier in China en die Colorado Rivier in Kanada. Hulle altwee toon duidelik aan dat sediment in suspensie ‘n groot bydrae het tot die gedrag van die vloedvlakte. Hierdie tesis ondersoek die proses waarby hierdie sediment op die vloedvlakte beland.

Soos waargeneem in talle riviere wêreldwyd is sediment in suspensie op die vloedvlakte geneigd om naby maar nie langs die hoofkanaal neer te sit nie. Hierdie gaping is die gevolge van die feit dat daar ‘n sone van hoër turbulensie plaasvind langs die hoofkanaal. As gevolg van die sone versnel die vloei op die vloedvlakte en vertraag die vloei in die hoof kanaal soos gesien kan word in die figuur hieronder:

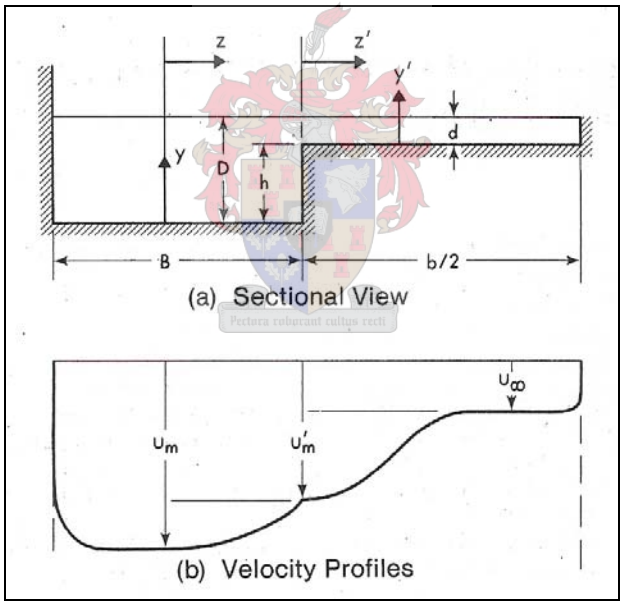

Die sone of gebied van skuifspanning het ook die gevolge dat sekondêre vloei patrone ontstaan soorgelyk aan die in die volgendde figuur. Die sekondêre stroom het die grootste rol om te speel in die verspreiding van gesuspendiërde particles na die vloedvlakte.

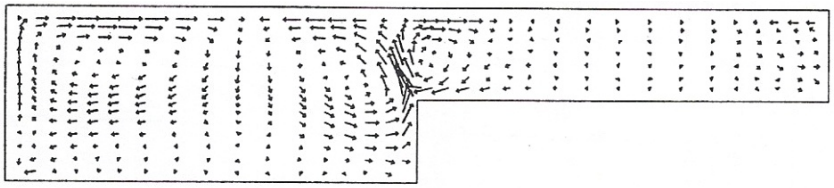

Die sekondêre strome kan wiskundig beskryf word maar is slegs in drie dimensies aanpasbaar. Dit is moontlik om hulle in ‘n twee dimensionele raamwerk te emuleer met behulp van sogenoemde dispersie faktore, maar nie elke twee dimensionele model wat beskikbaar is het hierdie faktore ingebou in die kode nie.

‘n Fisiese model is opgestel om die verspreiding van sediment na die vloedvlakte te meet. Die data wat ingesamel is, is dan gebruik om te sien of ‘n twee dimensionele model, naamliks CCHE2D, die verspreiding kan simuleer. Die gevolgtrekking is gemaak dat alhoewel die model die algemene verspreiding voorspel het, het dit nie die benodigde modules vir vertikale sekondêre stroom patrone ingebou nie. As gevolg daarvan kan dit nie gebruik word vir probleme wat trans-skuif sone verspreiding bevat nie.

ACKNOWLEDGEMENTS

I would like to express my appreciation toward all those who supported me both in terms of assistance and motivation. I would specifically like to mention my mentor Prof GR Basson for his patience and SANCOLD for their financial support. Further thanks go out to Ms MS Jacobs, Dr Julia Beck, Mr Noel Combrinck, Mr Ashley Lindoor and Dewet van Rooyen.

TABLE OF CONTENTS

Chapter 1 1
1 Introduction 1
1.1 Background 1
1.2 Motivation 1
1.3 Objectives 1
1.4 Outline of the thesis 2
Chapter 2 3
2 Floodplain Aspects 3
2.1 Inundation 4
2.2 Shear Layer 6
2.3 Sediment Deposition 7
2.4 Landforms 9
2.4.1 Levees 9
2.4.2 Anastomosing Rivers 13
2.4.3 Pans 18
2.4.4 Fertile Land 19
2.5 Floodplain Management 20
Chapter 3 21
3 Suspended Sediment 21
3.1 Origins 21
3.2 Mathematical Behaviour 24
3.2.1 Three Dimensions 27
3.2.2 Two Dimensions 28
3.2.3 One Dimension 29
3.2.4 Zero Dimension 30
3.3 Mixing Coefficients 30
3.3.1 Vertical Mixing 34
3.3.2 Transverse Mixing 37
3.3.3 Longitudinal Mixing 42
3.4 Particle Settling 43
3.4.1 Settling Velocity 43
3.4.2 Deposition 45
3.5 Boundary Shear Stress 48
3.6 Transport Across Shear Boundary 53
Chapter 4 61

4 Modelling 61
4.1 Physical Modelling 61
4.2 Mathematical Modelling 73
4.2.1 CCHE2D 73
4.2.2 Simulation 1 75
4.2.3 Simulation 2 78
4.2.4 Simulation 3 86
4.2.5 Enhanced CCHE2D 88
4.3 Conclusions 88
Chapter 5 90
5 Dam Impacts 90
5.1 Decrease in Flood Peaks and Frequency 90
5.2 Decrease in Sediment Inflow 91
5.3 Sediment Releases 92
5.4 Artificial Floods 94
5.4.1 Increase in Base Flow 94
5.4.2 Attenuated flow 94
5.5 Dam Removal 97
5.5.1 Planned Dam Removal 97
5.5.2 Unplanned Dam Removal 100
Chapter 6 102
6 Conclusions 102
Chapter 7 106
7 Recommendations 106
Chapter 8 107
8 References 107

LIST OF FIGURES

Figure 2-1: Basic Characteristics of a Floodplain 3
Figure 2-2: Flow Dynamics along a Shear Layer (Ahmadi & Rajaratnam, 1981) 5
Figure 2-3: Secondary Currents in Transverse Cross Section (Lin & Shiono, 1995) 6
Figure 2-4: Large Horizontal Eddies on Floodplain (Lin & Shiono, 1995) 6
Figure 2-5: Soil Depth Profile of Caesium Content at Krokfoss (Walling, Quine & He, 1992) 8
Figure 2-6: Soil Depth Profile of Caesium Content at Frogner (Walling, Quine & He, 1992) 8
Figure 2-7: Cross section at the city of Kaifeng (Leung, 1996) 11
Figure 2-8: Aerial view of the dike section near Kaifeng (Leung, 1996) 11
Figure 2-9: Flooded areas during the 1933 flood (Leung, 1996) 12
Figure 2-10: Erosion protection jetties (Leung, 1996) 12
Figure 2-11: The anastomosing upper Columbia River, Canada (Berendsen et al, 2002) 13
Figure 2-12: Geomorphologic map of the studied reach of the upper Columbia River. Flow is from right to left (Berendsen, Makaske & Smith, 2002) 15
Figure 2-13: Sediment deposition from the flood in relation to the topography of the floodplain cross-section (Berendsen, Makaske & Smith, 2002) 16
Figure 2-14: Pongola River, Kwa-Zulu Natal, South Africa. Flow is from South to North (Google Earth) 18
Figure 3-1: Initiation of motion and suspension for a current over a plane bed (van Rijn, 1993) . 23
Figure 3-2: Schematic of transport due to advection, turbulent diffusion and dispersion (Martin & McMutcheon, 1999) 25
Figure 3-3: Schematic Representation of the Diffusion and of the Convection-Diffusion in both the Laminar and Turbulent Regimes (Graf, 2003) 26
Figure 3-4: Vertical and Lateral velocity Distribution (Martin & McCutcheon, 1999) 31
Figure 3-5: Evolution of the Concentration introduced uniformly over the cross section (Graf, 2003) 32
Figure 3-6: Experimental Values of Sediment and Fluid Momentum Diffusion Coefficients (Graf, 2003) 33
Figure 3-7: Concentration Profiles (van Rijn, 1993) 37
Figure 3-8: Variation of ε_z with depth for channels of different widths and roughnesses (Lau & Krishnappan, 1977) 39
Figure 3-9: Variation of ε_z with depth at constant W/H ratios (Lau & Krishnappan, 1977) 40
Figure 3-10: Variation of the *C* factor with W/H and *f* (Lau & Krishnappan, 1977) 41
Figure 3-11: Variation of the *C* factor with W/H and *f* (Lau & Krishnappan, 1977) 42
Figure 3-12: Settling Velocity as a Function of Particle Diameter (Graf, 2003) 45
Figure 3-13: Velocity and Bed Shear Profiles (Ahmadi & Rajaratnam, 1981) 50
Figure 3-14: Experimental Distribution of Boundary Shear Stress (Ahmadi & Rajaratnam, 1981) 50
Figure 3-15: Similarity of the Excess Bed Shear Stress on the Floodplain (Ahmadi & Rajaratnam, 1981) 51

Figure 3-16: Bed Shear Stress in the Main Channel, $\lambda=z/(b/2)$ (Ahmadi & Rajaratnam, 1981).... 52
Figure 3-17: Behaviour of $A(\eta)$ Function (Ahmadi & Rajaratnam, 1981) 54
Figure 3-18: Predicted and Measured Secondary Flow (Lin & Shiono, 1995)..... 55
Figure 3-19: Contours of Streamwise Velocity (Lin & Shiono, 1995)..... 56
Figure 3-20: Depth Averaged Non-Dimensional Eddy Viscosity (Lin & Shiono, 1995)..... 56
Figure 3-21: Large Vortex Motion at the Free Surface (Lin & Shiono, 1995)..... 57
Figure 3-22: Flow Patterns Resulting from Secondary Flow (Lin & Shiono, 1995)..... 57
Figure 3-23: Streamwise Velocity Contours and Lateral Streamlines for an Asymmetric Smooth Channel (Naot et al, 1993) 58
Figure 3-24: Change of Bed Shear Stress with Depth (Naot et al, 1993) 59
Figure 3-25: Streamwise Velocity Contours and Lateral Streamlines for a Symmetric Wide Channel (Naot et al, 1993) 59
Figure 3-26: Streamwise Velocity Contours and Lateral Streamlines for a Rough Floodplain (Naot et al, 1993)..... 60
Figure 4-1: View of flume looking upstream 62
Figure 4-2: Laboratory flume 62
Figure 4-3: Schematic of experiment..... 63
Figure 4-4: Sediment container 63
Figure 4-5: Positions of Sampling Points 64
Figure 4-6: Suction tubes 65
Figure 4-7: Vacuum chamber 65
Figure 4-8: Vertical suspended sediment concentration 66
Figure 4-9: Plan View of Bed Profile..... 67
Figure 4-10: Cross Section of Flume..... 67
Figure 4-11: Plan View of Observed Suspended Sediment Concentration of Test 1 (g/ℓ)..... 68
Figure 4-12: Plan View of Observed Suspended Sediment Concentration of Test 2 (g/ℓ)..... 68
Figure 4-13: Plan View of Observed Suspended Sediment Concentration of Test 3 (g/ℓ)..... 68
Figure 4-14: Plan View of Observed Suspended Sediment Concentration of Test 4 (g/ℓ)..... 68
Figure 4-15: Suspended Sediment Concentrations for the consecutive transverse cross sections – Test 1..... 71
Figure 4-16: Suspended Sediment Concentrations for the consecutive transverse cross sections – Test 2..... 71
Figure 4-17: Suspended Sediment Concentrations for the consecutive transverse cross sections – Test 3..... 72
Figure 4-18: Suspended Sediment Concentrations for the consecutive transverse cross sections – Test 4..... 72
Figure 4-19: Cross section of Simulation 1 (not to scale) 75
Figure 4-20: Plan View of Bed Profile of Simulation 1..... 75
Figure 4-21: Flow field of Bousmar & Zech study (flow is from R to L)..... 76

Figure 4-22: Water surface profile of Simulation 1 76
Figure 4-23: Velocity profile of Simulation 1 76
Figure 4-24: Velocity profile close up of Simulation 1 77
Figure 4-25: Transverse velocity profile of Simulation 1 77
Figure 4-26: Bed Shear Stress profile of Simulation 1 78
Figure 4-27: Cross Section of Simulation 2 (not to scale) 79
Figure 4-28: Plan View Bathymetry of Simulation 2 79
Figure 4-29: Water surface elevation for Simulation 2 80
Figure 4-30: Velocity profile for Simulation 2 81
Figure 4-31: Simulated Sediment Concentrations 1 82
Figure 4-32: Simulated Sediment Concentrations 2 82
Figure 4-33: Simulated Sediment Concentrations 3 82
Figure 4-34: Simulated Sediment Concentrations 4 82
Figure 4-35: Simulated Sediment Concentrations 5 83
Figure 4-36: Simulated Sediment Concentrations 6 83
Figure 4-37: Simulated Sediment Concentrations 7 83
Figure 4-38: Simulated vs Observed Relative Concentrations at 1 m 85
Figure 4-39: Simulated vs Observed Relative Concentrations at 3 m 85
Figure 4-40: Simulated vs Observed Relative Concentrations at 6 m 85
Figure 4-41: Simulated vs Observed Relative Concentrations at 9 m 85
Figure 4-42: Simulated Surface Elevation for Simulation 3 87
Figure 4-43: Simulated Velocity Profile for Simulation 3 87
Figure 4-44: Simulated Sediment Concentrations 87
Figure 5-1: Relationship between the Flood and Sediment Peak (Shen, 2000) 93
Figure 5-2: Attenuation of Pongolapoort flood release (DWAF, 2006) 96
Figure 5-3: Bathymetry of Pongola Study (DWAF, 2006) 96
Figure 5-4: Matilija Dam (Matilija Coalition, 2002) 98
Figure 5-5: Matilija dam wall and sediment deposits, (Matilija Coalition, 2002) 98
Figure 5-6: Matilija ecosystem restoration project (Matilija Coalition, 2002) 99
Figure 6-1: Secondary currents driven by shear layer 102
Figure 6-2: Plan View of Observed Physical Model Suspended Sediment Concentration (g/ℓ) (H=0.135) 104
Figure 6-3: Plan View of Observed Physical Model Suspended Sediment Concentration (g/ℓ) (H=0.15) 104

LIST OF TABLES

Table 4-1: Experiments conducted 66
Table 4-2: Velocity measurements (m/s) 69
Table 4-3: Model Parameters for Simulation 2 80
Table 5-1: Pongolapoort Flood Peaks (DWAF, 2006) 90

LIST OF SYMBOLS

a	Reference level above river bed
b	Length scale
C	Concentration
c	Dimensionless transverse dispersion proportionality constant
C_a	Concentration at reference level a
CCHE2D	Centre for Computational Hydrodynamics and Engineering – 2 Dimensional
C_D	Drag coefficient
C_e	Depth averaged concentration for the equilibrium condition
C_o	Maximum concentration (065)
D_*	Dimensionless particle diameter
d_{50}	Mean particle diameter
D_x	Longitudinal dispersion coefficient (depth averaged)
D_y	Vertical dispersion coefficient (depth averaged)
D_z	Transverse dispersion coefficient (depth averaged)
F	Dimensionless shape factor
f	Friction factor
F_d	Fluid drag force
F_g	Gravity force
g	Acceleration due to gravity
H	Depth of flow
H_C	Depth in the main channel
H_P	Depth on the floodplain
K	Friction coefficient
p	Probability of deposition
Re	Reynolds number
s	Relative density / specific gravity in water (2.65)
S	Source sink term
S_0	Longitudinal bed gradient
t	Time
u	Longitudinal component of convective velocity
u_*	Shear velocity
$u_{*,crs}$	Critical bed shear velocity for initiation of suspension
U'_m	Velocity at the main channel – floodplain interface
U_∞	Undisturbed velocity on the floodplain

U_C	Undisturbed channel flow velocity (Manning)
u_i	Convective component in one of the three spatial dimensions
U_m	Undisturbed velocity in the main channel
U_P	Undisturbed floodplain flow velocity (Manning)
v	Longitudinal component of convective velocity
w	Vertical component of convective velocity
W	Width
x	Longitudinal distance
x_i	One of the three spatial dimensions
y	Vertical distance
Z	Rouse number (suspension number)
z	Transverse distance
z'	Distance over floodplain measured from the shear boundary interface
α	Reduction factor for settling velocity
β	Proportionality factor between ε_m and ε_s
ε	General mixing coefficient
ε_i	Diffusivity in the one of the three spatial dimensions
ε_m	Diffusivity for linear momentum
ε_s	Diffusivity for sediment
η	Function representing Z/b
θ	Mobility number
θ_{crs}	Critical mobility number
κ	von Karman constant
ν	Kinematic viscosity
ν_t	Eddy viscosity coefficient
ρ	Density of water
ρ_s	Particle density
τ	Vertical shear stress
τ'_0	Bed shear stress at the interface
τ_0	Bottom shear stress
τ_0	Disturbed distribution of bed shear stress
τ_∞	Undisturbed bed shear stress on the floodplain
τ_b	Applied bed shear stress
$\tau_{b,\,dep}$	Bed shear stress required for full deposition
φ	Factor for high sediment concentrations
ψ	Factor incorporating stratification of suspended sediment
ω_s	Particle fall velocity in clear still water

CHAPTER 1

1 INTRODUCTION

1.1 Background

The floodplain of a river forms a close relationship with the stream that created it. Not only does the river influence the characteristics of the floodplain, the floodplain can also very easily influence its river. The floodplain can be a temporary storage for vast volumes of flow during floods. This much is obvious but it should also be forthcoming that large amounts of sediment are stored here. It is from this sediment that the floodplain gets most of its characteristics and as such a floodplain can be defined as “a flat expanse of land on either side of a river where sediment has been deposited by a flooding river”.

1.2 Motivation

Rivers are complex systems that can be thought of being in dynamic equilibrium with the environment in which they exist, meaning that there is a general balance between erosion and deposition. Current understanding however is that the state in which a river and its associated features finds itself, is rather a consequence of the varying factors that are able to influence its behaviour. Therefore, if there is sufficient knowledge of the behaviour of these factors, the behaviour of the river itself can be more accurately understood and hence predicted. And seeing that predicting a river’s behaviour is the prime goal of practically all hydrologic and hydrodynamic models and methods, these various factors should be the focus of constant research.

This thesis thus aims to develop an understanding of one such a factor, namely that of floodplain sedimentation, and the interrelationship of the floodplain with the main channel.

1.3 Objectives

The objectives of this thesis are to investigate the behaviour of suspended sediment in a river and how this behaviour changes as the flow in the river overtops its banks. This overbank flow creates a special interaction between the main channel and floodplain flows, and it is this interaction zone that will be focussed on since it is the driving force for much of the observed behaviour.

1.4 Outline of the thesis

The thesis starts out by investigating various physical phenomena which are related to suspended sediment movement. Chapter 2 not only includes the effects suspended sediment has on a floodplain but it also provides certain case studies where the management of suspended sediment was identified as a key role player. The following section, Chapter 3 describes the literature review conducted for this research. It outlines the many equations and related behavioural patterns that describe suspended sediment transport. Chapter 4 is the section where both the physical as well as the mathematical modelling that was conducted is reported. Drawing upon the information presented in the previous chapters, Chapter 0 provides some guidelines and possible effects dam operators and managers should be aware of concerning the consequences of the fact that reservoirs store large amounts of sediment.

CHAPTER 2

2 FLOODPLAIN ASPECTS

This chapter looks at some of the aspects concerning the influence a river has on the floodplain it created. The basic geomorphic form of a river, especially in its lower reaches, consists of a broad and flat landscape with low gradients both in the longitudinal and transverse directions. Many rivers at this stage of their course tend to meander upon a bed of alluvial silt deposited there by the river itself. This alluvium is accreted or removed depending upon the flow conditions in the river. As shown below in Figure 2-11 floods can cover a very large area due to the low gradients involved and so the sediment these floods transport can be carried a long way from the main channel.

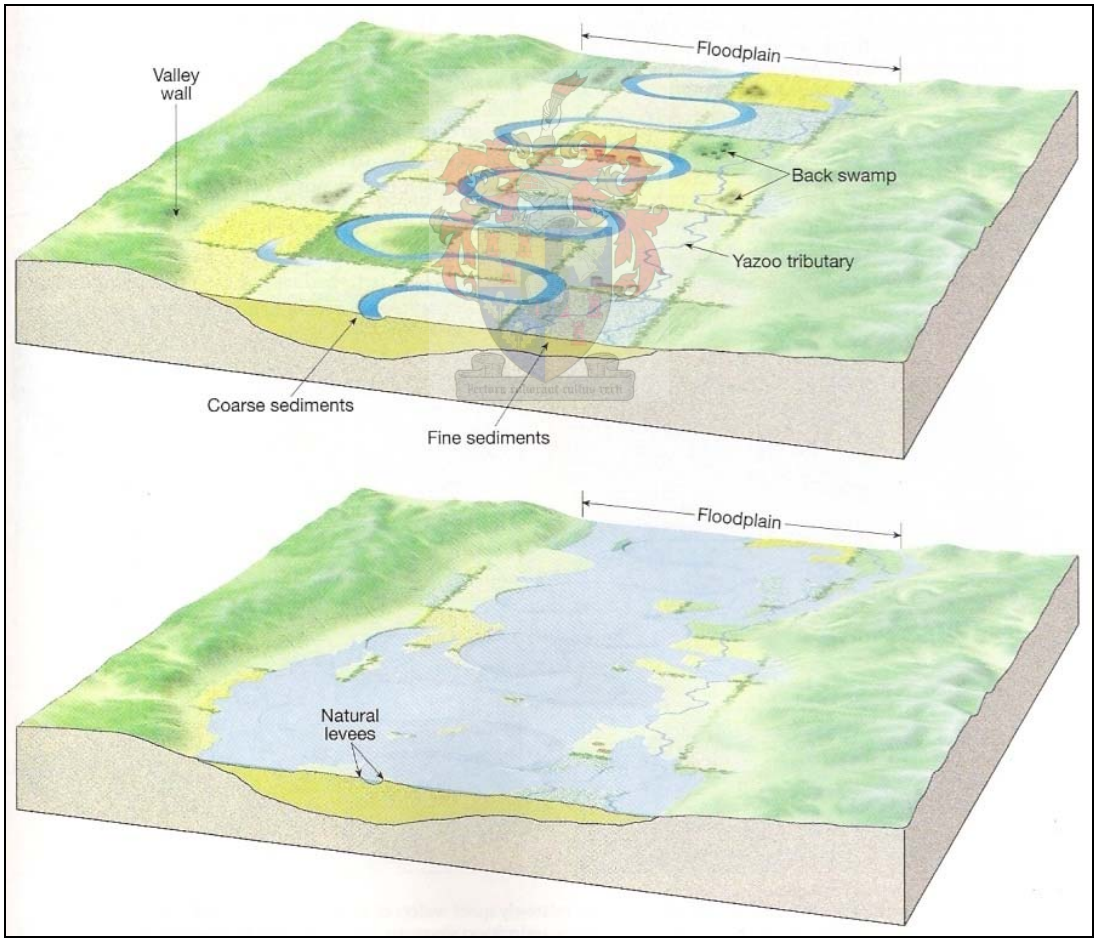

Figure 2-11: Basic Characteristics of a Floodplain

2.1 Inundation

Under normal, base flow conditions there is a general equilibrium between the processes of erosion and deposition in the river channel. Floods caused by rainfall, snowmelt or other non-natural events such as dam releases, supplement this base flow and thus also change the behaviour of its erosion and deposition activities.

An increase in flow can be large enough so that the main river channel alone is incapable of containing the flow within its banks. Water levels rise and start exceeding the ground levels of the adjoining floodplain. Such inundation of normally dry land constitutes a flood.

Initially, when the water levels are relatively low, flow on the floodplain is slow or even stagnant. Water possibly won't even be flowing in the direction of the main channel. As the flood waters rise however, floodplain flows become more influenced by the flows in the main channel. The nature of this influence is the exchange of momentum of the flow from the main channel to the flow on the floodplain. The method by which this is achieved is via a shear layer between the main channel and the floodplain, roughly where the top of the river bank is.

It is this shear layer between the two flows that causes a momentum and turbulence transfer from the fast flowing main channel to the floodplain. It has been the subject of much research over the last few decades, especially in terms of the determination of the total discharge of the so-called compound section. If the shear layer is ignored in such calculations the discharge given by the Chezy or Manning equations is greater than the actual observed discharge. As such it is evident that the floodplain has a retarding effect on the flow in the main channel, making floods flow slower than the general flow equations would predict. Figure 2-22 shows that the converse of this statement, that the floodplain flows quicker as a result of the main channel flow, is also true.

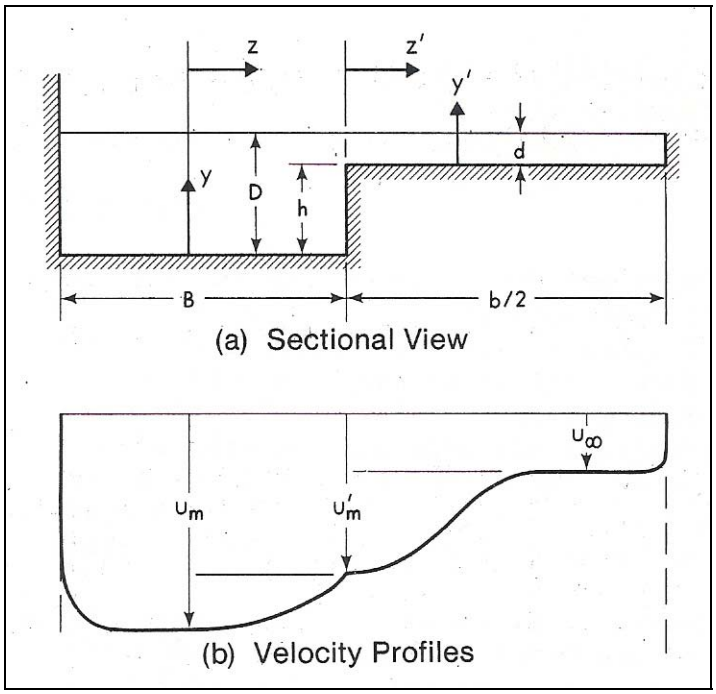

Figure 2-22: Flow Dynamics along a Shear Layer (Ahmadi & Rajaratnam, 1981)

In Figure 2-22, u_m represents the undisturbed or unaffected velocity in the main channel and u_∞ the undisturbed velocity on the floodplain. As can be seen from the figure, these velocities only assert themselves a certain distance away from the boundary between the main channel and the floodplain. Close to the boundary the flow in the main channel is slower and on the floodplain it is faster as energy from the main channel flow is transferred to the floodplain flow. The flow at the interface itself travels at u'_m.

The floodplains considered in this study are generally well developed and thus can be expected to have small transverse and longitudinal gradients. Water on the floodplain can thus be expected to flow very wide and very shallow. Local concentrations around buildings and the like can however cause supercritical flow where large scale erosion can take place. On the contrary, collections of buildings or other infrastructure on the plain can act as obstructions to the flow and cause damming up of the flow. Large scale deposition can thus be expected to occur here.

All water on the floodplain during a flood originates from the river's main channel, except for small and almost negligible contributions from ephemeral tributaries and rainfall. It can therefore be deduced that this is likewise the case for the sediment in suspension. Despite such a logic argument this statement is fallacious because it is possible for sediment to be entrained on the floodplain. It must be recalled however that one of the purposes of this thesis is to investigate the dispersion rates of sediment resultant from the main channel sediment transport.

2.2 Shear Layer

The shear layer does not only exist on a river between the main channel and its floodplain. It occurs in general between any two flows where one is travelling slower than the other regardless of the circumstances. As such, research into the dissipation of the energy or the mixing of a jet in a larger mass of water is also valid here.

Such shear layers are responsible for transporting momentum from the faster moving flow to the slower moving one. As such this interaction zone, henceforth called the main channel floodplain interface (M/F interface) is a region of high turbulence yet strangely enough this does not necessarily mean an increase in suspended sediment transport. It will be shown later that the lateral transport of the solute is mainly dominated by secondary currents (Lau & Krishnappan, 1977) (also see Figure 2-33), generated by differential bed shear stress, which in turn are a direct result of the shear layer. Despite the increase in turbulence and a subsequent increase in turbulent mixing the decrease in transport caused by secondary currents actually causes a decrease in lateral suspended sediment. This statement however ignores the fact that there are also large horizontal (vertical axis) eddies at work, such as those shown in Figure 2-44.

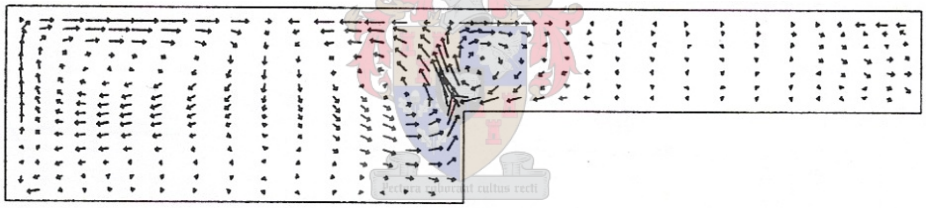

Figure 2-33: Secondary Currents in Transverse Cross Section (Lin & Shiono, 1995)

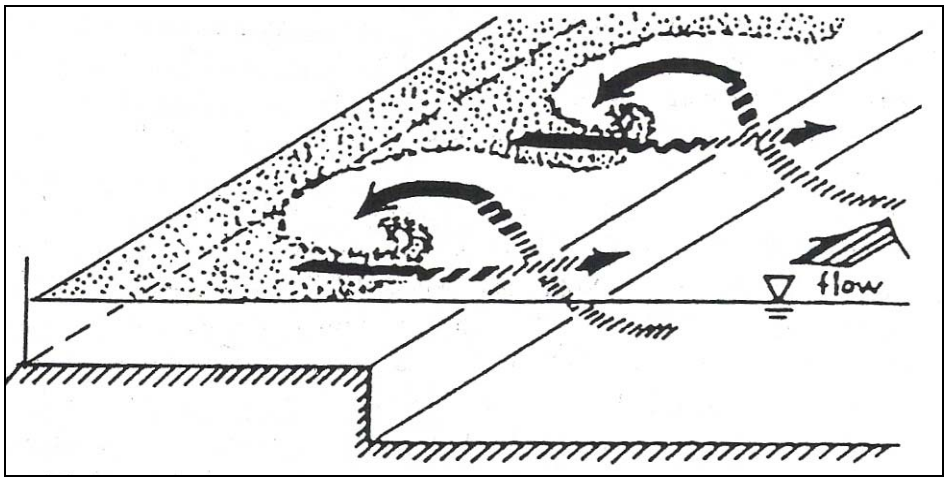

Figure 2-44: Large Horizontal Eddies on Floodplain (Lin & Shiono, 1995)

2.3 Sediment Deposition

In general, sediment on a floodplain mainly undergoes deposition. It acts as a sediment trap. The amount deposited is, of course, dependent on the amount of sediment available and the prevailing flow conditions. The question is how much sediment on the floodplain originated from the main channel? How much of that sediment is deposited, and how much is removed and deposited downstream?

The suspended sediment enters the floodplain from the main channel and begins depositing almost instantly. As is evident from the existence of levees, in general the highest accumulations occur near the channel and then decrease as distance from the main channel increases. The amount of dispersion that occurs before a particle deposits depends on the turbulence profile on the floodplain as well as the momentum transfer between the main channel and the floodplain.

Studies into the rates of deposition on floodplains have revealed that as much as 40% of suspended sediment in the main channel can be deposited on the floodplain (Walling & Owens, 2003). Such a high percentage has the implication that during floods, floodplain deposition can play a large role in the amount of sediment actually transported downstream. Such suspended sediment budget studies prove that there is more than one way to combat sediment related problems.

To determine deposition rates radionuclides such as Caesium-137 and Lead-210 along with sediment core samples can be used. Average annual sedimentation rates so measured are usually in the order of 1 $g.cm^{-2}.yr^{-1}$ over a period of 30-40 years (MS Encarta).

Caesium-137 is a radionuclide which is found in the majority of soils around the world which have been exposed to the atmosphere in the last 50 years or so. The reason it so useful in determining the sedimentation rate is that practically all this Caesium-137 has a common source, namely the large scale nuclear weapons testing of the 1950's and 60's as well as the later accident at Chernobyl. Thereby if a soil profile like the examples shown below (Figure 2-55 and Figure 2-66) which depict two sites along the river Leira in Norway are analysed for Caesium-137 the average annual sedimentation rate can be determined.

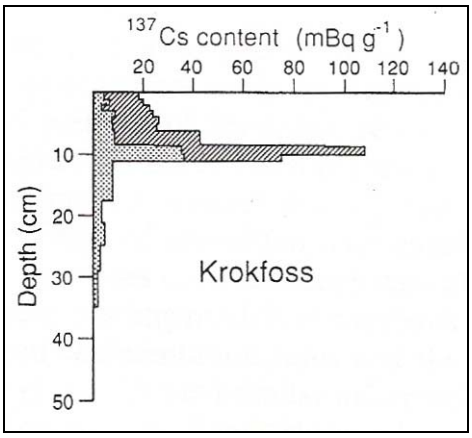

Figure 2-55: Soil Depth Profile of Caesium Content at Krokfoss (Walling, Quine & He, 1992)

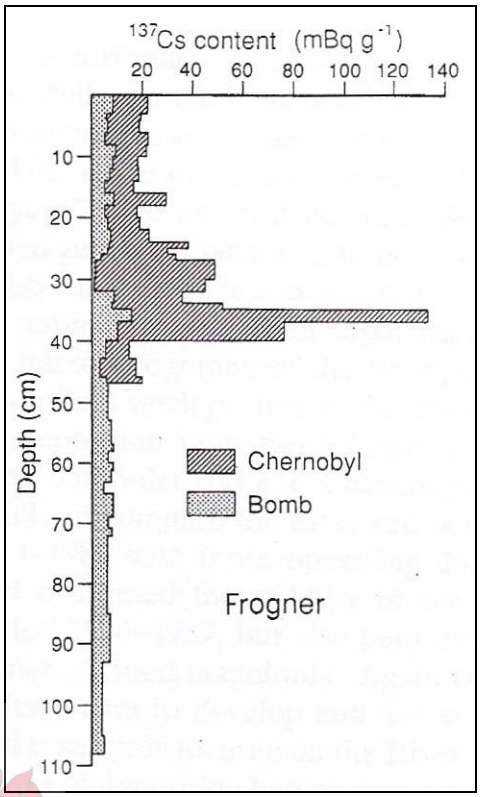

Figure 2-66: Soil Depth Profile of Caesium Content at Frogner (Walling, Quine & He, 1992)

The depth below the surface this layer of Caesium-137 is found is then divided by the number of years since the accident or the weapons testing to obtain an overall average sedimentation rate over that period. It is also of interest to note that some of the Caesium found can be attributed to the Chernobyl rather than the weapons testing. Thus in certain cases even this general sedimentation rate can be refined further.

Care must however be exercised in simply accepting this average yearly rate of deposition. Site circumstances must be taken into account. Factors such as biological activity and farming all have significant effects on the soil profile and so must be taken into account. Other site specific attributes have even been used to prove that the rate determined is actually not valid for the entire period under study but only for a single large-scale flood event (Walling et al, 1992).

Further dating methods other than radionuclides have also proven useful. They include macro- and micro-fossils, volcanic events, sediment traps as well as carbon dating.

The rates of sedimentation so determined can play a vital role in determining the human impact on fluvial systems or in the calibration of models aiming to predict the distribution of deposition. This data can then aid in the mitigation of environmental problems where sediment-associated pollutants are involved. The accumulation of phosphorous is a prime example. Most studies show that in general there is an exponential decrease with distance from the main channel, but there can be significant deviations due to microtopography and secondary flow routes.

Still, it must be noted that another role an overbank flood plays is that of sediment flushing, which under healthy conditions will prevent an excessive build up of such pollutants. This is especially true of gravel rivers where large floods are known to flush out unnatural fine sediment which has gotten there by a variety of ways (Toda et al, 2005).

2.4 Landforms

There are various ways to determine the amount of sediment that is transferred to a floodplain. The easiest and most inexpensive of these methods is to look, by way of chronologic aerial and oblique photographs, at the size and regularity of sediment related landforms found on the floodplain. Such methods are not in the least quantitative but they can indicate areas of low and high sedimentation.

2.4.1 Levees

The clearest indication of a sediment flux from the river is the presence of natural levees on both sides of a river channel. As sediment is carried onto the floodplain, the coarser fractions quickly find themselves in a flow which is unable to carry them, thus they settle down not far from the main river channel. Smaller fractions such as clay or silt will settle farther away. As more and more sand is deposited on top of the river banks the longitudinal ridges that form can eventually create a continuous sand bank on either side of the river.

Such levees can be a great advantage to those living near rivers since smaller floods which would normally flow onto the floodplain now flow confined to the main channel. Long term false confidence can however be placed in such structures, whether they are natural or man-made, with disastrous consequences. There are numerous recorded events of the failure of such embankments due to even small floods having overtopped or breached them. The reason for this is that the discharge capacity of such canalised rivers decreases over time. Sediment carried by any particular flood that would have been deposited on the floodplain now settles out in the main channel, thus raising the bed level.

A prime example is the Huang He (Yellow) River in China. The river received its Western name from the colour of its water, which is a perennial ochre-yellow hue due to its high sediment content – up to 1.6 billion tons per annum, the highest in the world (World Bank, 1993) (Wikipedia). Because of the incredibly high concentrations of the sediment, on average 37.6 kg/m³ (compared to 0.07 for the Amazon and 0.6 for the Mississippi), much of this sediment is deposited. It is estimated that only 1.2 billion tons is discharged to sea, the rest is deposited in the river (Leung, 1996) (Cowen, 2000)

The ancient Chinese used this sediment deposited in the main channel to artificially enhance the natural levees along the river for flood protection. As the river deposited more and more sediment, thereby raising the bed, so were the levees raised, until after some 4000 years the river bed rose as high as 10 meters above the surrounding floodplain, creating a suspended river, as is visible in Figure 2-77 and Figure 2-88 (MS Encarta). The river levees are estimated to have been breached more than 1500 times and the river changed course 26 times in the last three thousand years. The present course was adopted in 1897, yet to this day floods continue to threaten the people living on the floodplain. The last major flood, indeed the most deadly natural disaster on record, occurred in 1931 which is estimated to be responsible for the death of nearly four million people (Wikipedia) (Cowen, 2000)

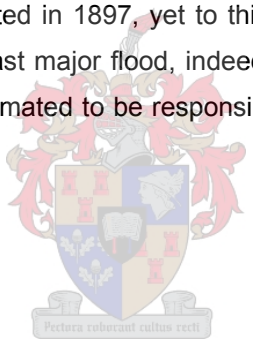

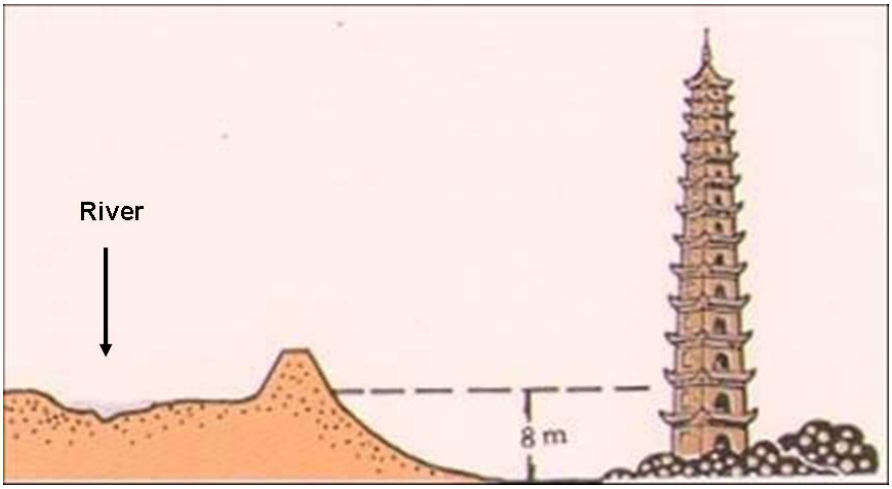

Figure 2-77: Cross section at the city of Kaifeng (Leung, 1996)

Figure 2-88: Aerial view of the dike section near Kaifeng (Leung, 1996)

Currently the lower 786 km of the river is lined with flood protection dikes as can be seen by the two cross-dashed parallel red lines in Figure 2-99 which border the river. These dikes, despite having failed numerous times have remained relatively intact over the last 50 years. This is partly due to a succession of jetties (Figure 2-1010) which help to keep the river's main current in its centre thereby preventing it from eroding levee foundations.

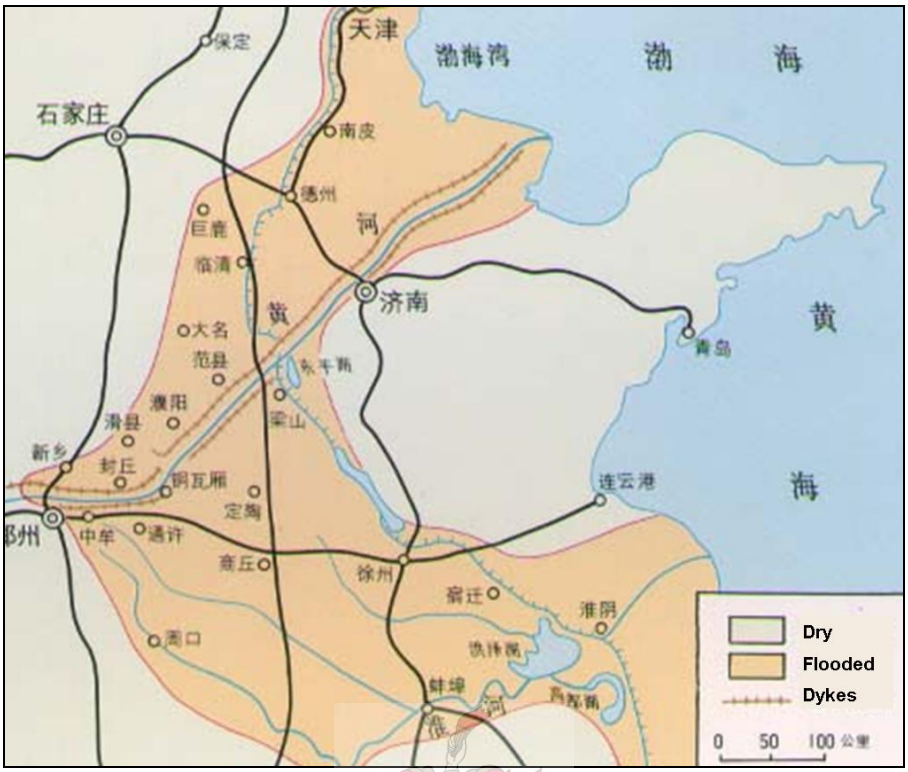

Figure 2-99: Flooded areas during the 1933 flood (Leung, 1996)

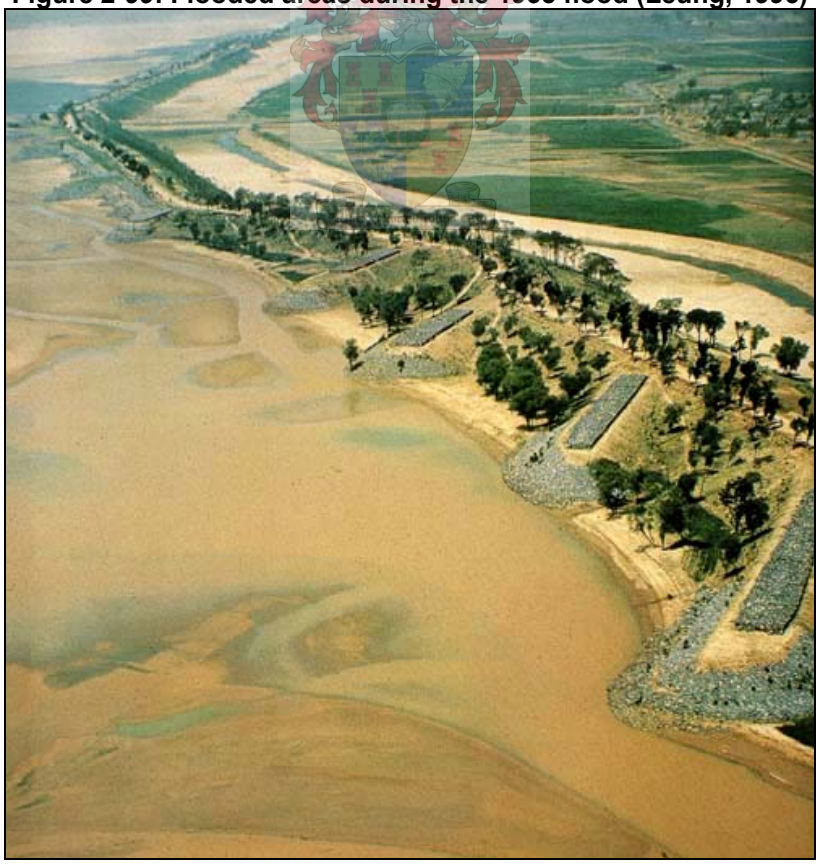

Figure 2-1010: Erosion protection jetties (Leung, 1996)

Another vital and more effective element in the managing of a river such as the Huang He, besides the maintaining of levees, is the managing of the catchment sediment yield. Over 90% of the sediment in the Huang He originates from a region called the Loess Plateau. Poor farming practices, thick deposits of aeolian loess and region specific climatic conditions are the cause behind large scale erosion. Efforts such as afforestation, terracing and other soil conservation methods are underway to combat these processes. The project, funded by the World Bank, is a long term one and as yet the Yellow River continues to rise in bed level at an average 1 m every 10 years (Leung, 1996) (World Bank, 1993).

The above is a clear indication that when it comes to the transport of suspended sediment in rivers there is a natural flux of sediment onto the floodplain, and when such a process is interrupted, the river in question can behave erratically.

2.4.2 Anastomosing Rivers

Another very clear indication of the influence of overbank sedimentation is the existence of anastomosing rivers such as the one shown in Figure 2-1111. Anastomosing rivers are those rivers that due to avulsions change course periodically resulting in a floodplain that consists of several channels, some newly formed and other older ones silting up. They can be defined as a river that is composed of two or more interconnected channels that enclose floodplains. Such rivers can be distinguished from braiding rivers in that braided rivers are characterised by convex bar like islands instead of interchannel floodplains.

Figure 2-1111: The anastomosing upper Columbia River, Canada (Berendsen et al, 2002)

A study was conducted recently on the Columbia River in Canada focusing on the frequency and causes of such avulsions. The study titled "*Avulsions, channel evolution and floodplain sedimentation rates of the anastomosing upper Columbia River, British Columbia, Canada*" is summarised below (Berendsen, Makaske & Smith, 2002).

The age of a set of channels in a particular reach was determined using ^{14}C dating of subsurface floodplain organic material from beneath levees. Also under investigation was the theory that the very existence and frequency of avulsions are related to the amount of floodplain sedimentation that occurs. Floodplain sedimentation rates were determined and from this several conclusions as to transverse sediment depositions were made.

Anastomosis occurs on several rivers worldwide regardless of their physiographic setting. The Rhine-Meuse delta for example is set in a coastal plain and is thus in contrast with the anastomosing Columbia River which is set in a montane environment. The setting of a river is therefore not an influence on whether or not a river is prone to anastomosis.

Two types of dating techniques for measuring sedimentation rates were used in the study. The first involved the drilling of a set of cores along a predetermined cross section (see Figure 2-1212). These cores were then split up, described and dated in 10 cm sections. As mentioned before, Carbon-14 dating was used on the peaty organic substances in the alluvium profile. These dates were then subsequently confirmed using terrestrial macrofossils and ash layers from known volcanic eruptions in the region.

The second dating technique is aimed at estimating short-term sedimentation rates. The sediment deposited during a single flood event was measured using sediment traps in the form of artificial grass mats. The short-term sedimentation rates would invariably result in higher rates than their long-term counterparts indicate. But, considering the effects of settling and compaction the incongruity in values is expected.

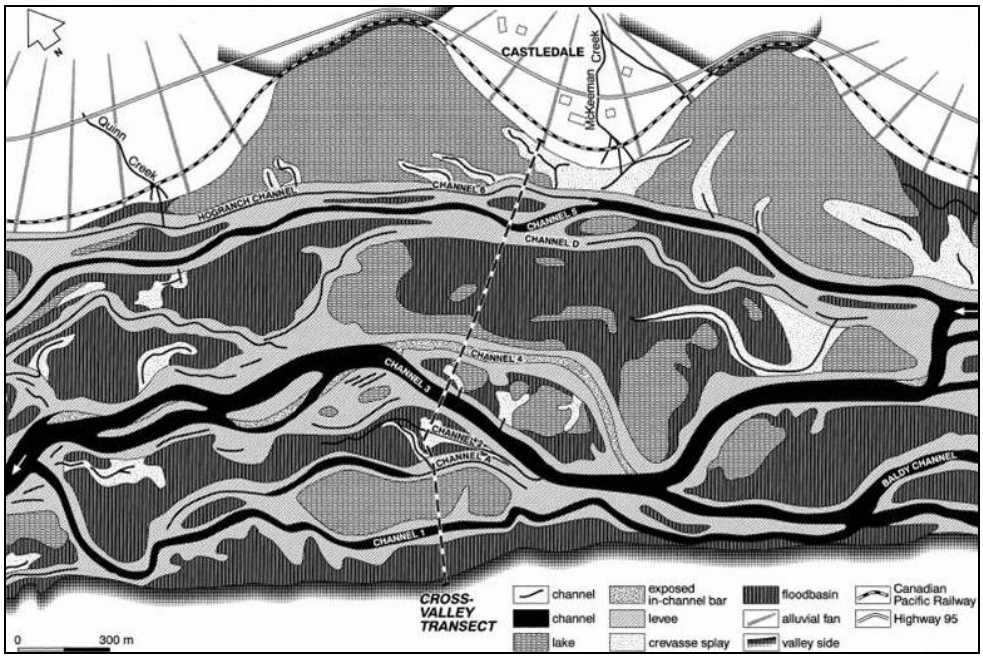

Figure 2-1212: Geomorphologic map of the studied reach of the upper Columbia River. Flow is from right to left (Berendsen, Makaske & Smith, 2002)

Results of the study estimate the long-term average floodplain sedimentation rate to be 1.75 mm/a. Average levee sedimentation rates were nearly four times higher than floodplain rates, and it was determined that levee deposits vary noticeably as a function of the distance from the channel. Values of up to 6 mm/a were calculated near the channel and roughly 2 mm/a at more distant levee sites.

The short-term average sedimentation rates from the single flood event was in the order of 0.8 mm/a. This value is somewhat lower than the long-term average but this can be attributed to the relatively low magnitude of the flood that was measured. The flood was so small in fact that certain sections of the higher levees remained unaffected. As can be seen from Figure 2-1313 the measured sediment thicknesses ranged from 4.7 to 0 mm. The larger values were experienced at levees that were inundated during the flood. Higher levees, such as those adjoining channel 3, were unaffected due to their elevation above the flood waters.

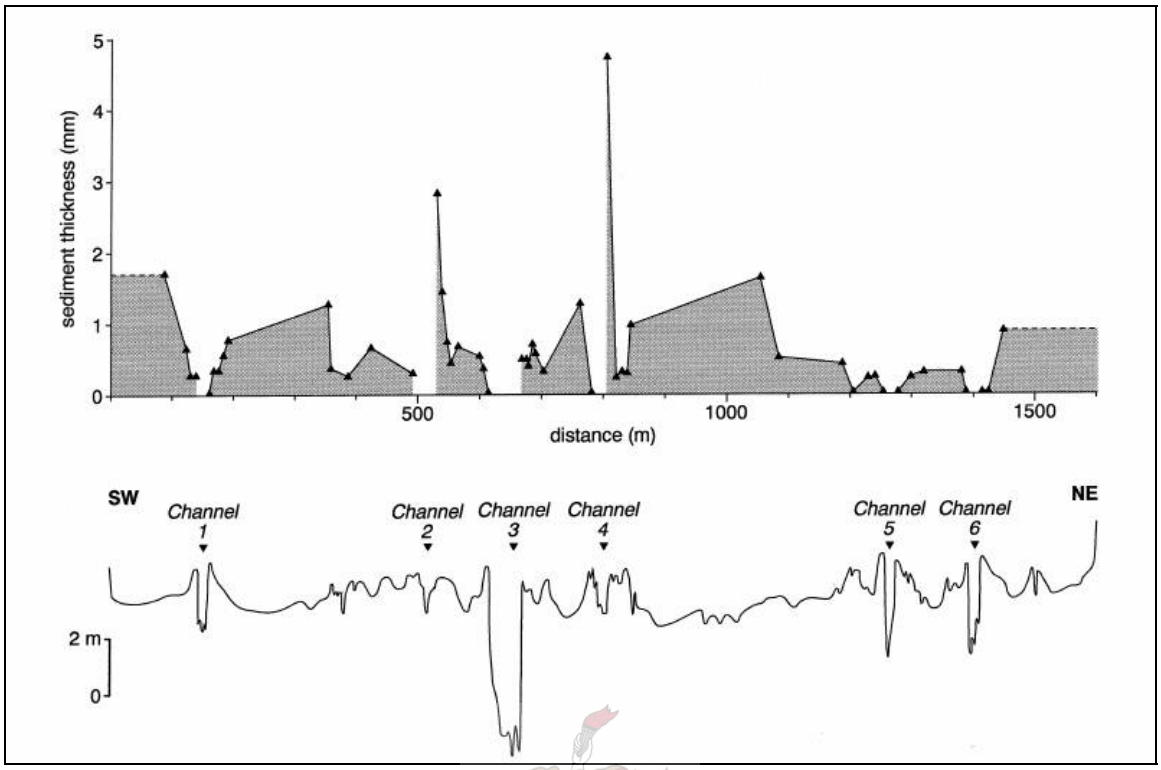

Figure 2-1313: Sediment deposition from the flood in relation to the topography of the floodplain cross-section (Berendsen, Makaske & Smith, 2002)

Apart from the peaks there was the odd occurrence that the majority of the sedimentation occurred on the floodplains and relatively little settled on the levees. This phenomenon was attributed to the amount of time that the various sections were inundated. The deepest part of the floodplain remained under water the longest and thus received most sediment, whereas the higher levees remained completely dry.

Thus in order for the pronounced levees, which are a prerequisite for avulsions, to develop the timing of the flood hydrographs must be strongly peaked. Such peak flows would cause the levee sedimentation to outpace the floodplain sedimentation. In other words rapid sedimentation on levees and not on the floodplains requires a strongly peaked flow regime with bankfull discharge frequently exceeded to enable sediment to be transported from the main channel.

Without such a peaked regime, the floodplain relief would be able to keep pace with that of the levees, and as such avulsions will occur less often. It must be noted however that sediment deposition is not the only cause for avulsions. In the Columbia River especially events such as log jams and beaver dams are characteristics which cause the river to change course more frequently than observed elsewhere.

Cumulative levee sedimentation can become so excessive that the levees become the highest landform on the floodplain. Thus, during floods, the point of highest unit discharge moves away from the main channel to another less resistant point on the floodplain (which may very well have been a previous channel), which erodes and in time becomes the new active main channel. The old main channel, having a reduced supply of water, starts to silt up either laterally or vertically and may eventually be abandoned by the river entirely.

Although it is evident that in the Columbia River differential floodplain sedimentation and log jams are conducive for avulsions and abandonment of channels, the driving force which controls the switch between bed scour and accretion has yet to be refined. Time dependant characteristics such as channel history and bank vegetation have been proposed to play a big role.

It is interesting to make a comparison to the previous section where the Yellow River was discussed. Though that river is no longer flowing in its natural state it is clear that it too with its high levees would change course regularly. Thus even without the problems of a suspended river, it would change course on its own account.

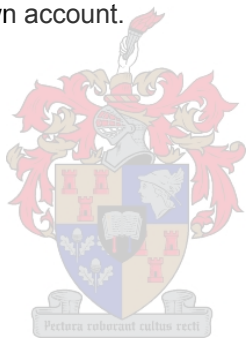

2.4.3 Pans

As is the case with the Pongola River, certain rivers, due to their sediment dynamics can create a system of freshwater pans on the floodplain which are periodically cut off from the main river channel by levees. An aerial view of the Pongola River is presented in Figure 2-1414. It shows numerous pans which lie on the floodplain alongside the main river channel.

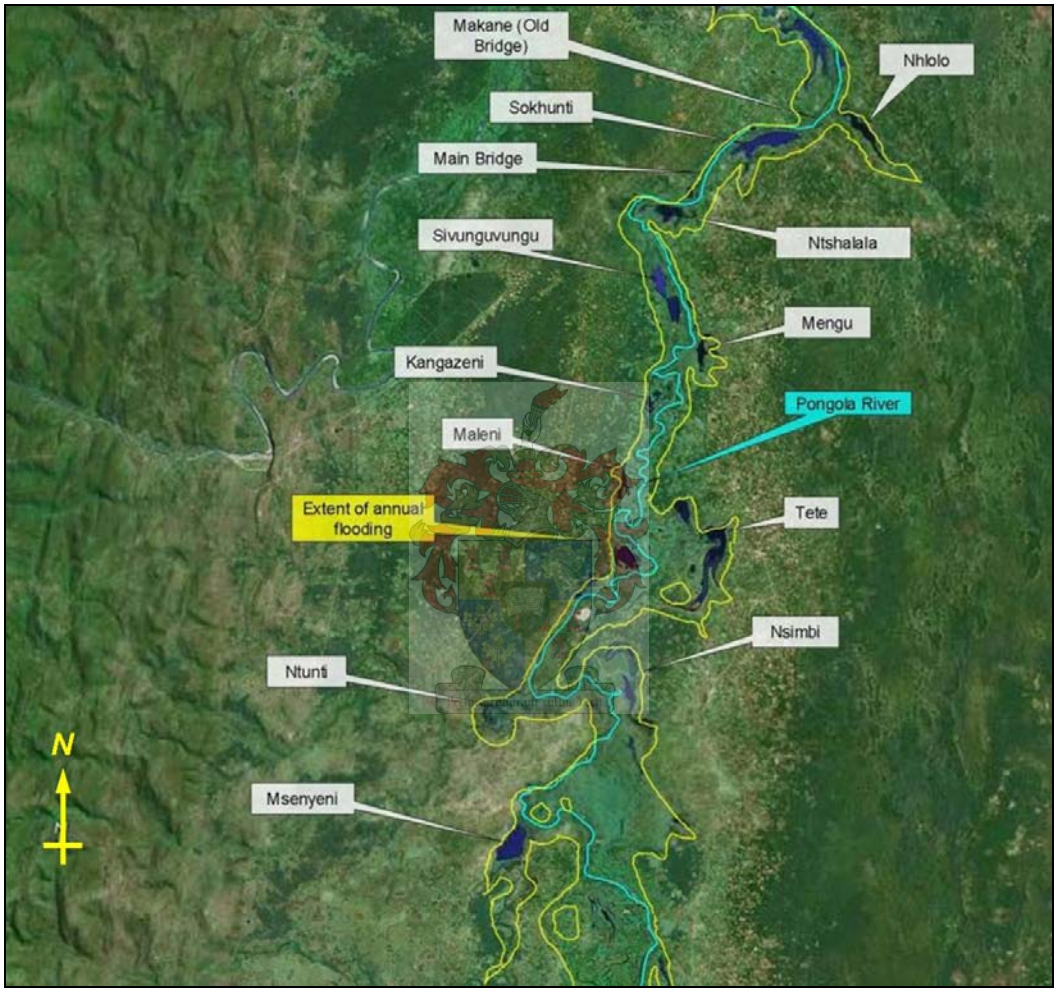

Figure 2-1414: Pongola River, Kwa-Zulu Natal, South Africa. Flow is from South to North (Google Earth)

The differential floodplain deposition patterns causing the development of levees can have the effect of cutting off water from the river. These slack water swamps and pans are replenished from time to time by floods from the main river or from tributaries. These replenishing flows, as is the case for the Pongola River, have the tendency to stick to certain preferred flow paths.

These paths are thus of interest since severe scour would be expected here. Though scour does take place it is not as excessive as would be expected from such a large volume of water moving through such a relatively narrow channel. Vegetation in these preferred channels probably plays a very large role not only in retarding flow velocities but also in protecting soil against scour.

A further contributing factor to the limiting of scour is the highly cohesive nature of the sediment encountered in the Pongola River. It was observed that even with large changes in elevation from the pans to the river sediment did not easily erode away. The duration of floods which lasted only a few days also prevented large amounts of scour.

What is also of interest is the closure of these so-called preferred flow paths. It seems logical that such channels would be prone to erosion and so would not only serve as entrances to the pans but also as the exits in some cases. Such continuous erosion year after year would thus lead to the pans draining completely instead of retaining their water as they do now. It therefore seems logical that deposition is taking place in or near the entrances. A balance thus exists between the processes of erosion and deposition at these preferential flow paths.

As a narrow, sediment laden flow enters a large relatively stagnant body its load will deposit. This much is known, but what happens when flow not only comes from this one channel but also from the floodplain as overland flow. How will such flow patterns affect the pans? A further point of interest is the fact that the Pongola River is now regulated due to the Pongolapoort Dam and as such carries much less sediment than it naturally would. Has the decrease in sediment influx affected the river-pan system in any noticeable way?

No conclusive data has been collected in this regard but old maps from the area do show that the river has changed course in one of the flatter areas. Whether or not this was due to a decrease in sediment flow cannot be determined, but data has been collected over the past few years which, if studied further, might shed some light on how the pans are behaving in this sediment deprived environment (Beck & Basson, 2003) (DWAF, 2006).

2.4.4 Fertile Land

A further piece of evidence that confirms the large role floodplain sedimentation plays in the health of a river system is the use of floods by riverine farmers to recharge the nutrients on their lands. Probably the most famous instance of this phenomenon is the Nile River in Egypt.

This river is well known for its dependants, the Egyptians, who have relied upon the Nile to deliver a regular influx of sediment to recharge their fields. On average the Nile deposited some 12 million tons of sediment per annum on the floodplain and carried a further 124 million tons of sediment out to sea.

This process has however not been as consistent as is believed. Both sediment and climate models suggest that there have been periods in the distant past when the river did indeed flood but deposited almost no sediment compared to its normal load. The cause of this anomaly has been ascribed to natural cyclic climate systems which induced rain to fall in the catchment of the White Nile but not in that of the Blue Nile where the majority of the sediment is sourced (Krom et al, 2002).

The sediment related problems experienced currently are however not a result of climate change but rather the construction of the High Aswan Dam (HAD). Completed in 1970, it is Egypt's most important water resource, besides the Nile itself. Currently the High Aswan Dam silts up at a rate of around 60-70 Mm^3/a, forcing Egyptians to import nearly 13 thousand tons of fertilizer every year to keep the soil, which the Nile once supported with fertile depositions.

2.5 Floodplain Management

Floodplain management can refer to a number of activities and guidelines. These of course depend on the end goal of the manager. As such a floodplain can be used to store sediment and so prevent it from causing problems farther downstream. It has been shown that even at small rivers as much as 47% of the total sediment flux that flows through the system can be stored on the floodplain (Walling & Owens, 2003).

If the floodplain is undeveloped or contains agricultural lands these deposits can have a positive influence. If however the floodplain is the site of important infrastructure, possible damage caused by this deposition (for example the extensive clean-up operation) must be mitigated. Such measures can include the provision of flow paths not only to prevent deposition in certain places but to encourage it in others. This is to facilitate the subsequent removal of this sediment.

Such floodplain management plans must also include any sources of contaminants on the floodplain which could be spread should a flood manage to reach it. Again, measures not only at the source site itself but also downstream of the site can be put in place to prevent the contaminant from being transported but also to collect it in a spot downstream.

CHAPTER 3

3 SUSPENDED SEDIMENT

Suspended sediment can be defined as that part of the sediment load of a river which consists of fine soil particles that remain in suspension for a considerable period of time without contact with the bottom. Such material remains in suspension not by vertical velocity (u_y), which averages to zero in any case, but by the fluctuations in this velocity caused by turbulence as well as the tendency for particles to move from areas of high concentration to areas of low concentration according to Fick's Law.

Suspended sediment can be differentiated from bed load sediment in that more energy is required to get particles into this state and keep them there. There is no clear definable demarcation between bed and suspended transport. All that can be said is that as the energy of the flow increases, certain particles saltating along the bed will make longer jumps and thus become part of the suspended load.

How much of this stream energy is required to place and keep a particle in suspension will depend on its size, shape and density. The smaller, rougher and lighter a particle is the easier it will be for turbulence to keep it in suspension. At a given stream power therefore, the smaller sediment will be transported in suspension. Slightly larger particles will be moved as bed load and larger particles still will remain unmoved.

The theory behind the behaviour of suspended sediment in a water body is described in this chapter. The focus will be on the transport caused by rivers but the equations are just as valid for transport in larger bodies of water such as estuaries and reservoirs.

3.1 Origins

The origins of suspended sediment can refer to both the question of where spatially a certain particle came from but also how it was placed in suspension. The first question is relatively straightforward in that a sediment particle comes from the catchment upstream of its current location. Of course, such a vague statement is of no real value. A more precise description would be to state that particle was picked up or discharged into the river at some point upstream.

The forthcoming natural processes include erosion (turbulence bursting), in other words the suspension of material by the actions of the river itself. Other less obvious processes include the

segment of a river's transport load called wash load. Wash load is defined as that part of the river's total load which was not picked up by the river by its own actions. In other words, it is sediment that was placed in the river flow by either overland flow or aeolian transport. It can be identified by observing that the characteristics, such as size and composition, of the wash load particle do not conform to the characteristics of the sediment which is known to originate from the river. As such it is possible for an "upper reach" river which carries mostly cobbles to also carry an uncharacteristic suspended load of very fine material.

Unnatural sources of sediment refer to sediment which originates from human activities, a prime example being farming. Other examples include the passing of turbidity currents through a dam.

As to how suspended sediment is placed in suspension, there is a very wide range of literature which refers to this topic. The actual physical process is difficult to define and observe. The phenomenon of turbulence bursting where a turbulent eddy strikes the bed and suspends a great deal of sediment is clear enough but when it comes to the more general suspended sediment which originates from bed-load the distinction is less definable.

When can a particle of a certain size be said to stop saltating and be regarded as part of the suspended load? Due to this ill-defined limit, most definitions present boundary regions above or below which full scale suspended sediment does or does not take place.

Van Rijn (1993) reports that an upper boundary for fully a developed concentration profile can be stipulated by Bagnold (1966):

$$\frac{u_{*,crs}}{\omega_s} > 1 \tag{11}$$

which can then be expressed in terms of the mobility number,

$$\theta_{crs} = \frac{\left(u_{*,crs}\right)^2}{(s-1)gd_{50}} = \frac{\left(\omega_s\right)^2}{(s-1)gd_{50}} \tag{22}$$

in which θ_{crs} = critical mobility number

$u_{*,crs}$ = critical bed-shear velocity for initiation of suspension

ω_s = particle fall velocity in clear still water

d_{50} = mean particle diameter

g = acceleration of gravity

s = ρ_s / ρ , relative density

As a lower (or intermediate) boundary for suspension movement, a set of experiments conducted by van Rijn (1993) resulted in,

$$\begin{aligned} 1 < D_* \le 10: \quad & \frac{u_{*,crs}}{\omega_s} > \frac{4}{D_*}, \quad or \quad \theta_{crs} = \frac{16}{D_*^2}\frac{\omega_s^{\,2}}{(s-1)gd_{50}} \\ D_* > 10: \quad & \frac{u_{*,crs}}{\omega_s} > 0.4, \quad or \quad \theta_{crs} = 0.16\frac{\omega_s^{\,2}}{(s-1)gd_{50}} \end{aligned} \tag{33}$$

where D_* is the dimensionless particle diameter,

$$D_* = \left[\frac{(s-1)g}{\nu^2}\right]^{1/3} d_{50} \tag{44}$$

Both of these boundaries together with the well-known Shields parameters are plotted in Figure 3-11.

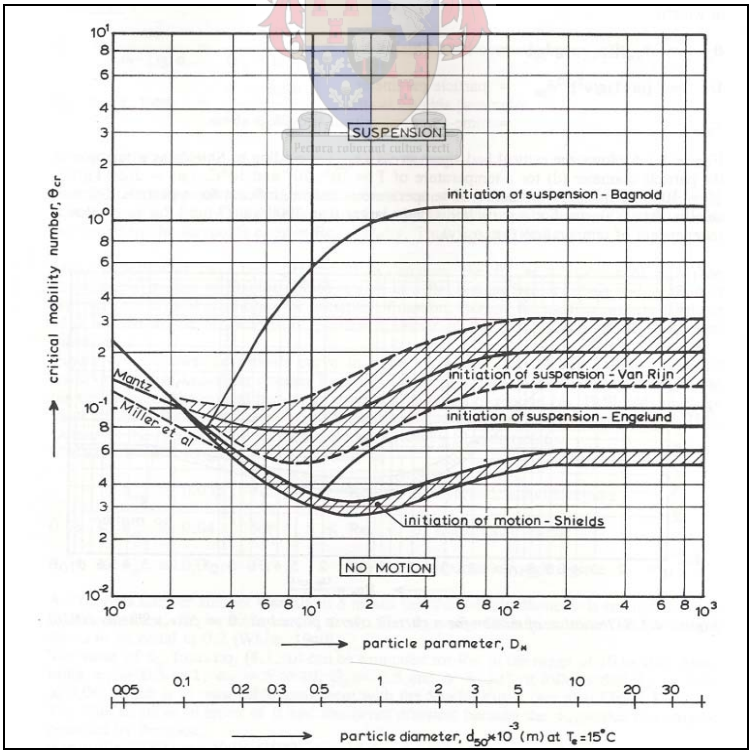

Figure 3-11: Initiation of motion and suspension for a current over a plane bed (van Rijn, 1993)

What the above figure clearly indicates is the entirely logical premise that the bigger a particle the more energy is required to suspend it. What is also evident is the very wide range of critical movement parameters provided by the various contributing researchers. What this confirms is that sediment movement is a highly stochastic process which cannot in practical terms be exactly defined, only general movement can be predicted with high levels of accuracy.

In both cases above the key parameters are bed shear stress (bed-shear velocity) and sediment fall velocity. Because of this in places where the bed shear stress decreases across a certain distance the larger sediment particles in suspension can be expected to settle out. It is for this reason that coarser sediment settles out on the floodplain near to the main channel and lighter smaller sediment is able to travel farther into the floodplain.

A more definitive description of this decrease in bed shear stress is given in section 3.5. Settling velocity is expanded upon in section 3.4.

The above discussion mainly focuses on the prediction of movement of material by using the shear stress as the defining parameter. It must be realised however that there are other parameters that can be used most notably the unit stream power method. The method basically revolves around the concept that movement will only occur once the unit stream power required to move a certain particle is exceeded by a multiple of the applied stream power (Armitage & McGahey, 2003).

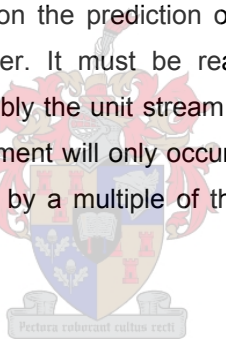

3.2 Mathematical Behaviour

The mixing of suspended sediment in a river is controlled by three basic processes namely molecular diffusion, turbulence diffusion and dispersion (see Figure 3-22 and Figure 3-33) (Martin, McMutcheon, 1999). In symbolic terms these mixing processes can be expressed similarly in that the degree of mixing is proportional to the concentration and turbulence gradients that occur. In general, they can be described as

$$\frac{\partial C}{\partial t} = \frac{\partial}{\partial x}\left(\varepsilon \frac{\partial C}{\partial x} \right) \tag{55}$$

where $\frac{\partial C}{\partial t}$ is the time rate of change of the concentration due to the mixing processes, x is a spatial dimension (longitudinal, transverse or vertical), C the mean concentration and ε is a

mixing coefficient (Martin, McMutcheon, 1999). The derivation of these mixing or dispersion coefficients will be covered in Section 3.3.

Another major factor involved in the mathematical description of suspended sediment transport is that of advection. Advection refers to the transport of the medium which carries the suspended sediment. In other words, the movement of the water at the velocity and direction dictated by the flow conditions of the river (Carrera, 1993).

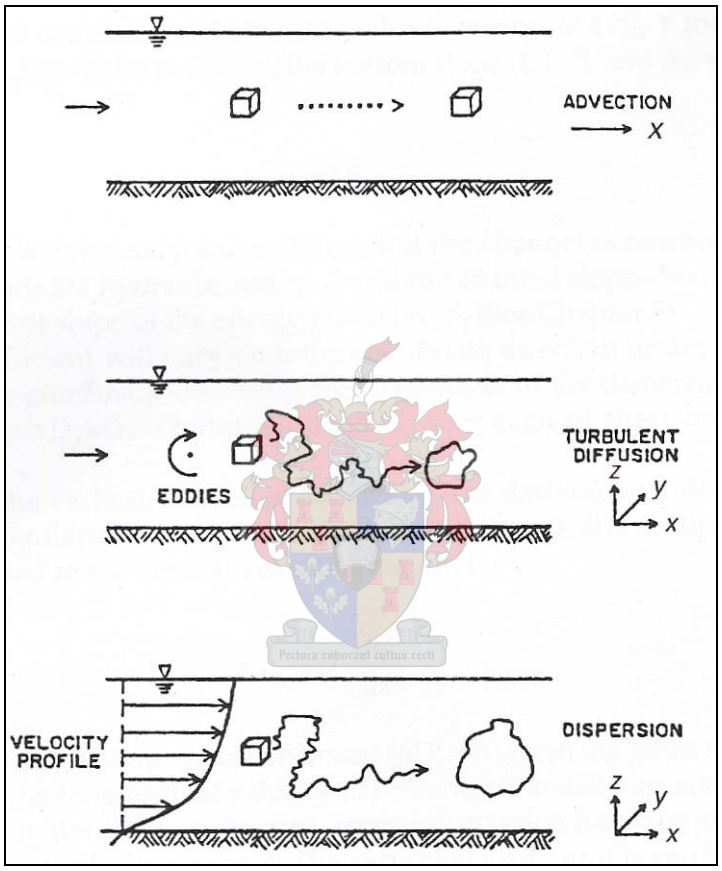

Figure 3-22: Schematic of transport due to advection, turbulent diffusion and dispersion (Martin & McMutcheon, 1999)

Figure 3-33 describes the difference between the different modes of suspended sediment transport very well. Figure 3-33-a depicts the spreading of a suspended sample in a still body of water. Movement only occurs due to the molecular motion of the fluid, also known as Brownian motion. Figure 3-33-b shows the spreading of solute under non-turbulent laminar conditions. In this case suspended sediment is transported via both dispersion as well as advection. In Figure 3-33-c turbulent mixing is presented. As is evident from the graphic, turbulent mixing causes the solute to spread farther or at a faster rate than the other two processes.

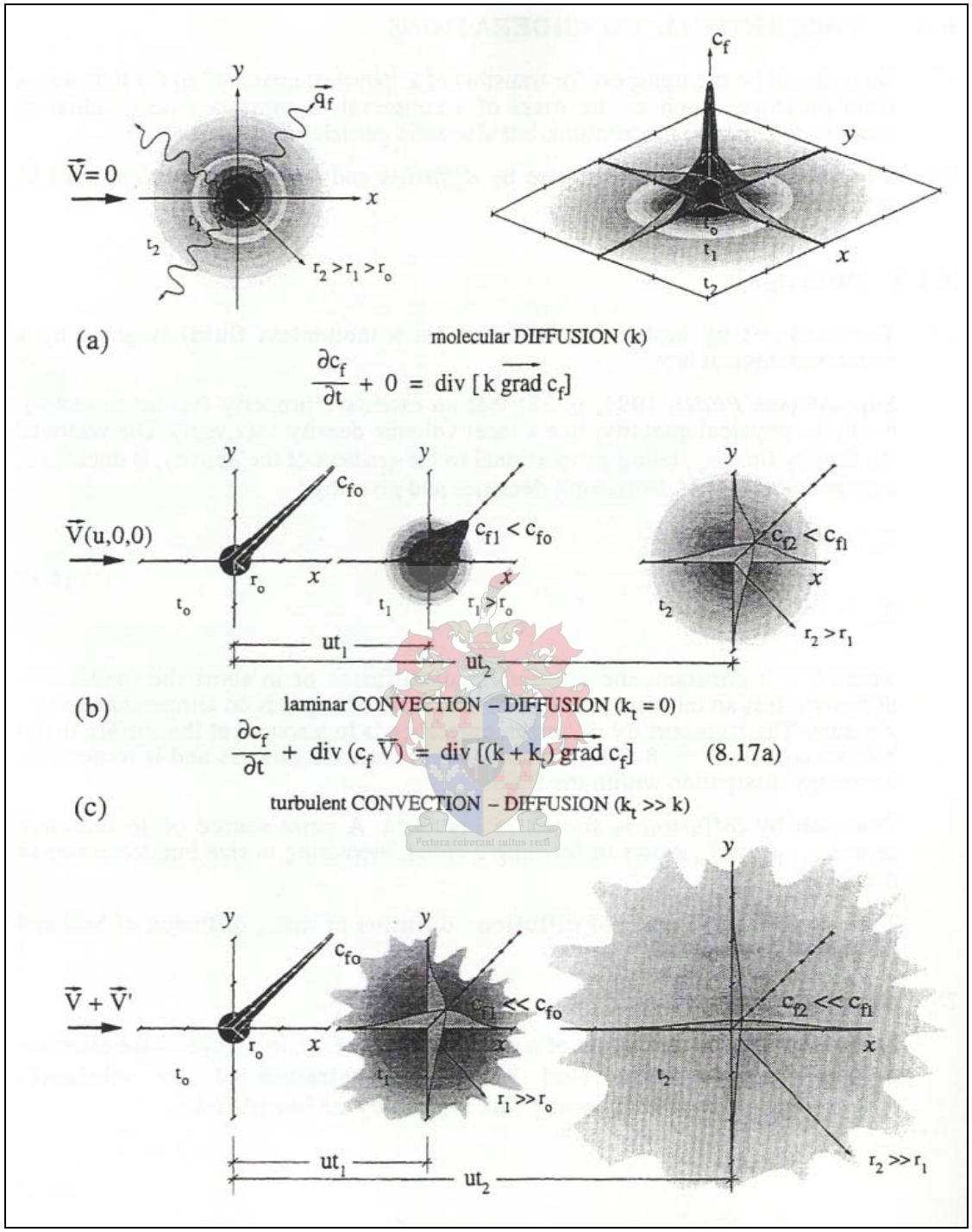

Figure 3-33: Schematic Representation of the Diffusion and of the Convection-Diffusion in both the Laminar and Turbulent Regimes (Graf, 2003)

3.2.1 Three Dimensions

These two processes, namely advection and diffusion, together form the basis of the aptly named advection-diffusion equation. The basic premise is that of considering the mass balance of sediment in a defined volume under the influence of diffusive and convective transport. The general three-dimensional equation describing the distribution of sediment concentration looks as follows:

$$\frac{\delta C}{\delta t} + \sum_{i=1}^{3} u_i \frac{\delta C}{\delta x_i} = \sum_{i=1}^{3} \frac{\delta}{\delta x_i}\left(\varepsilon_i \frac{\delta C}{\delta x_i}\right) \tag{66}$$

where,

C = concentration

t = time

x_i = the three direction coordinates

u_i = the convective velocity components in the three directions determined from the continuity and momentum equations

ε_i = the diffusivities (diffusion coefficients) in the coordinate directions

For the purposes of this thesis the convention that the longitudinal, vertical and transverse directions are represented by *x*, *y* and *z* respectively and time by *t* are used. The $\frac{\delta C}{\delta t}$ term represents the change in concentration in time and is usually the dependent variable in the equation. The $\sum_{i=1}^{3} u_i \frac{\delta C}{\delta x_i}$ term expresses the advection (or convection) process as a change in concentration over distance at a certain velocity. The final term symbolises the dispersion of the solute. Whilst the other terms are fairly straightforward in their physical meanings the last term is less so, especially considering the variable ε_i. These diffusivities in the general three-dimensional formula indicate the magnitude of the diffusive transport in the various directions. In layman's terms it describes the fact that particles will move from areas of high concentration to areas of low concentration at a rate proportional to the concentration gradient between the two areas.

Written out in full over the three dimensions the equation becomes:

$$\frac{\delta C}{\delta t} = -u_x \frac{\delta C}{\delta x} - \left(u_y - w\right)\frac{\delta C}{\delta y} - u_z \frac{\delta C}{\delta z} + \frac{\delta}{\delta x}\left(\varepsilon_x \frac{\delta C}{\delta x}\right) + \frac{\delta}{\delta z}\left(\varepsilon_z \frac{\delta C}{\delta z}\right) + \frac{\delta}{\delta x}\left(\varepsilon_y \frac{\delta C}{\delta y}\right) \quad (77)$$

Note that the vertical velocity component is taken as $u_y - w$, defining the resultant vertical velocity. However, it must also be noted that u_y is usually assumed to be equal to zero for river modelling since average vertical movement tends to nil.

For ease of use and faster modelling procedures equation (66) is readily simplified to two and even one dimensions. The main change between such reduced formulas and the general one, besides the omission of a coordinate direction, is the adjusting of the diffusion coefficient to allow for the omission. There are various methods of how such an adjustment should take place, most of them empirical. These are further described in Section 3.3.

3.2.2 Two Dimensions

Two dimensional modelling, as the name suggests, entails the omission of one of the coordinate directions. The question is which one. Such a choice would typically depend on the aim of the particular study. Take, for example, the intention of determining the deposition patterns with respect to transverse distance. How far away from the main channel does sediment accumulate on the floodplain surface? In order for the deposition patterns to be modelled the settling velocity of the suspended sediment must be included. This means that the vertical dispersion cannot be ignored. Put differently, the term $\frac{\delta C}{\delta x}$ which describes the longitudinal dispersion should be nullified. This can, however, only be true for steady, longitudinally uniform flow where the rate of erosion and deposition are equal over the entire section of the river under study (James, 1985). As a result, this kind of two dimensional modelling can produce interesting results in terms of deposition patterns but not successfully model dynamic systems.

Nonetheless, the formula looks as follows, with the steady state assumption as $\frac{\delta C}{\delta t} = 0$:

$$0 = \frac{\delta}{\delta y}\left(\varepsilon_y \frac{\delta C}{\delta y}\right) + \frac{\delta}{\delta z}\left(\varepsilon_z \frac{\delta C}{\delta z}\right) + w\frac{\delta C}{\delta y} - u\frac{\delta C}{\delta z} \quad (88)$$

Whilst ε_y describes the vertical dispersion the factor of interest is w which represents the convective velocity in the vertical direction which for suspended sediment is equal to the particle fall velocity. Take note that it is assumed to be positive downwards, hence the positive sign in equation (88). The transverse convective transport effects caused by secondary currents could possibly be accounted for in the transverse diffusivity ε_z, together with the usual dispersion effects. Thus for straight channels running parallel to the valley they flow in, there is no need for the last term in the above formula. However, if there is an additional transverse convective component, due to the river channel deviating from the ideal straight channel, the length averaged transverse velocity term u is required.

If on the other hand the purpose of the study was not to determine deposition patterns but say the prediction of solute spreading in a river or reservoir. In such a case it is the vertical dimension that is omitted i.e. assumed constant over time. Equation (66) would reduce to:

$$\frac{\delta C}{\delta t} = \frac{\delta}{\delta x}\left(\varepsilon_x \frac{\delta C}{\delta x}\right) + \frac{\delta}{\delta z}\left(\varepsilon_z \frac{\delta C}{\delta z}\right) - u\frac{\delta C}{\delta z} - v\frac{\delta C}{\delta x} \tag{99}$$

The above formula indicates that this model is capable of simulating dynamic, non-steady systems in that the $\frac{\delta C}{\delta t}$ term is not equal to zero. u and v represent the depth averaged velocities in the transverse and longitudinal directions respectively. The only real other difference between equation (88) and (99) is the omission of the settling velocity w.

3.2.3 One Dimension

The one dimensional version of the advection-dispersion equation is even more simplified than the two-dimensional case in that both the transverse and vertical transport is assumed to be in equilibrium. In terms of this thesis this assumption cannot be made but there are circumstances, such as straight regular channels with flow under the bankfull stage, where its use can be advantageous. The omission of two coordinate directions simulates the effect that the rates of dispersion in the vertical and transverse direction have reached equilibrium and will not change with time or with vertical and transverse distance. Therefore only longitudinal dispersion is accounted for. Uses for this equation format include the simulation of the progress and dilution of a pollutant down a river course (Bowie et al, 1985).

3.2.4 Zero Dimension

Technically there is no such thing as a zero-dimension equation, but in practice the general advection-dispersion equation can be averaged in all three spatial directions. Such equations are unable to predict the fluid dynamics of a system thus these models only predict the concentration field as it varies with time. As an example, the simplest representation of a lake is to consider it as a continuously stirred reactor (Bowie et al, 1985).

3.3 Mixing Coefficients

No matter how accurate the formulations of the basic physical mechanisms, good predictions of the transport of suspended sediment require sufficient data concerning rate constants and coefficients.

It is perhaps a good idea to now make a clear distinction between the definitions of dispersion and diffusion. Both are mathematically similarly described, though their values might differ from each other. Diffusion refers to the actual mixing of the suspended sediment through the water body, either by turbulence or by molecular movement. Dispersion on the other hand is not a physical mixing process as such but merely a consequence of the reduction of the full three-dimensional to lesser dimensions. (Martin & McMutcheon, 1999)

Take for example the averaging out of the vertical dimension. In such a case a non-uniform velocity distribution assumption across the depth of the water body must be made (see Figure 3-44). Advection will hence cause the suspended sediment to move at the mean water body velocity. Dispersion on the other hand is there to take into account the fact that particles travelling near the bottom of the water column will travel slower than the ones near the top. Therefore, ignoring longitudinal dispersion could result in the overestimation of peak concentrations and the underestimation of time of arrival i.e. a concentration-time distribution showing a gradual increase with a lower peak instead of a sharp rise and a high peak. This shear phenomenon causes a smearing of the concentrations in the same way longitudinal diffusion would (see Figure 3-55).

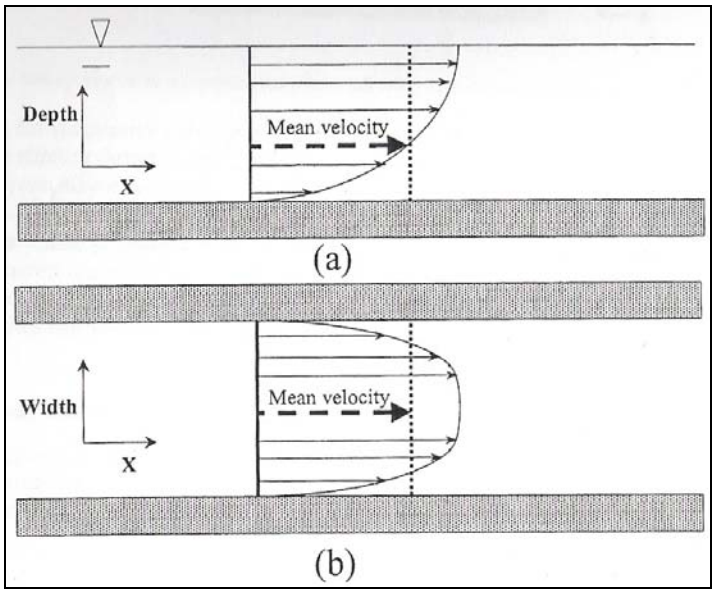

Figure 3-44: Vertical and Lateral velocity Distribution (Martin & McCutcheon, 1999)

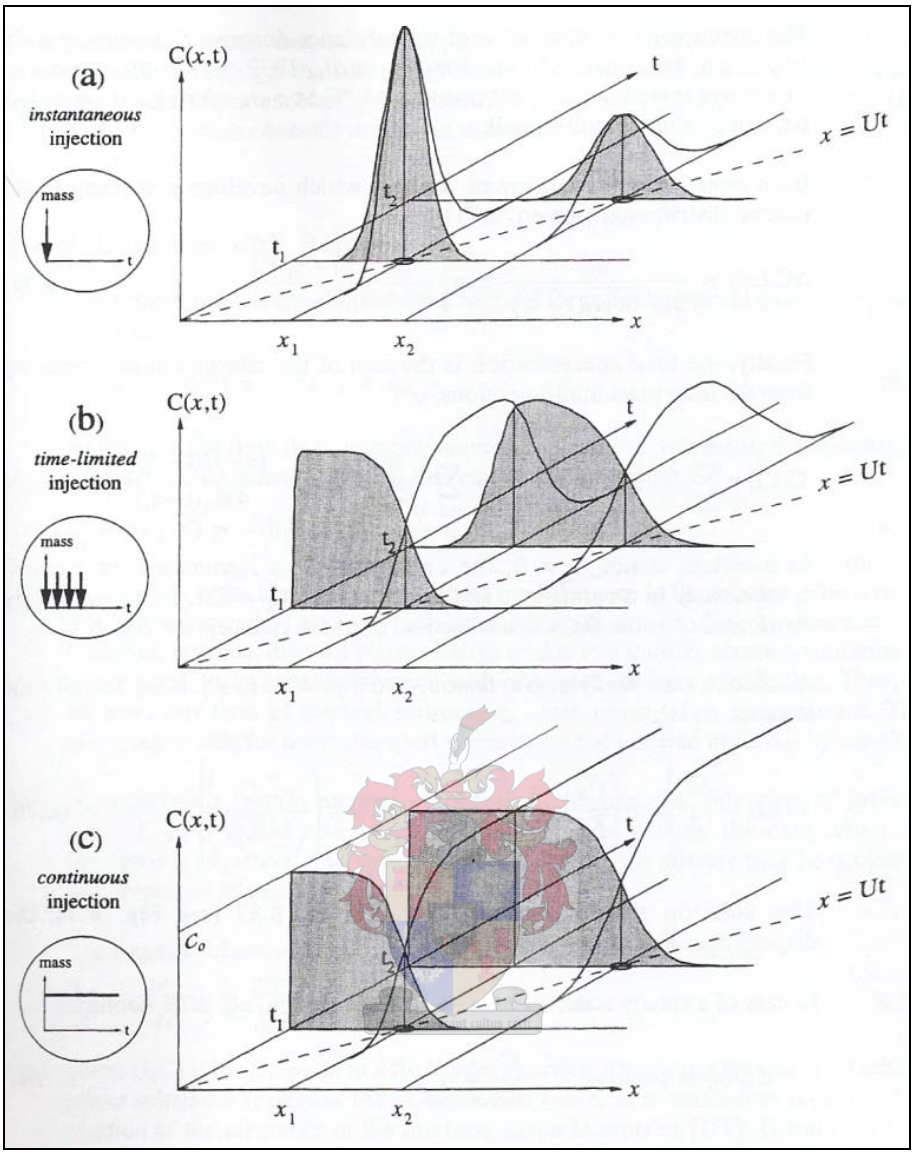

Figure 3-55: Evolution of the Concentration introduced uniformly over the cross section (Graf, 2003)

Diffusion (ε_i) therefore represents the mixing due to turbulence and advection and is as such only applicable in fully three dimensional flow. Dispersion (D_i) also represents mixing but it includes effects such as secondary flow and relative shear flow (DHI, 2003). Diffusion can be estimated theoretically though dispersion can only be determined by measuring field or laboratory conditions (DHI, 2003).

Theoretical estimations usually include the assumption that the diffusivity for sediment (ε_s) is proportional to the diffusivity for the fluid mass, which according to the Reynolds analogy is equal to the diffusivity for linear momentum (ε_m), i.e.

$$\varepsilon_s = \beta \varepsilon_m \tag{1010}$$

where β is the factor of proportionality. The value of this factor has been the subject of several studies which resulted in both $\beta<1$ and $\beta>1$ (see Figure 3-66). This apparent disagreement can however be explained. Experiments with suspended sediment conducted on a bed without bed-forms resulted in $\beta<1$. Under such circumstances turbulence is composed of rectilinear velocity fluctuations and so the inertia of the sediment particles prevents them from fully responding to these fluctuations (Cellino & Graf, 2002).

For the cases where $\beta>1$ was determined the bed had clear bed-forms. Therefore the turbulence structure contains eddies with a high degree of vorticity which results in the sediment particles leaving these eddies due to centripetal forces (James, 1985)(Cellino & Graf, 2002). As a consequence of this particles mix faster than the fluid that carries it, thus sediment diffusivity is larger than the fluid diffusivity. In most cases however, where the sediment in suspension is fine enough the assumption is made that $\beta=1$.

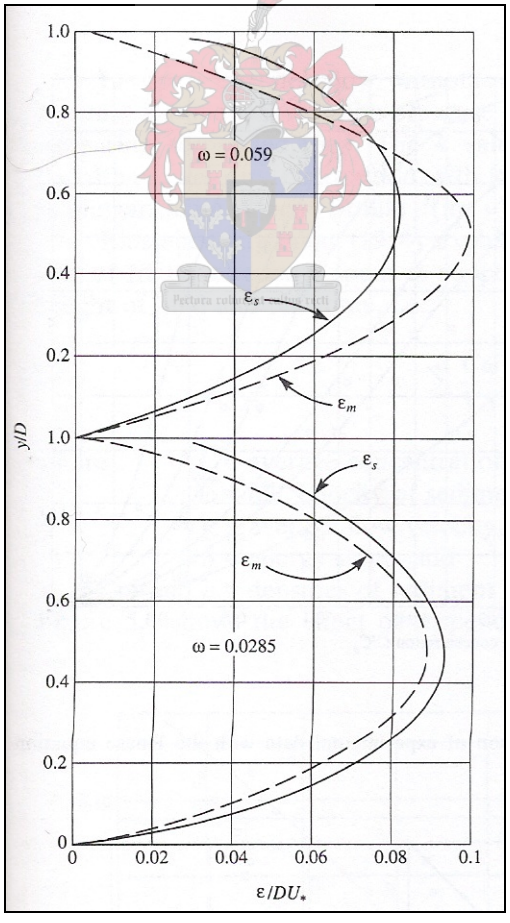

Figure 3-66: Experimental Values of Sediment and Fluid Momentum Diffusion Coefficients (Graf, 2003)

Formulas for the depth averaged value of β can be found in several texts, a few of which are given below.

van Rijn (1993) presents the following function:

$$\overline{\beta} = 1 + 2\left(\frac{\omega_s}{u_*}\right)^2 \quad for \quad 0.1 < \frac{\omega_s}{u_*} < 1 \tag{1111}$$

This equation has the consequence that $\overline{\beta}$ will always be larger than unity.

A subsequent depth averaged value determined by Cellino & Graf (2002) is

$$\overline{\beta} \approx \frac{3}{10} + \frac{3}{4} \cdot \frac{\omega_s}{u_*} \quad for \quad 0.2 < \frac{\omega_s}{u_*} < 0.6 \tag{1212}$$

A further factor ϕ (<1) can also be incorporated in β so as to include the effects of high concentrations of sediment (more than 10 kg/m^3). It expresses the retarding influence such high concentrations has on the turbulence structure of the fluid, thereby decreasing diffusivity.

3.3.1 Vertical Mixing

Mixing in the vertical direction is the reason sediment remains in suspension. The downward forces of gravity are counterbalanced not only by the upward forces of turbulence fluctuations but also the increase in concentration from the bed to the surface.

Assuming that the β coefficient is equal to unity, the sediment diffusivity can be derived by the equation for momentum diffusivity which according to Prandtl's mixing length theory is, (experimentally verified by Raudkivi, 1990)

$$\varepsilon_y = \beta \varepsilon_m = \kappa u_* H \frac{y}{H}\left(1 - \frac{y}{H}\right) \tag{1313}$$

This expression can be derived by considering that the vertical shear stress (τ) can be related to the vertical velocity gradient as follows:

$$\tau = -\rho\varepsilon_y \frac{\delta U}{\delta y} \tag{1414}$$

The velocity gradient is assumed to have a logarithmic profile where the deviation of the profile from the mean velocity is given by, (Martin, McMutcheon, 1999)

$$u(y) = \frac{u_*}{\kappa}\left(1 + \ln\frac{y}{H}\right) \tag{1515}$$

where u_* is the shear velocity, κ the von-Karman constant (equal to 0.4) and H is the depth of flow. The above equations together with a shear stress distribution (similar to that in a circular pipe)

$$\tau = \tau_0\left(1 - \frac{y}{H}\right) \tag{1616}$$

and the fact that shear velocity is related to bottom shear stress via,

$$u_*^2 = \frac{\tau_0}{\rho} \tag{1717}$$

in which

$$\tau_0 = \rho g H S_0 \tag{1818}$$

form equation (1313). Averaging it over the depth leads to the useful result that (Fisher et al, 1979)

$$D_y = 0.067 H u_* \tag{1919}$$

This means that the vertical dispersion coefficient is directly proportional to the shear velocity as well as the depth of flow.

Equation (1313) can also be used to find a concentration profile across the depth of the water body. Taking ε_y and substituting it in the vertical form of the convection-diffusion equation (i.e. assuming no movement along the transverse and longitudinal directions), then upon integration between the limits, $a<y<h$, the well known Rouse equation is obtained:

$$\frac{c}{c_a} = \left(\frac{H-y}{y} \frac{a}{H-a} \right)^Z \tag{2020}$$

where a = Reference level a small distance above the bed

c_a = Concentration at reference level a

Z = Rouse (or suspension) number = $Z = \omega_s / \beta \kappa u_*$

Figure 3-77 shows the suspended sediment concentration profiles for a set of diffusivity distributions. Distributions include *constant, linear, parabolic*, and *parabolic constant*. The figure show that even though the parabolic distribution (such as in equation (1313)) is most satisfactory in a physical sense seeing that it is based on a linear shear stress distribution and a logarithmic velocity profile, it does however have a disadvantage. A parabolic shape implies that there is zero concentration at the surface. A more realistic approach would be to use the parabolic constant distribution for vertical diffusivity: (van Rijn, 1993)

$$\begin{aligned} \beta \varepsilon_m &= \kappa u_* H \frac{y}{H}\left(1-\frac{y}{H}\right) \quad \text{for} \quad \frac{z}{H} < 0.5 \\ \beta \varepsilon_m &= 0.25 \kappa u_* H \quad \text{for} \quad \frac{z}{H} \geq 0.5 \end{aligned} \tag{2121}$$

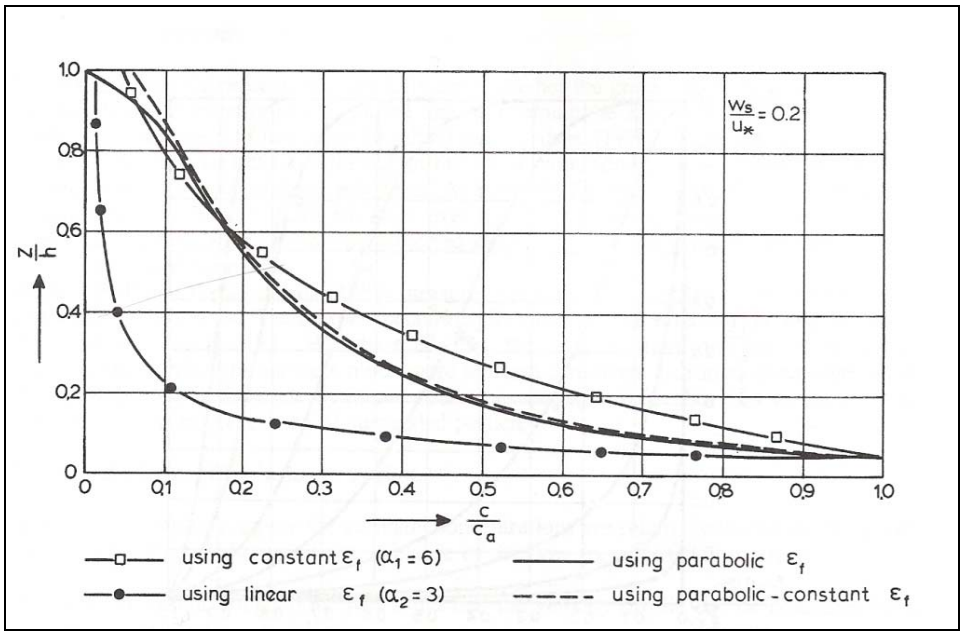

Figure 3-77: Concentration Profiles (van Rijn, 1993)

For ease of use within computer models the parabolic distribution is usually used since by examining Figure 3-77 not much accuracy is lost between the two, except at the surface of the flow.

3.3.2 Transverse Mixing

Much research has been conducted into the spreading of materials in open channels. In terms of lateral or transverse spreading there is a general custom to assume that the transverse dispersion coefficient is proportional to the product of shear velocity and average depth, i.e.

$$D_z \sim Hu_* \tag{2222}$$

or,

$$D_z = CHu_* \tag{2323}$$

In other terms,

$$C = \frac{D_z}{Hu_*} \tag{2424}$$

This dimensionless transverse dispersion proportionality constant, *C*, has been measured under various circumstances in the field as well as in the laboratory and is typically on the order of two times greater than its vertical counterpart. However, the results of these tests indicate that *C* shows considerable variations even in straight rectangular channels. Experiments have suggested that the (Darcy-Weisbach) friction factor, *f*, as well as the width-to-depth, $\frac{W}{H}$, ratio have an effect on *C*, insomuch that both together form a function describing the behaviour of *C*. The reasons cited for this is that the friction factor which is related to shear velocity via,

$$f = 8\left(\frac{u_*}{u}\right)^2 \tag{2525}$$

is the variable that generates the turbulence which causes the mixing in the first place. The second factor, the width-to-depth ratio, plays a major factor in the occurrence of secondary circulation in a channel. And seeing as secondary circulation practically amounts to transverse advection, *W/H* can have a large role to play. It should be noted that the width-to-depth ratio representing the secondary circulation in the channel would only affect C and thus D_z if the case being handled is a two or a one dimensional case. The use of the fully three dimensional equation negates the need to include the effect of secondary circulation in the transverse diffusion coefficient.

The data of several previous studies were sourced and together with a fresh set of experiments the following conclusions were made regarding the behaviour of $D_z / u_* H$ (Lau & Krishnappan, 1977).

The results indicate that as the width-to-depth ratio is increased, the spreading rate D_z decreases and vice versa. The way in which the width-to-depth ratio was changed also revealed further information. Take for example the method of keeping the depth and bed roughness constant, D_z decreased as the width was increased. This can only be the effect of secondary circulation. If both the depth and roughness are unchanged there should be no difference in the turbulence structure, therefore changes in the dispersion ratio can only be ascribed to secondary circulation. As W/H is reduced, secondary circulation increases and as a result so does D_z as is evident from Figure 3-88. The figure shows that for the same roughness type an increase in width for a constant depth there is a decrease in the transverse dispersivity.

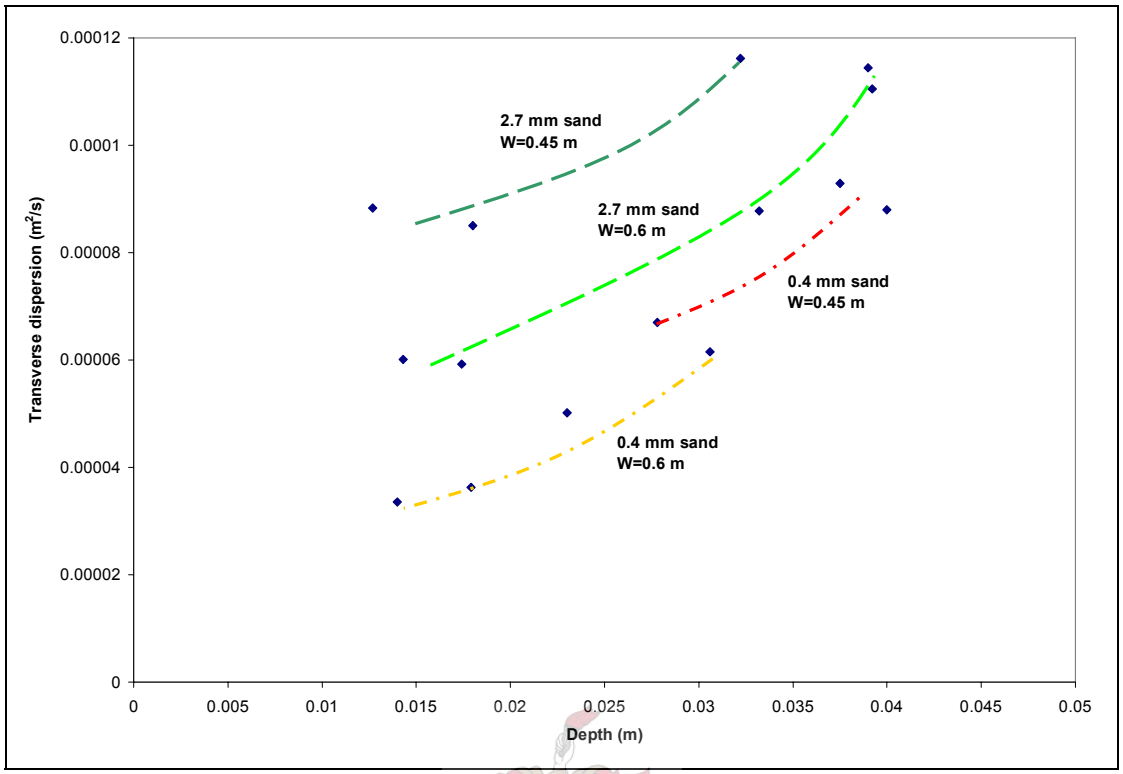

Figure 3-88: Variation of ε_z with depth for channels of different widths and roughnesses (Lau & Krishnappan, 1977)

The cause of this secondary circulation is the uneven distribution of bottom shear stress which will be further expanded upon in section 3.5.

If the W/H ratio is varied by altering the depth the changes in the transport rate are caused by both secondary circulation as well as the turbulence structure. Discovering which one of the processes is dominant can be ascertained from Figure 3-99.

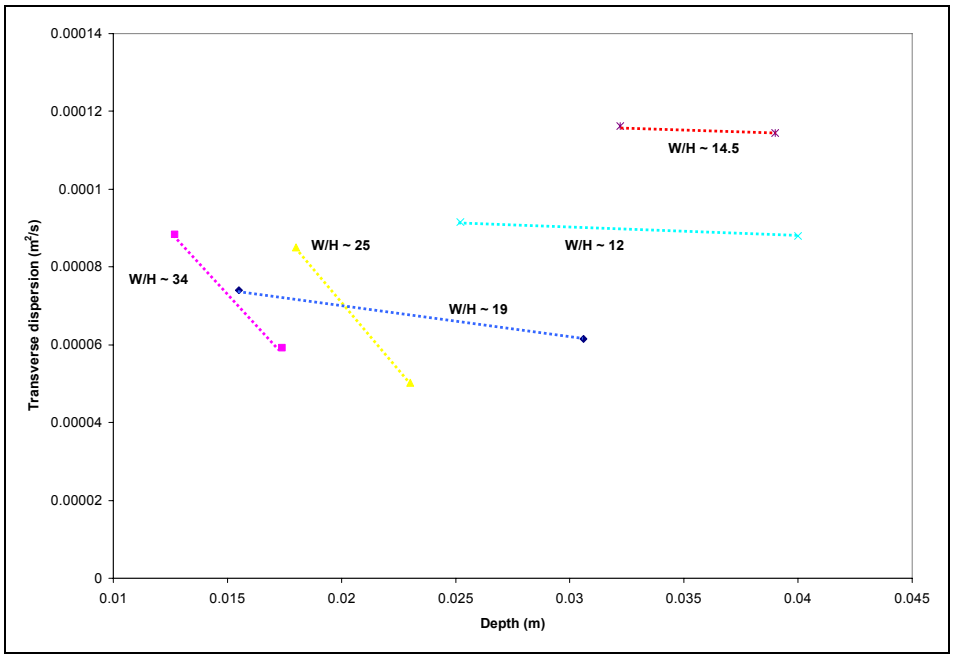

Figure 3-99: Variation of ε_z with depth at constant W/H ratios (Lau & Krishnappan, 1977)

While deeper flow would accompany a smaller bed shear and so less intense turbulence, the turbulence scale would however increase since the size of the largest eddies is proportional to the depth. The nett result of these two competing effects, as is evidenced by the all the experiments conducted as part of the study, is that as depth increases there is a decrease in D_z with all other variables kept constant. This proves that the increase in turbulence scale is not as effective as is the reduction in turbulence intensity.

But as mentioned previously, the lab tests show an increase in D_z with depth. This can therefore be attributed to the increase in secondary circulation which more than compensated for the decrease in diffusive transport. This result has the far reaching implication that it is secondary currents and not turbulence which dominate transverse sediment transport (Lau & Krishnappan, 1977).

The effect of the friction factor was also examined by Lau & Krishnappan (1977). It was determined that in most cases there is an increase in D_z with an increase in roughness. Though this may seem intuitive it is not true of all cases. This phenomenon can be explained by considering that at small width-to-depth ratios the transport due to secondary circulation is the dominant process over that of turbulence. Therefore the transport rates would not be much affected by whether or not the flow is over a smooth or rough boundary. And since the rougher

flow has a higher value of shear velocity, u_*, it is entirely possible for the transport rate (equation (2424)) to be smaller at a higher friction factor as can be seen from the line representing the friction factor of 0.07 in Figure 3-1010.

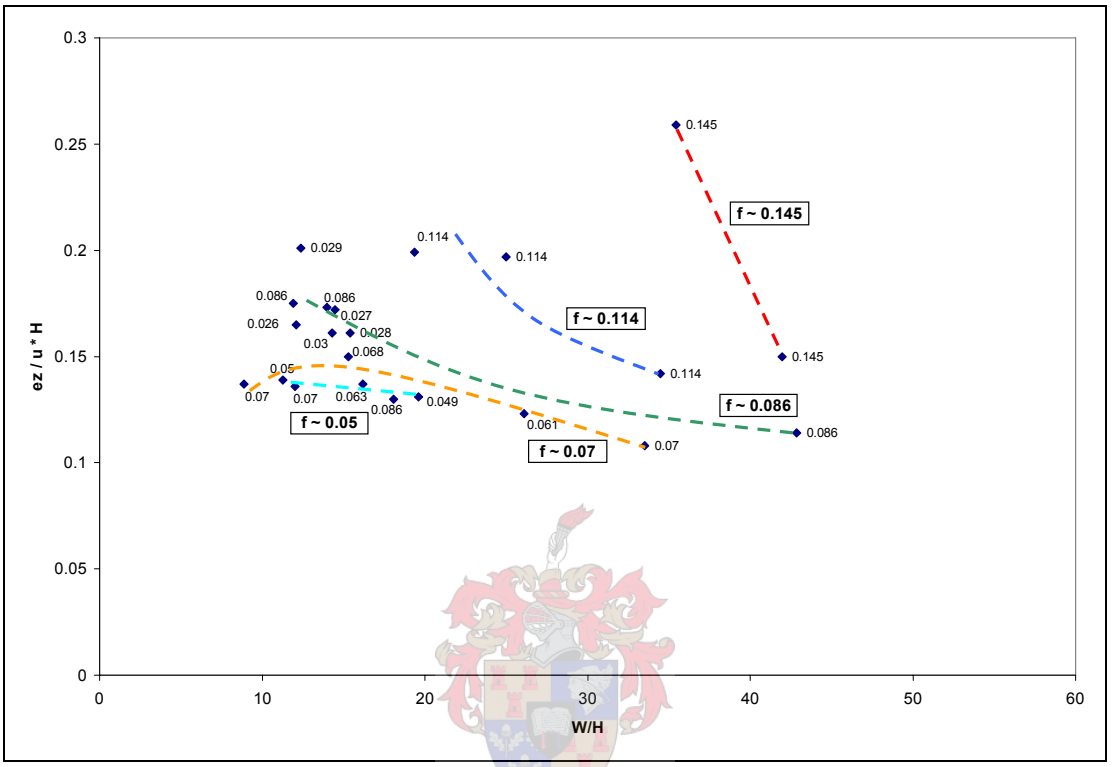

Figure 3-1010: Variation of the *C* factor with W/H and *f* (Lau & Krishnappan, 1977)

From the above discussion it is clear that it is difficult to reliably describe the behaviour of the transverse dispersion in terms of u_* and H. The reason is that these two factors predominantly relate to turbulence which has been proven not to be the dominant role player. Lau & Krishnappan (1977) have proposed alternative factors which could better represent D_z. Although a few were presented the one which has the most practical value is that instead of

$$C = \frac{D_z}{Hu_*} \rightarrow C = \frac{D_z}{Wu_*} \tag{2626}$$

In other words, transverse transport is no longer so much dependant on depth (*H*) but rather on width (w). A plot of the data is shown in Figure 3-1111 from which it is evident that all the data collapses onto one curve. Even though the effect of friction is still evident it has far less influence than the previously used factors.

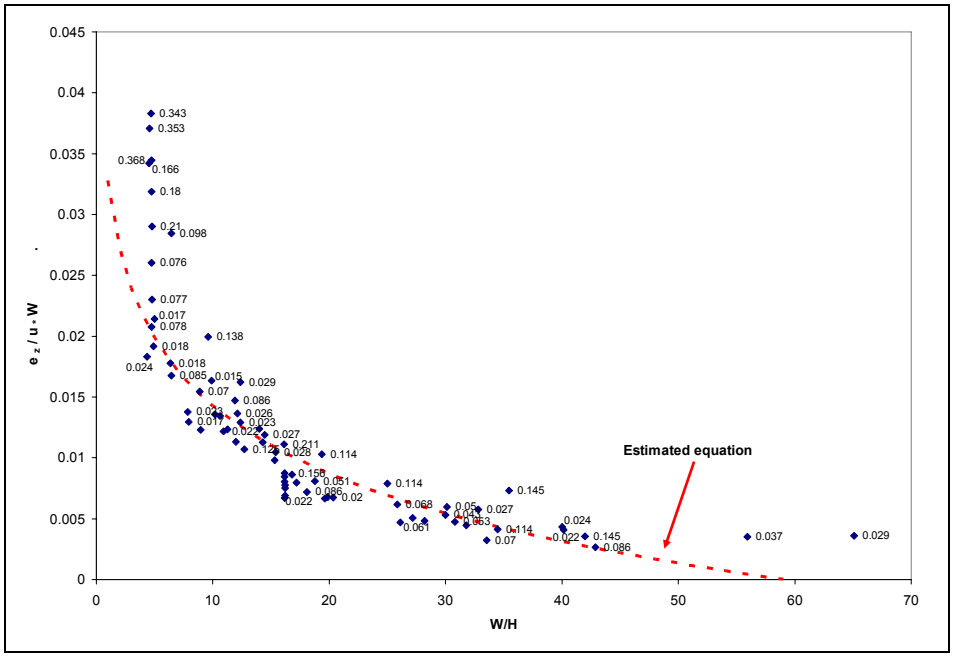

Figure 3-1111: Variation of the *C* factor with W/H and *f* (Lau & Krishnappan, 1977)

The data in the figure was used to estimate a curve, of which the formula is presented below (James, 1985):

$$\frac{D_z}{Wu_*} = 0.001\left(32.77 - 8.03\ln\left(\frac{W}{H}\right)\right) \quad for \quad 5 < \frac{W}{H} < 45 \qquad (2727)$$

It is clear from the figure that this formula is not valid for the entire range of $\frac{W}{H}$ values but only for a set of limits. It is however noted that the ratio of most natural rivers where suspended sediment is of concern do fall within these bounds.

3.3.3 Longitudinal Mixing

Diffusive mixing in the longitudinal direction can be regarded as being of the same order as that for transverse diffusive mixing, as there is no fundamental difference between the two. When it comes to dispersion however the processes are somewhat different as was mentioned in the beginning of this chapter (Fisher et al, 1979). Therefore, in practical terms, there is little interest in the longitudinal diffusivity but rather in the much larger diffusion coefficient. Other reasons for this apparent lack of data probably come from the difficulty in measuring longitudinal diffusion in dye

spreading experiments and having to separate the effects of longitudinal turbulence fluctuations caused by shear flow from the diffusion caused by turbulence.

Elder (1959) determined that

$$D_x = 5.93 H u_* \tag{2828}$$

However, Fisher et al (1979) indicated that in real streams the dispersion is almost always greater than this value and instead proposed:

$$D_x = 0.011 \frac{W^2 U^2}{H u_*} \tag{2929}$$

where W is the mean width, U the mean stream velocity, H the mean stream depth and u_* the shear velocity.

3.4 Particle Settling

Once a particle has become suspended its behaviour within the flow will depend on its settling velocity and the flow conditions. The particle will then fall towards the bed under the influence of gravity or be held in suspension when the vertical velocity component of the fluid's turbulence is greater than the particle's settling velocity.

3.4.1 Settling Velocity

As a particle falls through a liquid it accelerates until it reaches a terminal velocity, termed its settling velocity, ω_s. At this point the forces of gravity are counterbalanced by the drag forces of the fluid on the particle. For a perfect sphere the fluid drag force equals (van Rijn, 1993)

$$F_d = \frac{1}{2}\left(C_D \rho \omega_s^{\,2}\right) \cdot \frac{1}{4}\left(\pi d^2\right) \tag{3030}$$

and the gravity force,

$$F_g = \frac{1}{6}\left(\rho_s - \rho\right) g d^3 \tag{3131}$$

which gives

$$\omega_s = \sqrt{\frac{4(s-1)gd}{3C_D}} \tag{3232}$$

where ω_s = terminal fall velocity in a still fluid
d = sphere particle diameter
s = specific gravity (2.65)
C_D = drag coefficient
g = acceleration due to gravity

The drag coefficient is a function of the Reynolds number ($\mathrm{Re} = \omega_s d/\nu$) and a certain shape factor. Within the Stokes region (Re < 1) the drag coefficient is equal to 24/Re, yielding:

$$\omega_s = \frac{(s-1)gd^2}{18\nu} \tag{3333}$$

Outside the Stokes range however the drag coefficient becomes difficult to define in simple terms, but it generally decreases until it reaches a constant value.

For non-spherical particles such as natural sediment the terminal fall velocities can be calculated from the following formulas (van Rijn, 1993):

$$\omega_s = \frac{(s-1)gd^2}{18\nu} \quad for \quad 1 < d \le 100\mu m \tag{3434}$$

$$\omega_s = \frac{10\nu}{d}\left[\left(1+\frac{0.01(s-1)gd^3}{\nu^2}\right)-1\right] \quad for \quad 100 < d < 1000\mu m \tag{3535}$$

$$\omega_s = 1.1\sqrt{(s-1)gd} \quad for \quad d \ge 1000\mu m \tag{3636}$$

For the purposes of investigating suspended sediment equation (3434) is the most relevant. As can be seen it is the same equation as for the spherical particle. The reason for this is that the shape and roughness of the particle only becomes apparent at larger sizes. Figure 3-1212 presents the above equations graphically.

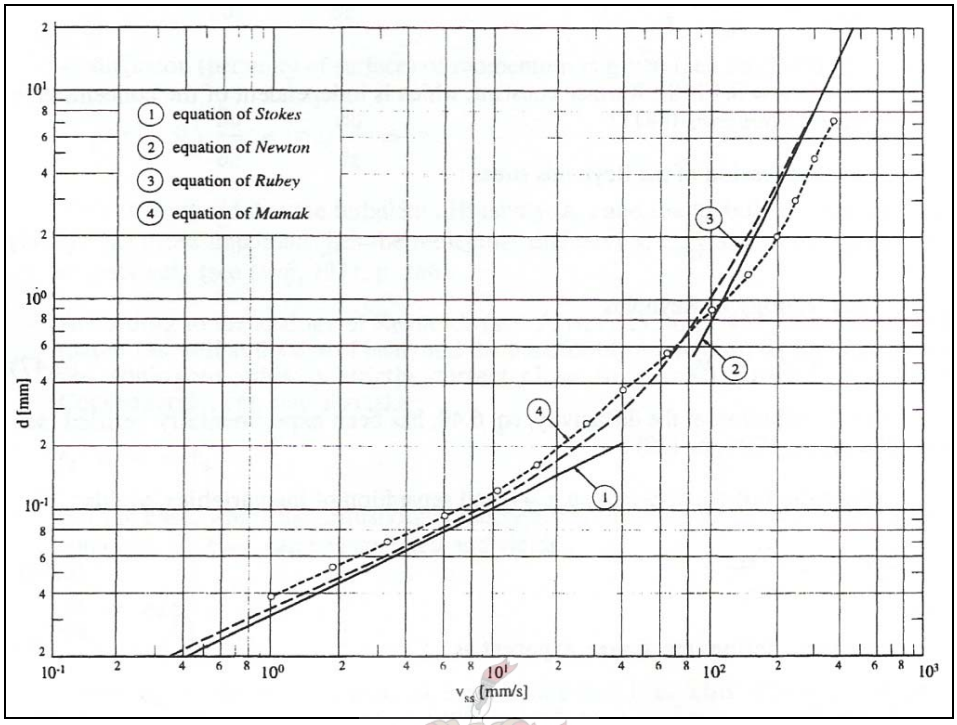

Figure 3-1212: Settling Velocity as a Function of Particle Diameter (Graf, 2003)

The settling velocity determined for clear water at a certain temperature can then be affected by other factors not the least of which include the presence of neighbouring particles which reduce its speed. However, for this effect to have a significant influence concentrations need to be high and as such the fall velocity in clear water is usually utilised.

3.4.2 Deposition

One further factor which can be important in the modelling of water quality is the assumption that the solute is not a reactant in any chemical or biological processes in the water volume. As such, no allowance for the decay of the suspended sediment is made in equation (66), i.e. the sediment is assumed to be passive. There is however another very important omission from the above the equation. When modelling suspended sediment behaviour in a mathematical model it is of key importance to include a source-sink term. As such the general equation becomes

$$\frac{\delta C}{\delta t} + \sum_{i=1}^{3} u_i \frac{\delta C}{\delta x_i} - \sum_{i=1}^{3} \frac{\delta}{\delta x_i}\left(\varepsilon_i \frac{\delta C}{\delta x_i}\right) = S \qquad (3737)$$

The source term, *S*, represents the local balance of suspension and deposition. Various modellers represent this term in different ways, but in general the *S* term is proportional to the product of the settling velocity and a certain reference suspended sediment concentration.

van Rijn (1993) describes the deposition rate as

$$S = \alpha C \omega_s \tag{3838}$$

in which C = sediment concentration near the bed

ω_s = (concentration dependent) settling velocity in still water

α = coefficient (≤ 1)

The α term can be thought of as a reduction factor of the settling velocity caused by turbulence and the vertical sediment concentration gradients, which yield an upward flux of sediment. It can be related to the bed shear stress as follows:

$$\alpha = 1 - \frac{\tau_b}{\tau_{d,dep}} \tag{3939}$$

where τ_b is the applied shear bed stress and $\tau_{b,dep}$ is the critical bed shear stress required for full deposition to occur. This critical bed shear stress, $\tau_{b,dep}$, is however a term describing a highly stochastic process in that at that bed shear stress some particles may settle and others may not. The value only describes a rough average of when settling is taking place. Considering this, the ratio $\frac{\tau_b}{\tau_{d,dep}}$ can be replaced by a probability of deposition, *p*.

This probability would then depend on the factors such as the characteristics of the bed surface, the particles themselves as well as the flow. For granular beds the entrainment probability defined by Engelund & Fredsøe (1976) is

$$p = 1 - \left(1 + \left(\frac{K\pi/6}{\theta - \theta_{crs}}\right)^4\right)^{-1/4} \tag{4040}$$

K is a friction coefficient and θ is given by the more general version of equation (22).

The technical documentation for a two dimensional, depth averaged, hydrodynamic/morphologic model environment, namely CCHE2D (Jia & Wang, 2001) proposes a similar formula to equation (3838). The local depth averaged balance between sedimentation and suspension can be represented by:

$$S = -\frac{1}{H}\left(\omega_s C_a + \beta v_t \left.\frac{\delta C}{\delta y}\right|_a\right) \tag{4141}$$

in which C_a = sediment concentration near the bed surface with reference height a

β = coefficient used to convert the diffusivity of turbulent eddies to that of sediment

v_t = eddy diffusion coefficient

H = depth

Equation (4141) can then be reworked to form (Jia & Wang, 2001),

$$S = -\frac{\omega_s}{HF}\left(C - C_e\right) \tag{4242}$$

where

$$F = \frac{\left(\frac{a}{H}\right)^{z'} - \left(\frac{a}{H}\right)^{1.2}}{\left(1-\frac{a}{H}\right)^{z'}\left(1.2 - z'\right)} \tag{4343}$$

in which

$$z' = z + \psi \tag{4444}$$

$$z = \frac{\omega_s}{\beta \kappa u_*} \tag{4545}$$

$$\psi = 2.5\left(\frac{\omega_s}{u_*}\right)^{0.8}\left(\frac{C_a}{C_0}\right)^{0.4} \tag{4646}$$

and in this instance

$$\beta = 1 + 2\left(\frac{\omega_s}{u_*}\right)^2 \tag{4747}$$

C = depth averaged concentration

C_e = depth averaged concentration for the equilibrium condition

κ = von Karman constant (0.4)

u_* = overall bed shear velocity

C_0 = maximum concentration (0.65)

Equation (4242) and its parameters are largely empirical. F, called the shape factor is a dimensionless factor incorporating influences such as the vertical concentration profile (z) and stratification of suspended sediment (ψ) (van Rijn, 1993). The above equation is however useful because of its ability to simulate unsteady, non-equilibrium processes of sediment transport.

3.5 Boundary Shear Stress

As shown in the previous chapter formulations regarding dispersion are usually related to shear velocity (u_*) and thus to bottom shear stress (τ_0) seeing as it is these factors which control shear. They are related to each other via:

$$u_*^2 = \frac{\tau_0}{\rho} \tag{4848}$$

And for steady uniform flow in a wide channel,

$$\tau_0 = \rho g H S_0 \tag{4949}$$

where g is gravitational acceleration, ρ fluid density, H mean depth and S_0 the bottom slope. Together these form

$$u_* = \sqrt{gHS_0} \tag{5050}$$

The above equation is however only applicable in undisturbed flow conditions i.e. far away from any factors which may influence the flow regime. Such factors usually include vertical flow boundaries such as shear layers or vertical barriers.

What is most relevant to this thesis is that the presence of a shear layer between the main channel and the floodplain causes both an increase in shear flow over the floodplain and a decrease in shear flow in the main channel. What this means is that if the floodplain was not present then the flow in the main channel would be faster than if it was present. The converse can be said for flow on the floodplain.

What happens on the floodplain is that the vertical shear boundary increases the flow up to a certain transverse distance, beyond which the boundary shear stress may be regarded as being equal to that given in equation (4949) (see Figure 3-1313 and Figure 3-1414). The exact length of this distance is not required seeing as it has been built into the equation below. As *z*, the transverse distance from the shear boundary tends to infinity the bed shear stress tends toward its undisturbed value.

As is evident from Figure 3-1313-b the velocities on both the floodplain and the main channel tend toward the same value as they approach the shear layer interface, namely U'_m. The same can however not be said of the bed shear stress profile. Figure 3-1313-c shows a very clear jump in bed shear at the main channel – floodplain interface. Though this may seem aberrant, there is no reason to expect the two bed shear values to tend toward the same value. The reason for this is that the bed shear being measured in Figure 3-1313 may be measured at the same place horizontally but not vertically. The bed shear stress at z'=0 in the main channel is lower than its floodplain counterpart simply because of the solid side wall which induces a far larger frictional force on the main channel flow than does the shear layer on the floodplain flow.

An actual experimentally determined bed shear stress profile can be seen in Figure 3-1414 (Rajaratnam & Ahmadi, 1981). It shows that the bed shear stress on the floodplain was increased due to the interface and that when only considering the horizontal surfaces there is indeed a jump in the bed shear stress from the main channel to the floodplain. The figure also shows that this is not a real jump as such since the boundary shear stress profile of the right bank bridges the difference between the two.

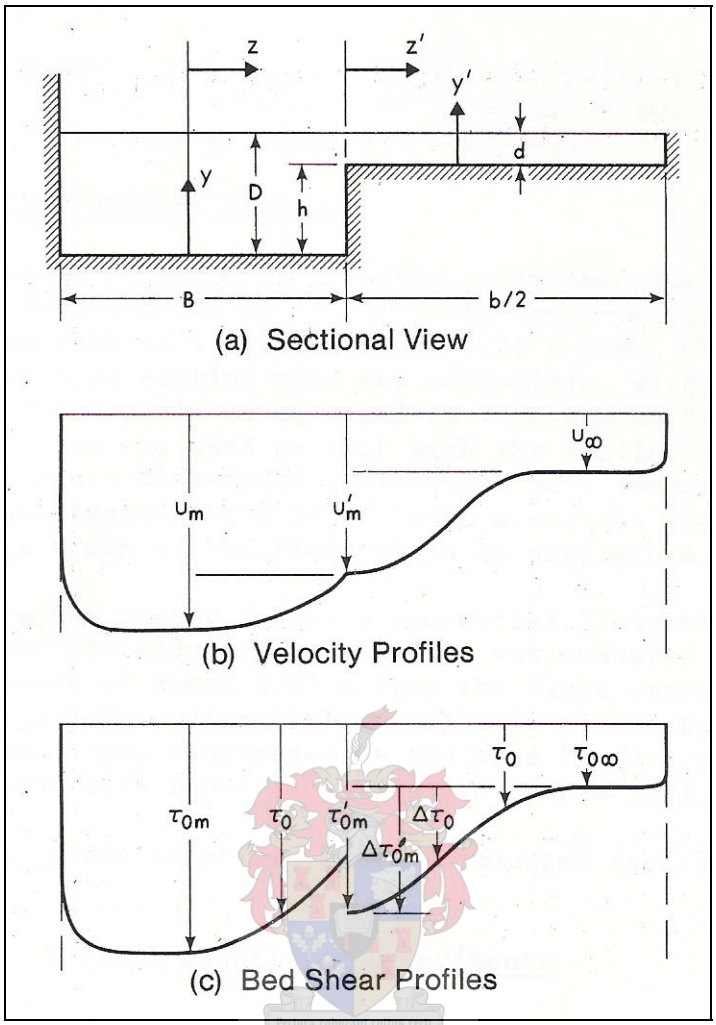

Figure 3-1313: Velocity and Bed Shear Profiles (Ahmadi & Rajaratnam, 1981)

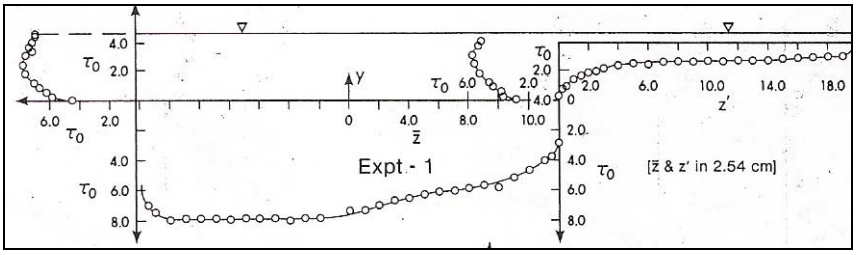

Figure 3-1414: Experimental Distribution of Boundary Shear Stress (Ahmadi & Rajaratnam, 1981)

Further experimental investigations into the variation of shear flow in a compound section conducted by Rajaratnam & Ahmadi (1981) resulted in the description of bed shear stress on the floodplain depicted in Figure 3-1515 and equation (51)

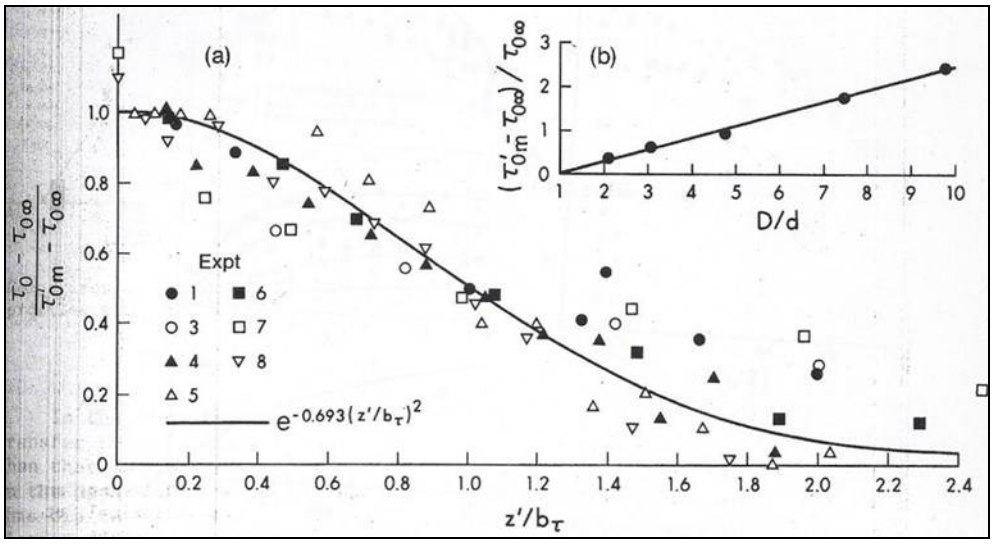

Figure 3-1515: Similarity of the Excess Bed Shear Stress on the Floodplain (Ahmadi & Rajaratnam, 1981)

$$\frac{\tau_0 - \tau_\infty}{\tau_0' - \tau_\infty} = e^{-0.693\left(z'/b\right)^2} \tag{5151}$$

which can be rewritten as

$$\tau_0 = \tau_\infty + \left(\tau_0' - \tau_\infty\right) e^{-0.693\left(z'/b\right)^2} \tag{5252}$$

where the boundary shear stress at the junction is

$$\tau_0' = \tau_\infty \left(1 + 0.24\left(\frac{H_C}{H_P} - 1\right)\right) \tag{5353}$$

and the length scale factor

$$b = 0.64 H_P \left(\frac{H_C}{H_P} - 1\right) \tag{5454}$$

in which τ_0 = the disturbed distribution of bed shear stress

τ_∞ = the undisturbed bed shear stress on the floodplain given by equation (4949)

z' = the distance over the floodplain measured from the shear boundary interface

b = a length scale

$\tau_0^{'}$ = the bed shear stress at the interface

H_P = the depth on the floodplain

H_C = the depth in the main channel

A relationship for the decrease in bed shear stress in the main channel was also investigated and resulted in Figure 3-1616 below. It shows that the bed shear stress is strongly related to the ratio of the depth of flow in the main channel to that on the floodplain. It also indicates that for any given ratio the difference between the undisturbed bed shear stress in the main channel, τ_{0m}, and the one at the shear boundary (the difference being represented by $\Delta\tau_0$) reaches a maximum value. Take for example a ratio of $\frac{D}{d}=10$, from Figure 3-1616-c it is evident that the maximum change from the undisturbed value is roughly 20%.

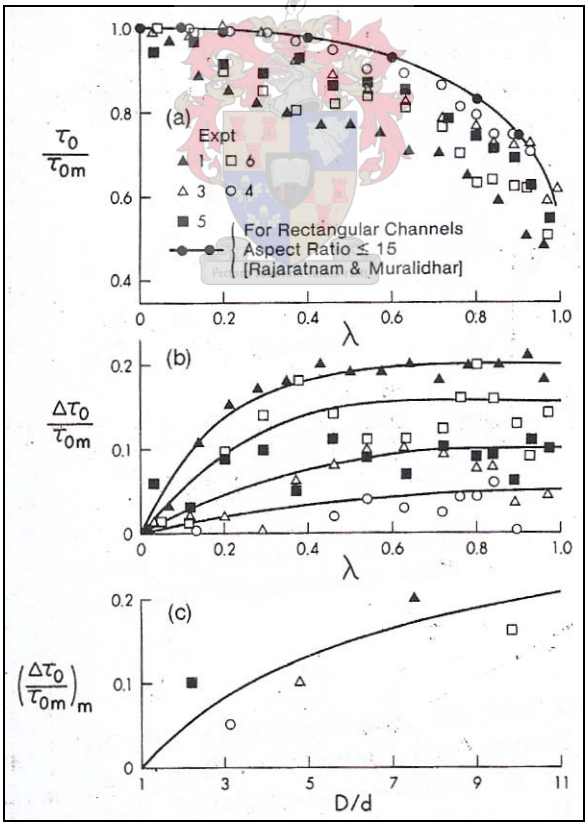

Figure 3-1616: Bed Shear Stress in the Main Channel, *λ=z/(b/2)* (Ahmadi & Rajaratnam, 1981)

Rajaratnam & Ahmadi (1981) also determined that the vertical velocity distribution was logarithmic at all locations even in the shear boundary layer if the above equations are used to determine u_*. It is therefore evident that the equation for the vertical mixing coefficient, derived based on this logarithmic distribution, is also applicable within the shear boundary layer between the main channel and the floodplain.

3.6 Transport Across Shear Boundary

As stated in the previous section, the vertical mixing coefficients derived in section 3.3 are valid everywhere in the river, including the shear boundary to the floodplain. The transverse equations however need to be revisited. Under normal uniform flow there is usually only a large velocity gradient in the vertical direction. At a vertical shear boundary however there is also a very apparent velocity gradient in the transverse direction. As such the normal transverse mixing coefficients do not apply here. Rajaratnam & Ahmadi (1981) have shown that within the "interaction zone" the transverse velocity distribution is dominated by the bed shear stress. They subsequently proposed a formula estimating the eddy viscosity which by assuming β is equal to unity can also describe transverse diffusivity:

$$\frac{D_z}{(U_C - U_P)} = \frac{0.3\left(\frac{H_C}{H_P} - 1\right)^3}{\left(\frac{U_C - U_P}{u_{*\infty}}\right)^2} \cdot A(\eta) \qquad (5555)$$

in which U_C = the undisturbed channel flow velocity (given by Manning)

U_P = the undisturbed floodplain flow velocity (given by Manning)

$u_{*\infty}$ = the undisturbed shear velocity

η = z/b see equation (5454)

The function $A(\eta)$ can be approximated by equation (56) and is depicted in Figure 3-1717

$$\begin{aligned} A &= -31.5\eta + 11.45 \quad for \quad \eta < 0.3 \\ A &= -2.37\eta + 2.71 \quad for \quad \eta > 0.3 \end{aligned} \qquad (5656)$$

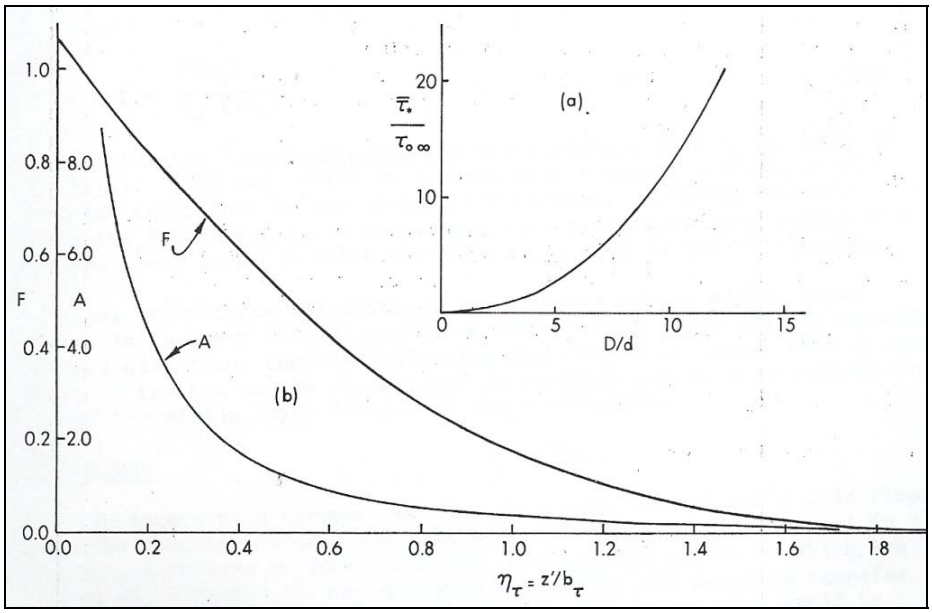

Figure 3-1717: Behaviour of *A(η)* Function (Ahmadi & Rajaratnam, 1981)

The remainder of this section will now describe some of the aspects concerning transport across this boundary which originate both from fieldwork as well as mathematical models on compound channels.

As was mentioned previously the process of transverse transport of solute is dominated by secondary currents and so being able to predict their behaviour can result in a good approximation of the movement of the suspended sediment they carry.

Lin & Shiono (1995) set up a hydraulics model which aimed to determine the effect of using a non-linear *k-ε* turbulence model instead of the linear one when considering the solute transport in a compound channel. Figure 3-1818 shows that the typical secondary flow patterns for a compound channel are well predicted. There is a strong inclined secondary current at the main channel – floodplain (M/F) junction as well as two twin vortices on each side of the junction. Besides the main channel and floodplain vortices there is also a third so-called free surface vortex on the other side of the main channel. This vortex would obviously not occur very often under natural circumstances since floodplains usually occur in symmetrical pairs.

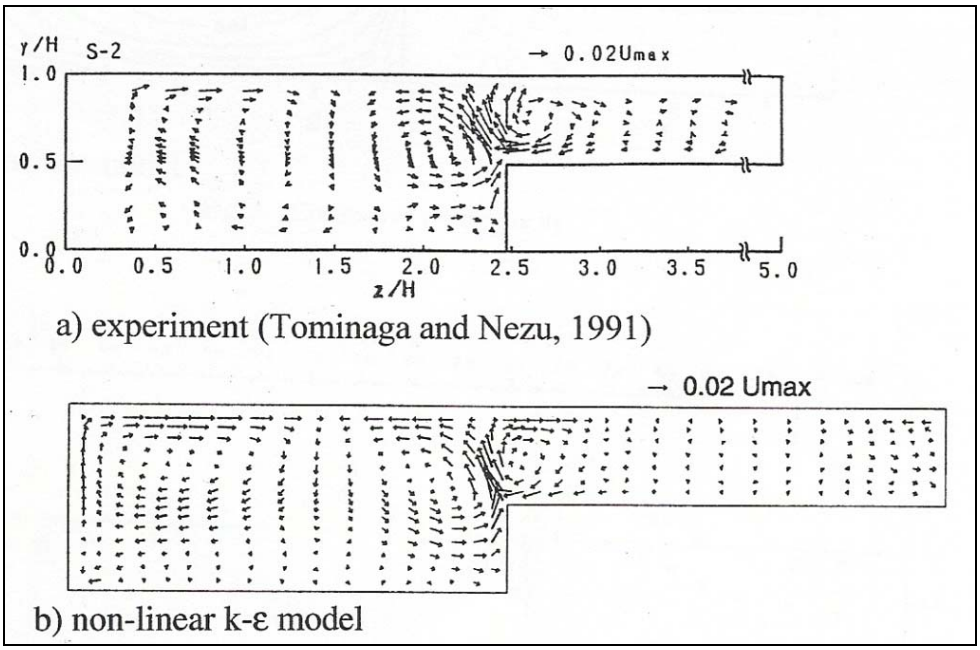

Figure 3-1818: Predicted and Measured Secondary Flow (Lin & Shiono, 1995)

The non-linear model was also capable of more accurately predicting the streamwise velocity which shows a trend of retarding somewhat in the region of the M/F junction (See Figure 3-1919). The significant effect that the transverse secondary currents have on the streamwise velocity is evident. Also modelled was the eddy viscosity from which diffusivity can be derived (see Figure 3-2020). The junction between the floodplain and main channel shows a distinct drop in diffusivity but with a peak right alongside it.

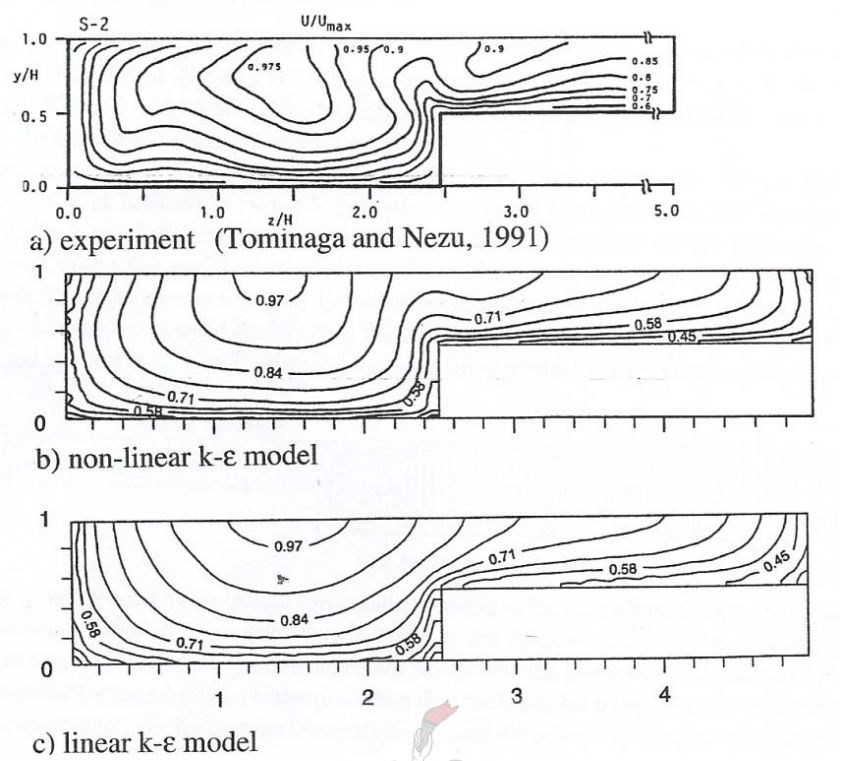

Figure 3-1919: Contours of Streamwise Velocity (Lin & Shiono, 1995)

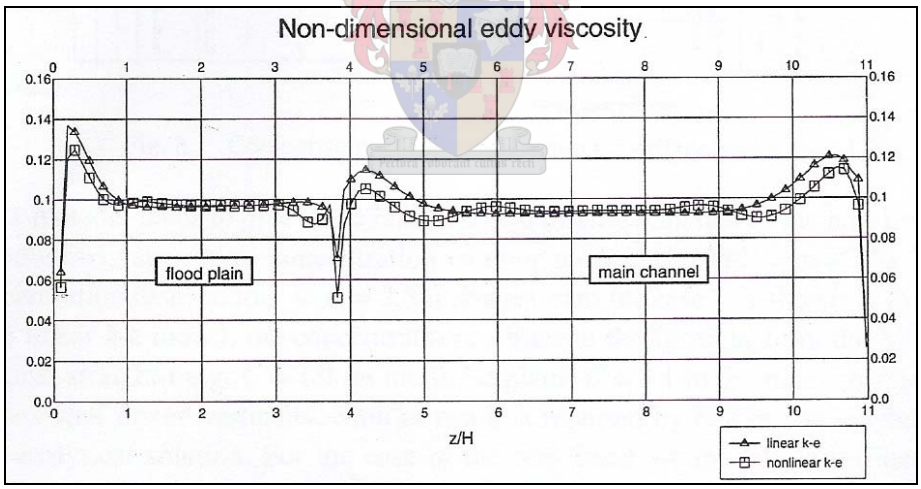

Figure 3-2020: Depth Averaged Non-Dimensional Eddy Viscosity (Lin & Shiono, 1995)

What effect this behaviour has on solute transport is clearly demonstrated by Figure 3-2121 and Figure 3-2222. They show that when a solute source is either placed on the floodplain or the main channel the consequence of it travelling across the M/F junction is that initially higher concentrations will be observed at the surface forming a ‘concave’ concentration distribution. Given time and distance this will then reach the equilibrium vertical concentration profile. A consequence of this is that the location where maximum deposition of suspended sediment

occurs will not be right at the interface as expected (because this is where the highest concentrations are). The secondary currents, which are stronger near the interface zone, carry any sediment that wants to settle close to the main channel back to the interface and up to the surface. From here it is then carried further onto the floodplain and subsequently settles a distance away from the M/F interface.

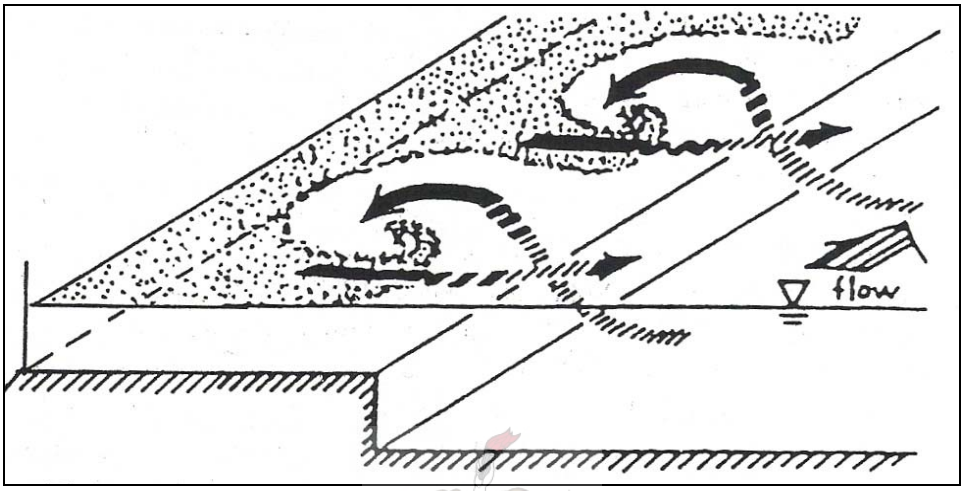

Figure 3-2121: Large Vortex Motion at the Free Surface (Lin & Shiono, 1995)

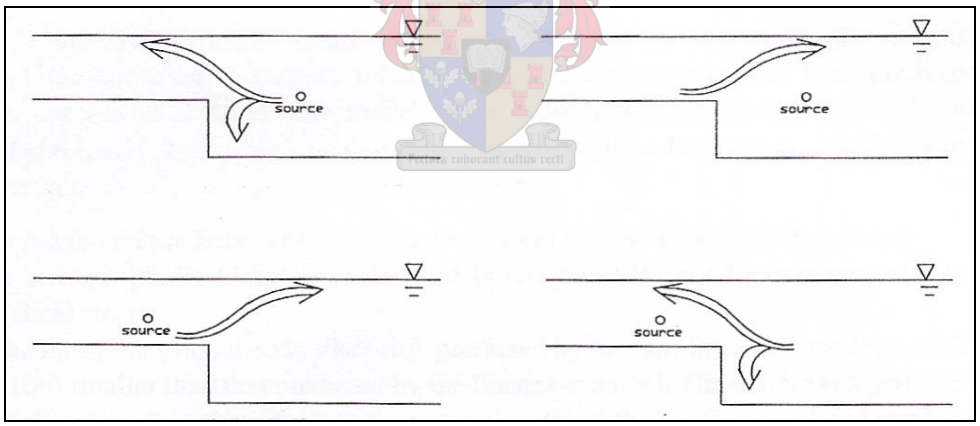

Figure 3-2222: Flow Patterns Resulting from Secondary Flow (Lin & Shiono, 1995)

A further conclusion drawn by the research paper was that in general it was observed that movement of solute was either from the floodplain to the main channel or visa versa and not both. This stands to reason seeing that suspended sediment would naturally travel from places of high concentration near the source to places of lower concentrations. The phenomenon is however not mutually exclusive therefore it is wholly possible for sediment to travel from the floodplain into the main channel and then back onto the floodplain. The total percentage of the sediment making this journey can nonetheless be expected to be small.

Another study (Naot et al, 1993) investigated the influence of various factors on the hydrodynamics of compound channels. The factors included the depth, width and floodplain roughness. For a smooth floodplain an increase in depth causes a drift of the maximum streamwise velocity towards the surface. For large floodplain depths a second zone of maximum velocities forms over the floodplain indicating that the entire cross section is tending toward acting like a single channel instead of a compound one.

With an increase in depth there is also an increase in the intensity of the vortex on the floodplain and a decrease for the vortex in the main channel. Thus it is evident that the increase in streamwise velocity on the floodplain is caused as a result of the increase in the transfer of momentum from the main channel to the floodplain which then also increases the intensity of the vortex there. Both of these effects can be seen in Figure 3-2323.

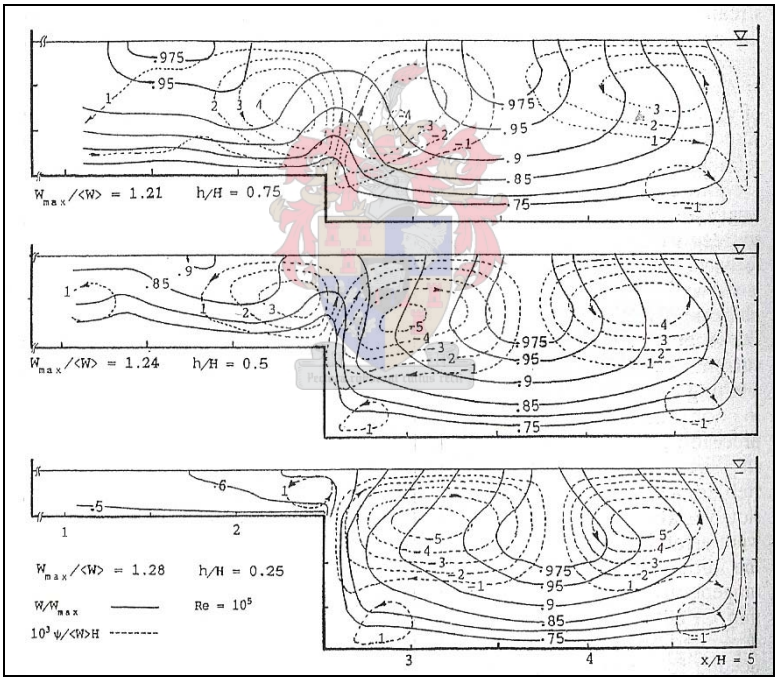

Figure 3-2323: Streamwise Velocity Contours and Lateral Streamlines for an Asymmetric Smooth Channel (Naot et al, 1993)

Figure 3-2424 also shows that as the depth increases (from h/H = 0.25 to h/H = 0.75) the local shear stresses start equalising. An increase in shear stress is observed on the floodplain and a decrease in the main channel.

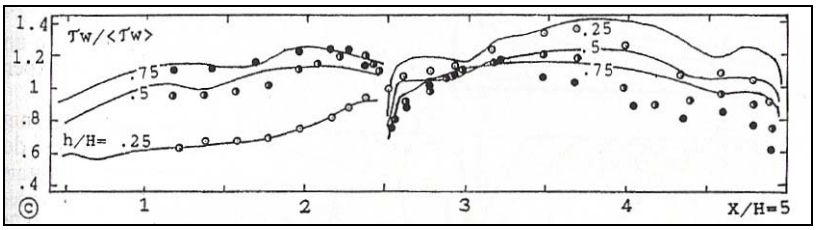

Figure 3-2424: Change of Bed Shear Stress with Depth (Naot et al, 1993)

The above results are however applicable for an asymmetric channel with a relatively narrow main channel. Increasing the width of the main channel thus places it more on par with a natural symmetric channel insomuch that the effect of the far main channel wall is almost entirely removed. The result of this is that the same trends are witnessed but that their intensity is of a lesser degree. Both the increase in streamwise floodplain velocity and floodplain vorticity is less pronounced. Comparing Figure 3-2323 to Figure 3-2525 shows this clearly.

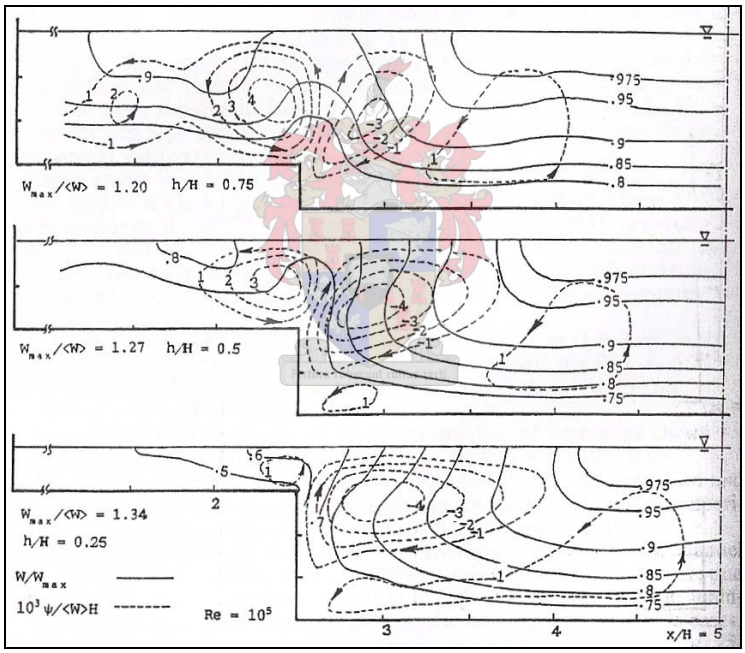

Figure 3-2525: Streamwise Velocity Contours and Lateral Streamlines for a Symmetric Wide Channel (Naot et al, 1993)

An increase in the floodplain roughness for the case where h/H = 0.5, enhances an increase in the intensity of the floodplain vortex but a decrease in the streamwise velocity there. Floodplain roughness thereby increases the transverse dispersion coefficients as was evidenced in section 3.3.2. (see Figure 3-2626)

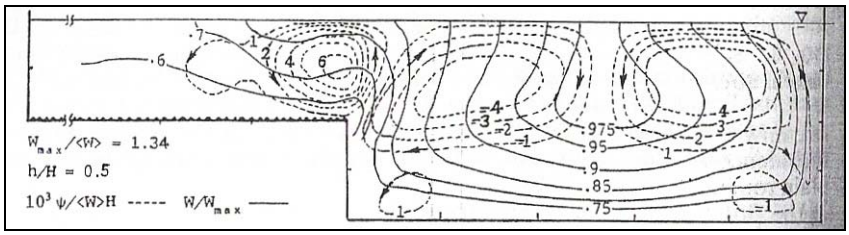

Figure 3-2626: Streamwise Velocity Contours and Lateral Streamlines for a Rough Floodplain (Naot et al, 1993)

CHAPTER 4

4 MODELLING

4.1 Physical Modelling

A physical laboratory model was set up for this thesis for the purpose of investigating and subsequently calibrating a series of computer simulations. The basic premise consisted of a straight rectangular channel alongside a wide floodplain. Sediment would be inserted in the main channel only and would then be allowed to spread across the shear boundary onto the floodplain. Suspended sediment samples would be taken at fixed control points to assess the distribution of the sediment under various flow conditions.

The experiment was conducted at the Hydraulics Laboratory of the Department of Civil Engineering, University of Stellenbosch. A two meter wide flume, fourteen meters long, was used to model the dispersion phenomena. The flume, shown below in Figure 4-11 and Figure 4-22, was partially filled with bricks to represent the floodplain, the channel on the left represents the channel.

The asymmetrical main channel was built with a width of 0.3 m which gives the remainder of the 2 m over to the floodplain. This results in a floodplain to channel width ratio of around 5.7. In general floodplains are not so flat but the model was aimed at determining the behaviour under ideal conditions. Because bricks were used as the floodplain, due to the ease and speed at which the model could be set up and adjusted if need be, the main channel had a depth of 0.11 m below the floodplain.

Since this depth was fixed the range of water levels that could be used during the tests was limited. The reason for this is that if the water level was made too deep then the influence zone depicted in Figure 2-22 would stretch out to include the wall of the flume which would then in turn have an effect on the results.

Figure 4-11: View of flume looking upstream

Figure 4-22: Laboratory flume

A basic longitudinal schematic of the experiment setup can be seen in Figure 4-33. On the upstream side a large pipe delivers the discharge from a constant head tank which is then measured by means of a V-weir before being released into the flume. After the flow has been stabilised by a wall of hollow bricks the sediment inflow is added into the channel part of the flow only. This sediment laden flow quickly mixes with the cleaner water and then moves into the main channel to subsequently disperse onto the floodplain. At the downstream end of the flume the water sediment mixture flows over a horizontal pivot sluice which controls the water level in the flume itself.

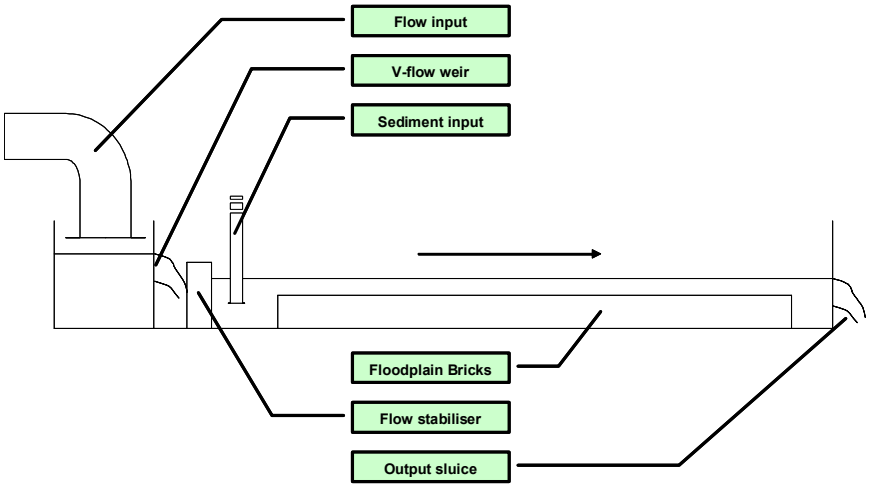

Figure 4-33: Schematic of experiment

The way in which the sediment is entrained in the flow is by pre-preparing a solution of sediment in a container and then pumping it at a desired rate into the main channel. The container used had a volume of 1.2 m^3 and for every experiment 6.6 kg of Western Ball Clay (median size of 0.14 μm, see Appendix) was added to it. The sediment was then mixed and kept in suspension using the influx of air through a tube at the bottom of the container. The resulting bubbles were sufficient in preventing the sediment from depositing. Figure 4-44 shows the container used to mix the sediment with the flume out of sight on the right.

Figure 4-44: Sediment container

Due to the fact that only 1200 liters of solution could be prepared at any one experiment it was the limiting factor in terms of the length of time that a test could be run. At the chosen rate of transfer roughly twenty minutes were available for each test. Therefore long term sediment movements could not be determined. Other studies have used a conveyor belt to directly deposit the dry sediment into the flow, which can be constantly reloaded. The problem with such a system is that it is difficult to deliver a constant concentration of suspended sediment. There are also concerns with the mixing of the dry sediment in the flow. Another problem resulting from the very fine sediment used is that any disturbances such as movement or wind easily cause it to blow away.

Once the sediment solution was mixed in the main channel flow and once it passed the barrier placed between the main channel and floodplain it began spreading onto the floodplain. There the concentration distributions at four transverse cross-sections were sampled. The sampling streamwise distances were 1, 3, 6 and 9 meters downstream of the point where sediment started spreading. In the transverse direction samples were taken in the middle of the channel and then 0.05, 0.15, 0.25, 0.45, 0.75, 1.15 and 1.65 meters from the edge of the floodplain, as can be seen in Figure 4-55.

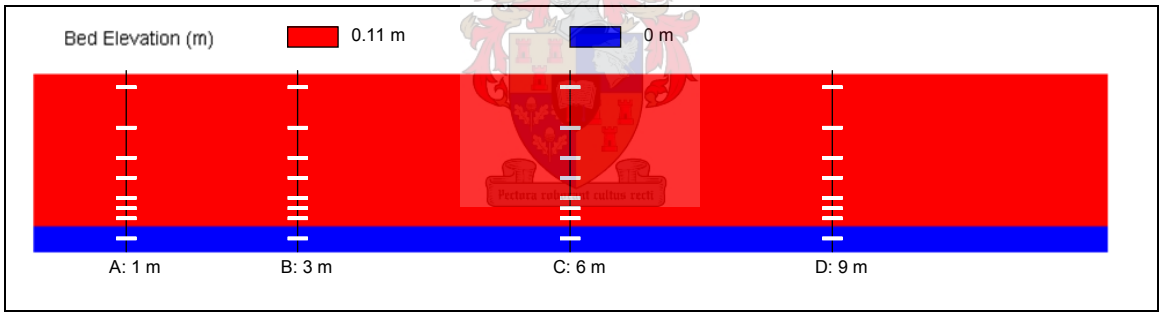

Figure 4-55: Positions of Sampling Points

The way in which the concentration samples were taken is via a set of suction tubes as shown in Figure 4-66. These tubes were then connected to a vacuum chamber (Figure 4-77) in which each of the tubes could empty their contents into a 500 ml bottle which was then removed and replaced with another for each measurement. Each of the tubes was the same length so that each bottle would fill at the same rate and not fill faster than others. The sample size was therefore relatively constant. The rate at which the samples were taken could be controlled by letting in a small amount of air into the chamber. In this way abstraction rates did not disturb the flow patterns. Care was also taken that before each measurement, the tubes were empty of fluid still there from the previous sample.

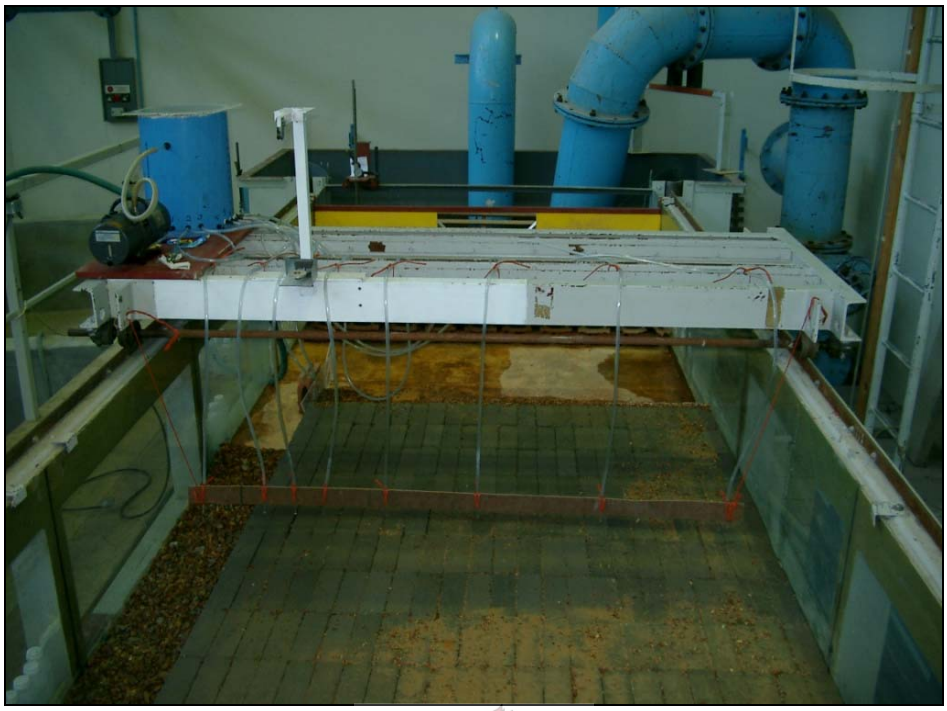

Figure 4-66: Suction tubes

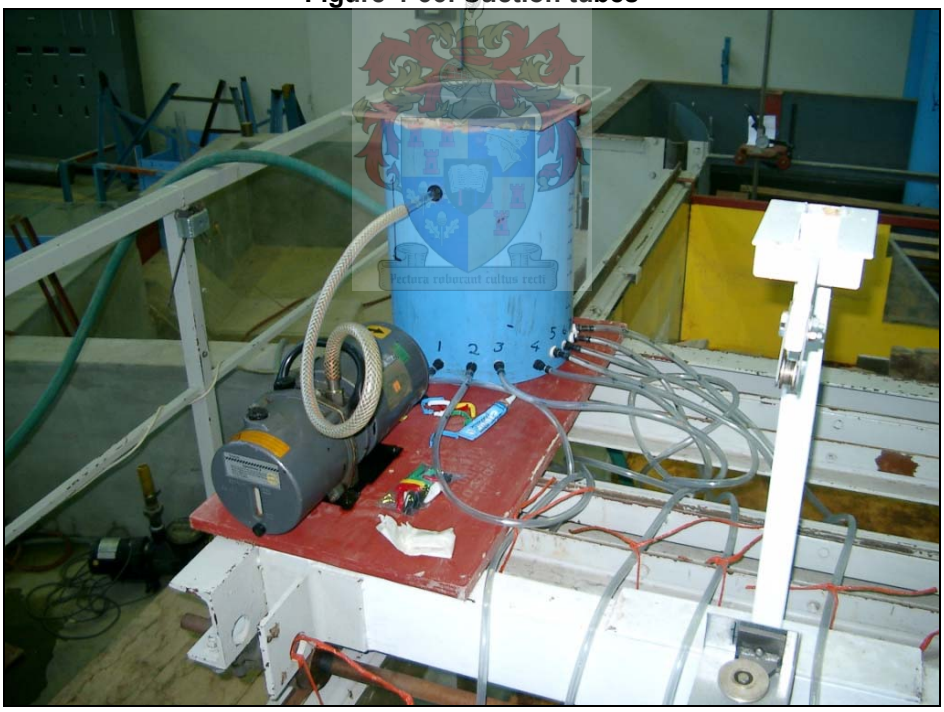

Figure 4-77: Vacuum chamber

The 500 ml sample bottles so obtained were then analysed by sucking the contents through filter papers which were subsequently weighed. Having the volume of each bottle (by weighing its contents) and also having the weight of the sediment it contained allows one to calculate the concentration at each sampling point. Take note that the sampling depth was at one third above

the bed of the floodplain depth including the main channel sampling point. This depth was chosen because at that depth there is little difference (roughly 15%) between the measured concentration and the depth averaged value. The reason for this is apparent from the Rouse concentration distribution profile as described in section 3.3.1 and depicted in Figure 4-88. The depth averaged concentration value is nearly equal to the actual concentration at a depth of 0.33 H. Take note that despite this fact, the sampled concentrations in both the main channel and floodplain were adjusted according to the Rouse equation (equation(2020)).

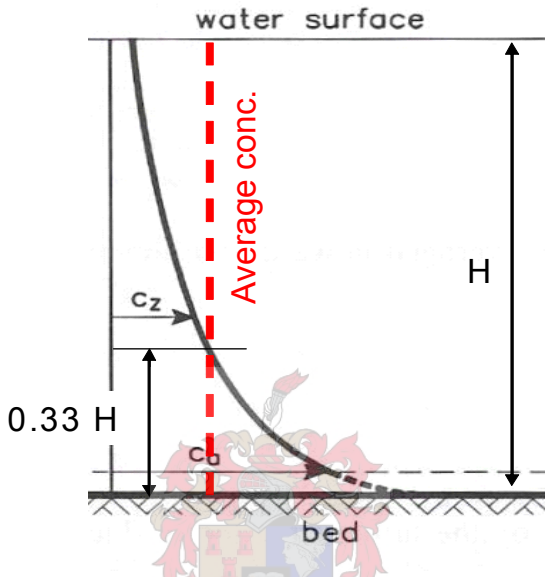

Figure 4-88: Vertical suspended sediment concentration

The scenarios that were conducted are shown below in Table 4-11.

Table 4-11: Experiments conducted

Test	Discharge (m^3/s)	Channel Depth (m)
1	0.01	0.0135
2	0.015	0.0135
3	0.01	0.015
4	0.015	0.015

Using the measurement grid described above thirty-two concentrations were determined for each test at a time of roughly 15 to 20 minutes after the commencement of the test. The timing is difficult to specify exactly since the sampling took longer in some instances than in others. Sampling was however only carried out once sediment movement onto the floodplain was observed. The concentration values so obtained were then interpolated to create the figures given below (see Figure 4-1111 to Figure 4-1414). Note that flow is from left to right as can be seen in Figure 4-99.

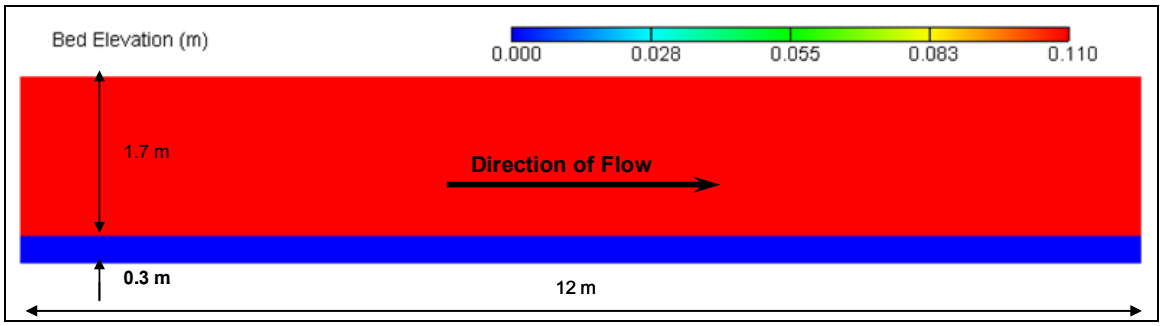

Figure 4-99: Plan View of Bed Profile

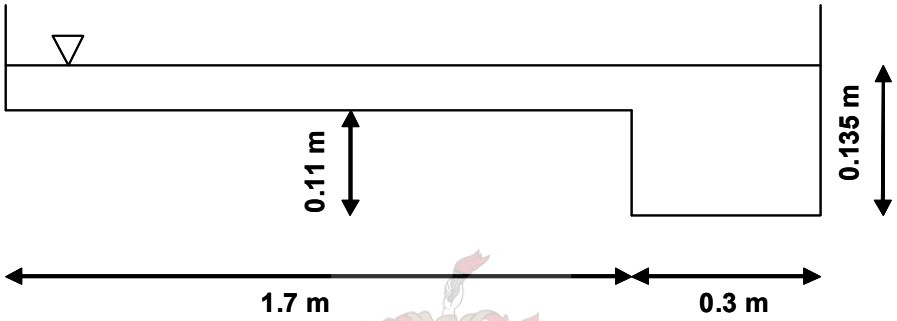

Figure 4-1010: Cross Section of Flume

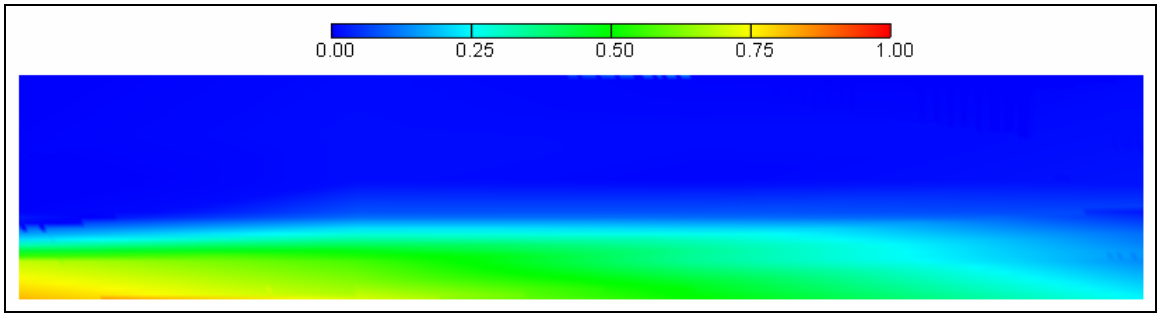

Figure 4-1111: Plan View of Observed Suspended Sediment Concentration of Test 1 (g/ℓ)

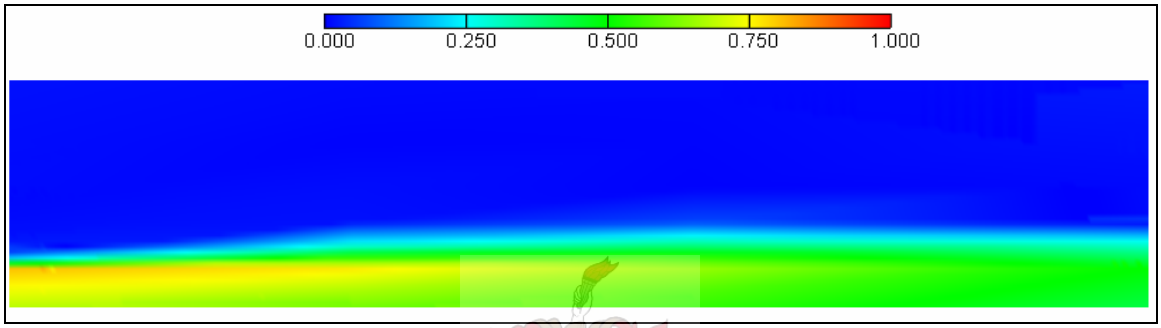

Figure 4-1212: Plan View of Observed Suspended Sediment Concentration of Test 2 (g/ℓ)

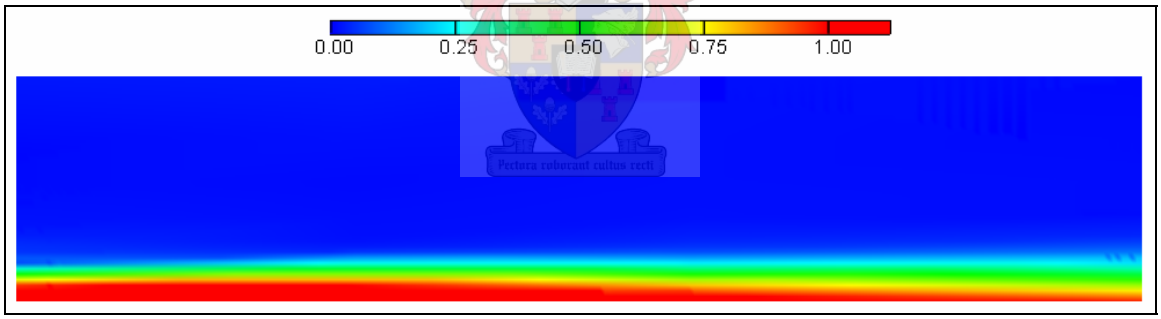

Figure 4-1313: Plan View of Observed Suspended Sediment Concentration of Test 3 (g/ℓ)

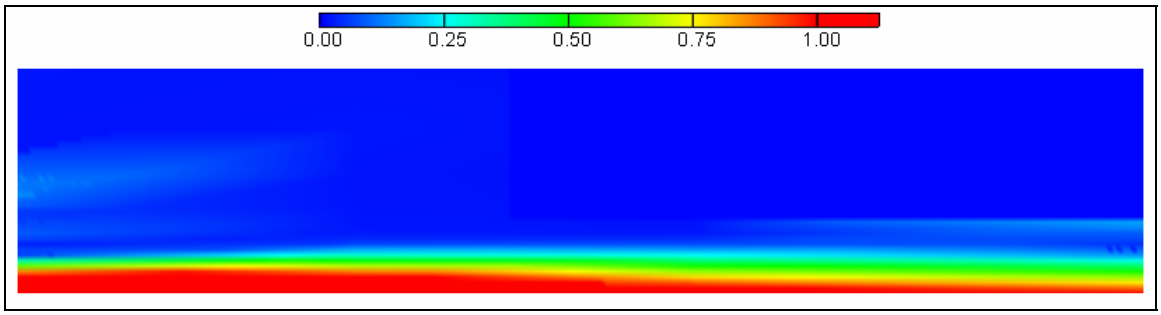

Figure 4-1414: Plan View of Observed Suspended Sediment Concentration of Test 4 (g/ℓ)

From a quick overview of the above rough graphical representations of the results it is clear that an increase in the discharge with depth remaining constant causes a more rapid movement of the sediment down the channel and floodplain. This is especially evident in noting the difference between Figure 4-1111 (which represents a discharge of 10 ℓ/s) and Figure 4-1212 (which represents a discharge of 15 ℓ/s). In Figure 4-1111 the sediment plume has not yet reached the end of the flume while at the same time the plume in Figure 4-1212 has done so.

The difference between the first two figures and the last two there seems to be an indication that there is considerably less lateral spreading taking place and as such the concentrations in the main channels are much higher than in the first two tests. As to the reason why the deeper flows cause less lateral transport, an explanation may be presented from section 3.6. Logically it seems to make more sense that deeper flows would equate to a greater area for which the suspended sediment to transport across.

Figure 3-2424 however shows that an increase in depth of flow brings about a decrease in bed shear stress and vortex intensity in the main channel. There is also the tendency toward an equalisation between the velocity on the floodplain and in the main channel. This invariably means that there is less friction between the two water bodies leading to less turbulence which then results in less transverse sediment dispersion as was observed in the experiments.

This can however not entirely be corroborated by the measurements. Rough flow velocity measurements were made by timing the movement of pieces of cork for a streamwise distance of two meters. Time was taken as the float moved over the first meter mark and then again over the second meter mark. These two measurements were then averaged to give the velocities as shown below in Table 4-22.

Table 4-22: Velocity measurements (m/s)

Discharge (m^3/s)	Flow Depth (m)			
	H = 0.135		H = 0.15	
	channel	floodplain	channel	floodplain
Q = 0.01	0.105	0.096	0.067	0.062
Q = 0.015	0.203	0.197	0.161	0.157

On average the flow velocity on the floodplain for the lower water elevation is roughly 94% of the flow velocity in the main channel. For the higher water level this figure increases by a meagre 1% indicating there might as well be no difference between them. The most likely reason for this

aberrant behaviour is that the flow being considered is not normal flow as the water level is not dependent on roughness but rather by the downstream sluice.

Performing some simple Manning calculations of an asymmetrical channel however clearly indicate that there is a definite decrease in the difference between the floodplain and main channel velocities as depth increases. Therefore the results from section 3.6 and the above experiments hold.

Another surprising aspect is that even for such a small increase in depth the change in behaviour is so profound. It is therefore likely that if the experiment was continued for a longer period of time then the sediment spreading in the deeper flows would start to mimic that in the shallower flow experiments. Thus the conclusion can be made that due to the stochastic nature of the movement of sediment it takes longer for sediment to travel onto the floodplain than pure theory suggests.

The next set of figures is presented on the next few pages. They show the concentrations at each of the four transverse cross sections where data was captured. In each case without fail there is transport from the region of high concentration in the main channel to the areas of low concentration on the floodplain.

There is also very clear evidence for longitudinal dispersive transport. As the sediment moves downstream the concentration in the main channel decreases. This can not only be prescribed to longitudinal transport but also the removal of the sediment in the main channel onto the floodplain. Thus there is also a suggestion that the system that was modelled was supply limited, which is understandable because there was only one sediment source and not a continuous one across the channel as would be the case in nature.

As was discussed previously there is once again the indication that for the deeper flows (experiments 3 and 4) there is the occurrence of relatively high suspended sediment concentrations in the main channel and lower ones on the floodplain.

Test number two does not generally match the trends set by the other tests. As can be seen from Figure 4-1616, the concentrations in the main channel are less than the ones on the adjacent floodplain. The precise reason is unclear but it is entirely possible that errors may have occurred during the sampling procedure.

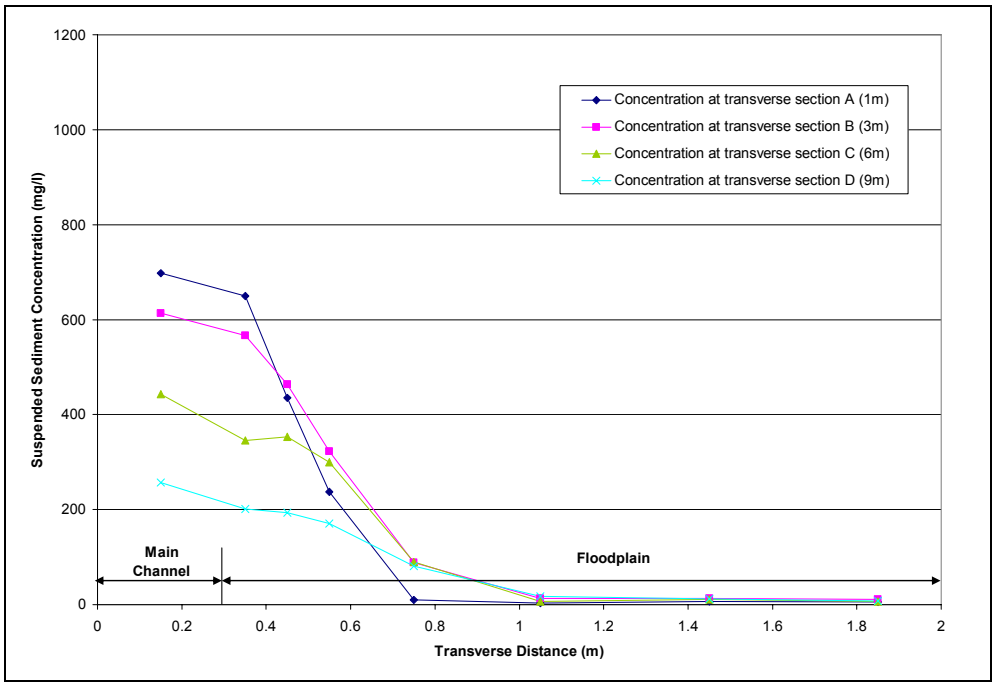

Figure 4-1515: Suspended Sediment Concentrations for the consecutive transverse cross sections – Test 1

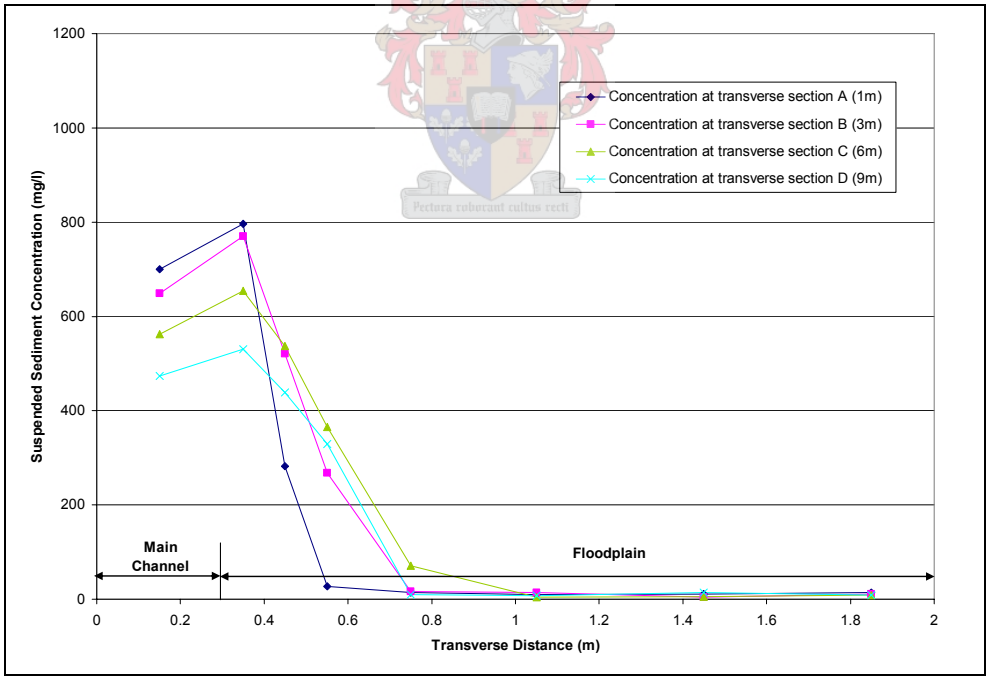

Figure 4-1616: Suspended Sediment Concentrations for the consecutive transverse cross sections – Test 2

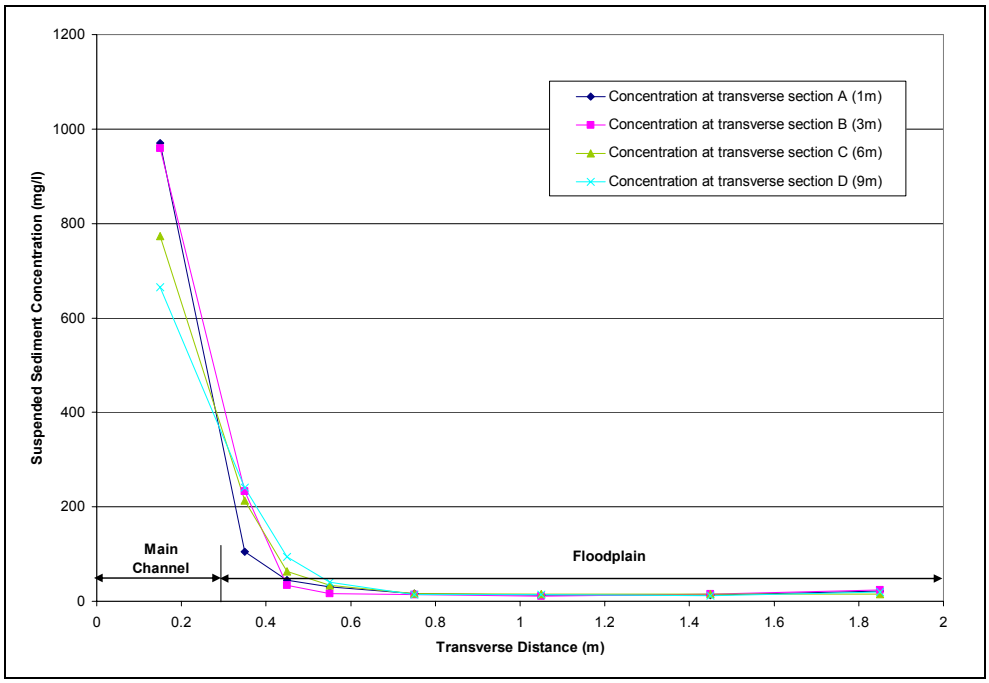

Figure 4-1717: Suspended Sediment Concentrations for the consecutive transverse cross sections – Test 3

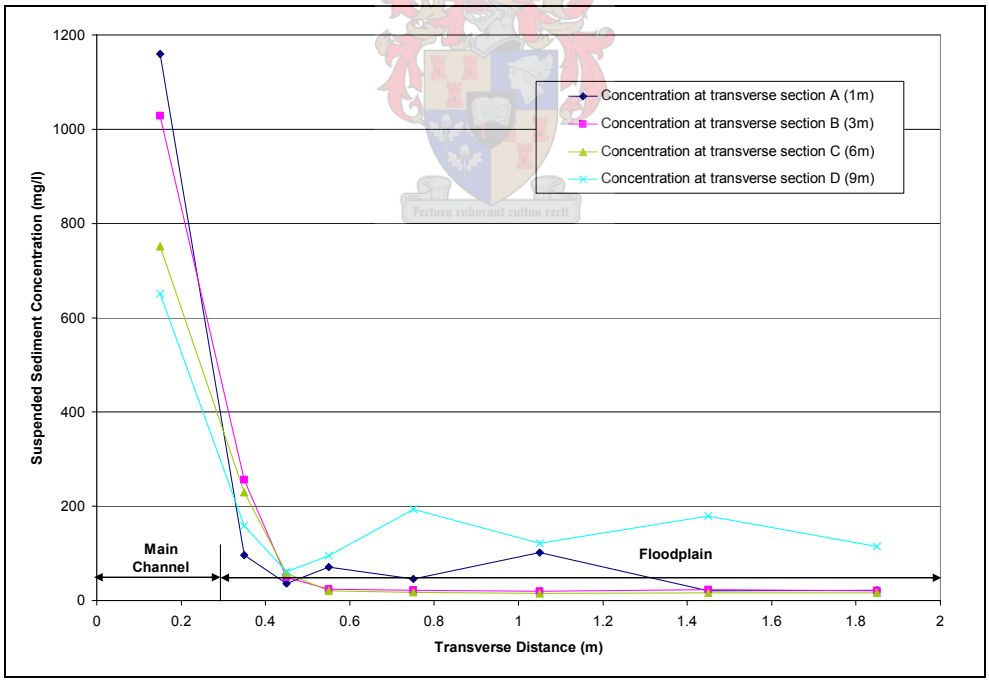

Figure 4-1818: Suspended Sediment Concentrations for the consecutive transverse cross sections – Test 4

The next section describes a range of both hydrodynamic and morphologic computer simulations which were carried out to further test the general trends observed in the physical models.

4.2 Mathematical Modelling

Numerous mathematical models have been developed over the years. As was explained in section 3.2, they can be classified according to how many dimensions they utilise in their calculations. In the past models have generally focussed on one-dimensional models though these days there has been a large scale movement toward two-dimensional modelling.

Three dimensional modelling is still in its infancy even though the mathematics behind the model has been around for several decades the current computer power that is generally available does not allow modelling of any but the simplest systems. There have been indications however that fully three dimensional models are being used to simulate hydrodynamic systems. Much work is however still needed in the three dimensional field concerning sediment transport.

One of the problems being encountered is the difficulty in defining the exact point at which sediment starts to move. Whereas one- and two-dimensional models could use generalisations in this regard, fully 3D models need to be more precise than that. Progress is however ongoing.

There are some though which are not convinced that fully three dimensional modelling is very effective except in terms of small local problems (van Rijn, 1993). If the problem is approached from a cost-benefit ratio three dimensional models always tend to cost more than the results they can provide. The reason for this is that a large amount of field data is required to effectively calibrate a three-dimensional model and it is this activity that carries the largest cost. But if this data is readily available the only other cost which must be considered is computer running time which with proper planning can be managed effectively.

4.2.1 CCHE2D

A mathematical model named CCHE2D which is reportedly capable of simulating both hydrodynamic and morphologic systems has been selected for a set of simulation runs. The reason for its selection is because not only is it freely available from the internet due to its development being funded by the government of the USA, but it is also more user friendly than some of the others available. A further reason is that the software was familiar to the candidate prior to the initiation of the study. The software was developed by Yaoxin Zhang and Abdul Khan at the National Centre for Computational Hydroscience and Engineering at The University of Mississippi (Jia & Wang, 2001).

In specific terms the program is a two dimensional, horizontal, integrated package for the simulation and analysis of free surface flows, sediment transport and morphological processes. There is a general procedure that must be followed for every simulation. The first activity is the generation of a grid upon which the bathymetry data can be superimposed. The smaller the grid cells or the closer the calculation points are to each other the more accurate the solution will be, but the more calculation points there are the longer the simulation time. Together with the bathymetry of the system, the model must also be provided with a water depth as well as a roughness factor at each node.

Secondly the boundary conditions for the simulation are specified. Aspects such as no-flow boundaries as well as inlet and outlet characteristics must be given. Generally for subcritical flow conditions all that is required at the upstream boundary is a discharge either in the form of a hydrograph over time or a constant value. Further data concerning the inflow of sediment can also be provided. At the downstream end a water level must be specified. In certain circumstances it may be difficult to determine what this water level should be, but it is usually a good idea to start the first simulation with a normal depth at the downstream end. This can then be changed depending on how the simulation behaves.

Taking all this information the program then uses finite difference techniques to discretise the system not only in the three spatial directions but also in time. A time step is defined as part of the setup process but some models do increase and decrease the time steps as the simulations progresses within certain error bounds. CCHE2D does this with its sediment transport module. If the flow of sediment is slow and steady it will increase the time step to speed up simulation time. If it however detects that large changes have taken place between the current time step and the previous one it will then repeat the calculations using a smaller time step, thereby making sure that the large change that was observed is not caused as a result of numerical errors brought about by the coarse time step. This method of calculation may sound advantageous but it has its complications as will be shown later.

The version of CCHE2D that will be used for the simulations is according to its documentation (Jia & Wang, 2001) capable of solving the depth-integrated convection diffusion equations for suspended sediment, such as the one presented in equation (88). This equation is then also augmented to include the settling out of sediment using a source-sink term as described in section 3.4.2. This augmentation was subsequently disabled so as not to allow the model to erode the bathymetry. This however has the consequence that no deposition can take place, but since the sediment being used is do fine very little deposition is expected as was observed in the physical experiments.

4.2.2 Simulation 1

The first simulation that was conducted is a control on the hydrodynamics module of CCHE2D to check whether or not it is fully capable of simulating the turbulence structures responsible for the phenomena described above. The model set up by (Bousmar & Zech, 2001) was reproduced in CCHE2D and run successfully.

The model consisted of a three meter long symmetrical compound channel as shown in Figure 4-1919 and Figure 4-2020.

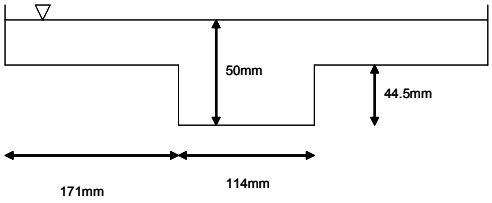

Figure 4-1919: Cross section of Simulation 1 (not to scale)

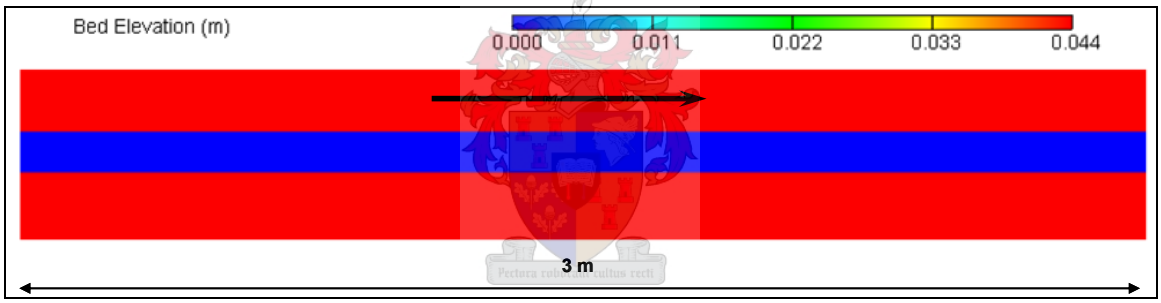

Figure 4-2020: Plan View of Bed Profile of Simulation 1

The bottom slope was taken as being 0.00085, the roughness value was specified as n = 0.0064 s/m$^{1/3}$ and the discharge at the inlet was equal to 2.5 ℓ/s. Because of the very small scale of the channel in question the grid size and time step likewise had to be small in order to maintain accuracy. One grid cell was 0.006 m by 0.006 m and the chosen time step is 0.002 s. This equates to 75 cells over the width and 500 cells along the length of the flume.

Once the run was completed it was concluded that CCHE2D was capable of simulating the complex horizontal flow processes since its results were practically identical to those of the Bousmar & Zech (2001) study as can be seen from comparing Figure 4-2121 and Figure 4-2424.

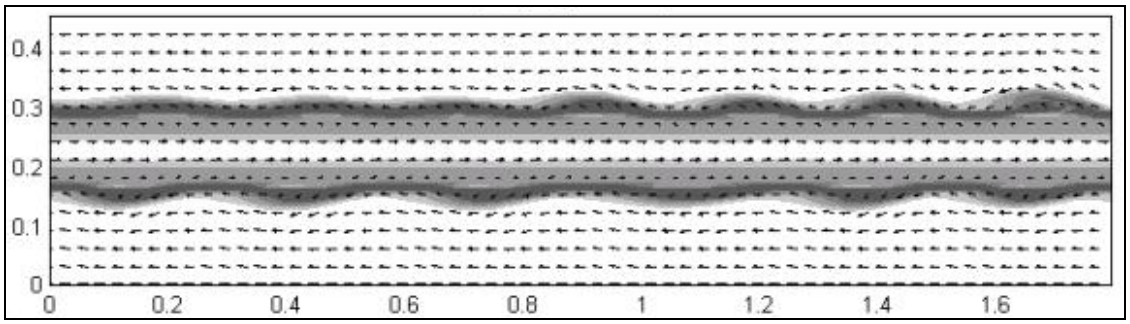

Figure 4-2121: Flow field of Bousmar & Zech study (flow is from R to L)

The water level plan profile can be seen in Figure 4-2222. Though from the large change in the colour scale it seems there is a large gradient from the upstream side (on the left) to the downstream side (on the right). By looking at the legend scale however it is clear that the maximum difference over the whole area is a mere two millimetres. What is evident is that because of the very small scale of the cell size that was chosen the small ripples that form on the turbulent flow have been accurately simulated.

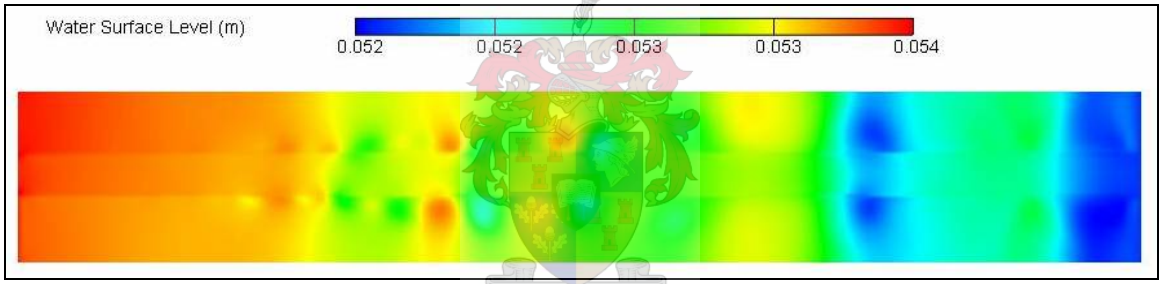

Figure 4-2222: Water surface profile of Simulation 1

The velocity profile is presented next in Figure 4-2323. The horizontal turbulent cells that form are clearly visible as they grow in size until the boundaries of the channel limit their growth any further. A close up of the velocity plot together with a set of vectors is shown in Figure 4-2424.

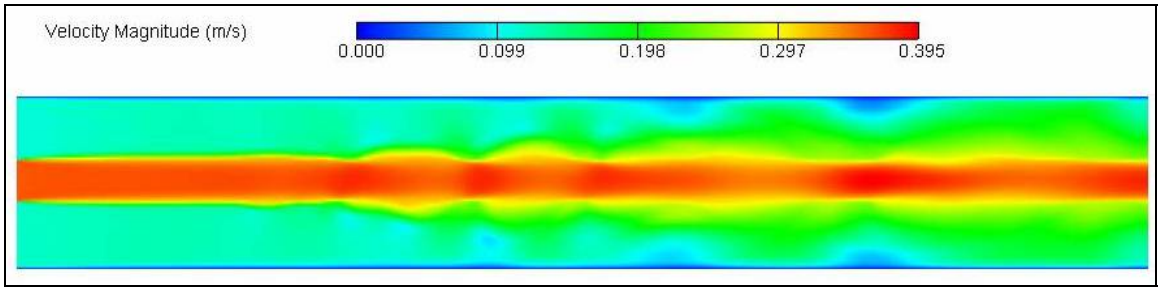

Figure 4-2323: Velocity profile of Simulation 1

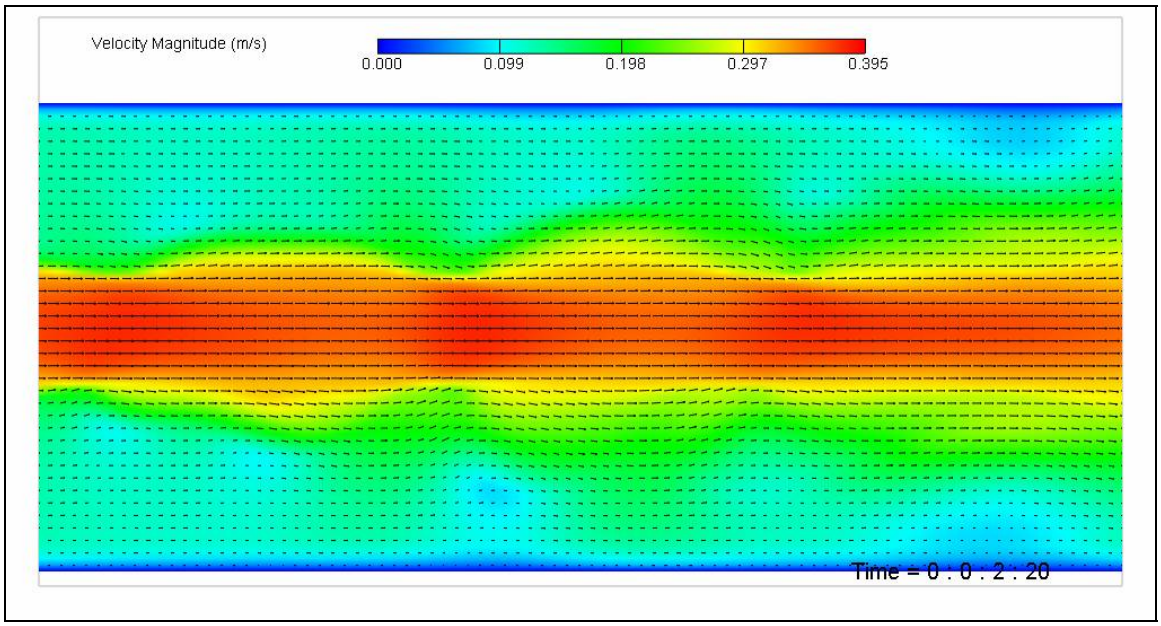

Figure 4-2424: Velocity profile close up of Simulation 1

Figure 4-2525 shows the transverse component of the above velocities and even though the magnitude of these are smaller than their longitudinal counterparts by an order of magnitude they are the ones responsible for the transfer of momentum (and so sediment) onto the floodplain. It is interesting to see that the vortices on either side of the channel occur in pairs in that they both flow toward or both flow away from the main channel. This is probably caused by the proximity of the two shear layers to each other, each situated above the edges of the main channel. If the main channel was wider it is likely that the observed vortices on both sides of the channel would soon lose synchronicity. Should the channel be wide enough so that the effect that the shear layer has on the main channel's bed shear magnitude has decreased to a negligible factor, the eddies generated would be independent of each other. This lack of synchronicity in wide channels, such as in nature, could in part explain the fact that it is rare to find straight natural channels.

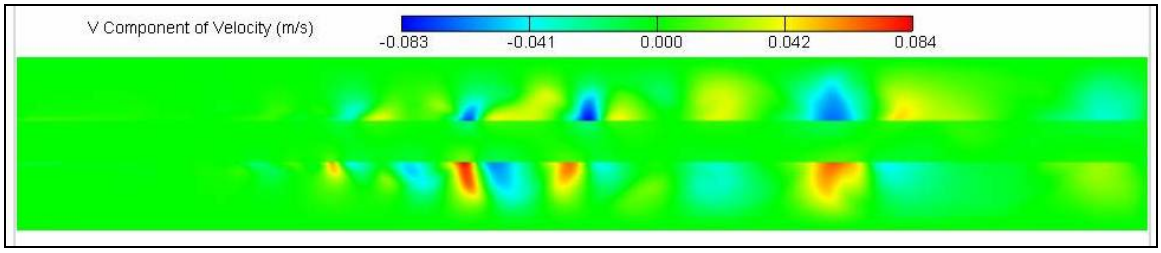

Figure 4-2525: Transverse velocity profile of Simulation 1

Figure 4-2626 demonstrates the capability of the model to simulate the bed shear stresses and the subsequent effects it would have on the transverse transport of suspended sediment are clear.

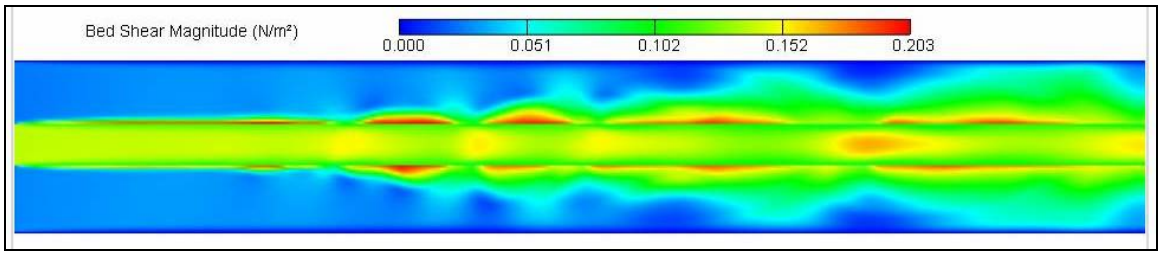

Figure 4-2626: Bed Shear Stress profile of Simulation 1

What is also clearly visible in all of the above figures is that it takes a certain distance before the turbulence structure begins to assert itself. This behaviour was not only evident in distance but also in time. The total simulation time is in the order of 140 seconds which results in the above final profiles but when the 'history' file is scrutinised it is clear that it takes nearly 100 seconds for the flow patterns to develop. It can thus be concluded that any changes that are brought about take a certain distance and a certain time to have an effect.

4.2.3 Simulation 2

The second simulation can basically be considered a calibration run of one of the physical experiments. The simulation involved not only the hydrodynamic simulation of the physical model but also the modelling of the transport of suspended sediment. In the first simulation it was determined that the chosen model is capable of successfully predicting the two dimensional flow field. This second run aims to determine if the same can be said of the sediment dynamics.

The physical model run that was selected is Test 2, i.e. a discharge of 0.015 m^3/s and a main channel depth of 0.135 m is shown in Figure 4-2727 and Figure 4-2828. The laboratory flume was reconstructed in the bathymetry where the main channel lies on the right hand side and has a width of 0.3 m. The remaining 1.7 m of the 2 m wide flume represents the level floodplain. The grid size that was used in the model is 0.02 m in width and 0.024 m in length. This equates to some 100 cells across the 2 m width of the section and 500 cells along the 12 m length. It was attempted to increase this grid size as it has a major influence on simulation running time, but it was quickly determined that even marginally increasing the size causes a significant change in the pattern of sediment movement. It was therefore decided to keep the small cell sizes for the initial simulation.

The consequence of this is that the timesteps likewise had to decrease in order to keep the simulation stable. A timestep of 0.1 s was used for the sediment simulations. This is indeed larger than the one used in Simulation 1, which indicates that in order to achieve the high accuracy that was aimed for in Simulation 1 both the cell and timesteps should be reduced. But given that Simulation 2 only aims to determine if the model is capable of cross-shear boundary sediment flow, such highly detailed models are not yet required.

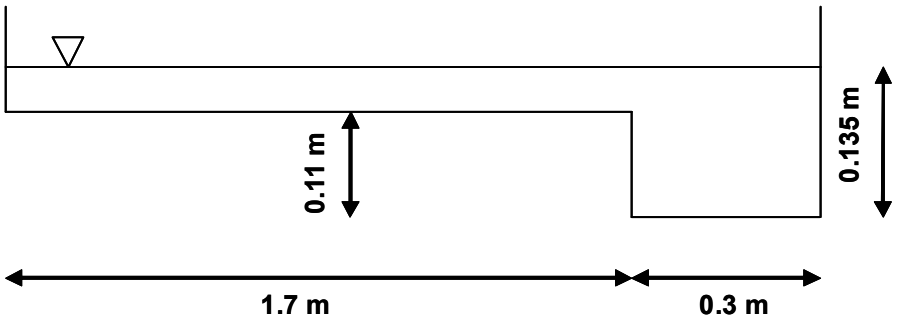

Figure 4-2727: Cross Section of Simulation 2 (not to scale)

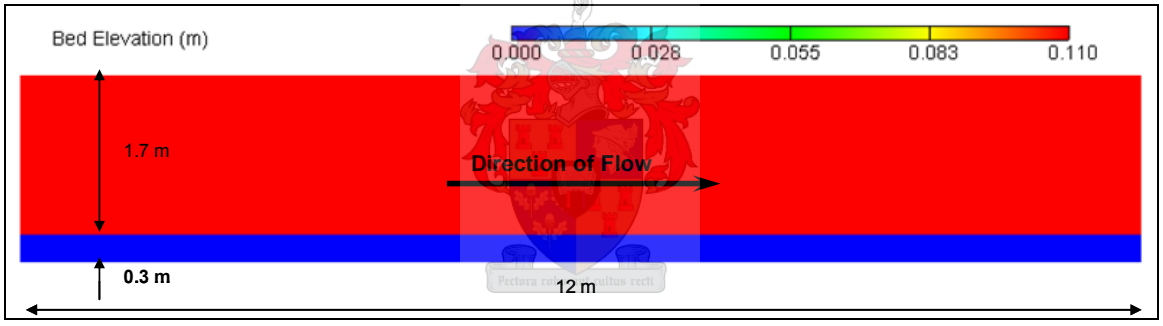

Figure 4-2828: Plan View Bathymetry of Simulation 2

As was mentioned in the beginning of this chapter, it was intended for this simulation run to be calibrated against the observed values but this was not possible since, as will be shown later, the travel times between the two models could not be correlated. For this reason, the model was calibrated using visual observations of phenomena. The calibration parameters that were used are the roughness values on the floodplain, time step as well as cell size. Table 4-33 gives some specifics concerning the available parameters in the model.

Table 4-33: Model Parameters for Simulation 2

Parameter	Value	Comment
Manning "n'' value on floodplain	0.011	Estimated using Manning equation
Manning "n'' value in main channel	0.006	Estimated using Manning equation
Cell size (m)	0.02 in width by 0.024 in length	
Timestep (s)	0.1	
Total run time (s)	10800	3 hours
Mean sediment size (mm)	0.00014	
Sediment specific gravity ()	2.65	
Flow input (ℓ/s)	15	
Suspended sediment input concentration (kg/m^3)	5	Across the entire cross section
Outlet water level (m)	0.135	
Initial water level (m)	0.135	
Turbulence model	Parabolic eddy viscosity model	coefficient of 2
Transport model	Total load as suspended sediment	Wu et al formula (Jia & Wang, 2001)

The figures below show some of the results from the simulation. Figure 4-2929 shows the water surface elevation and Figure 4-3030 the velocity field across the flume. Note that flow is as before from left to right.

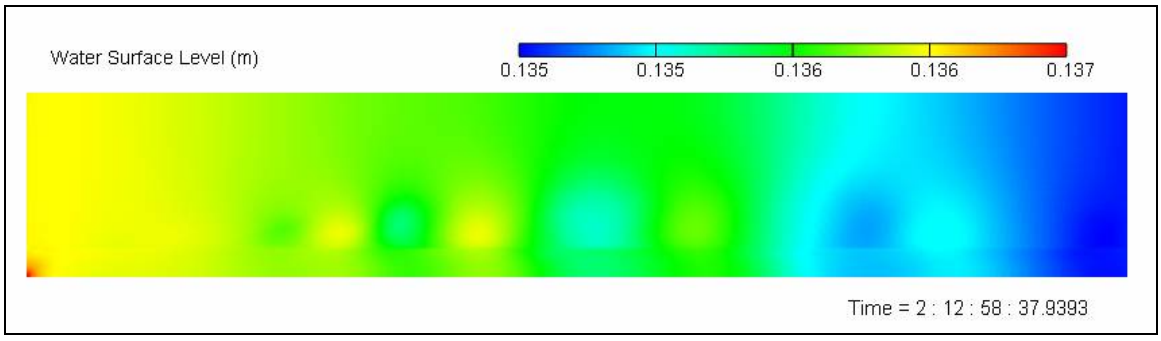

Figure 4-2929: Water surface elevation for Simulation 2

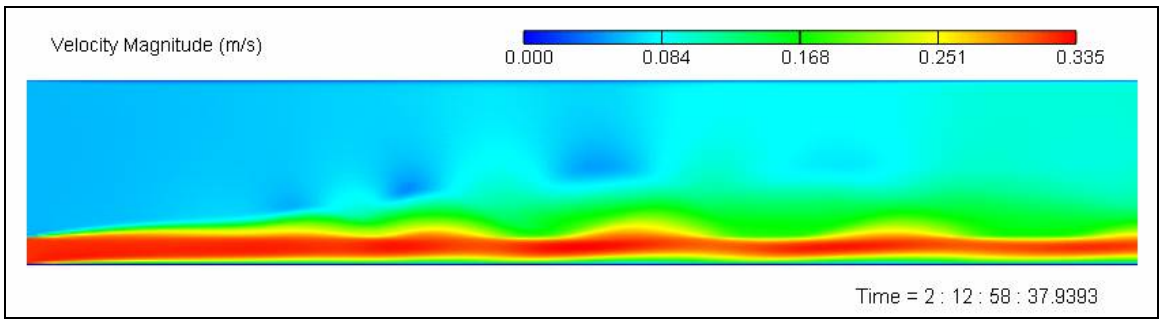

Figure 4-3030: Velocity profile for Simulation 2

It is clear from the above two figures that as in the previous simulation vertical axis eddies play a large role in transferring momentum from the main channel to the floodplain. It must however be noted that even though these eddies did occur in the physical tests they were not as large as estimated by the mathematical model. The eddies in the simulation start small but increase in size as they move downstream until the flume width limits their growth. The eddies in the physical model on the other hand grew only up to a point defined by the shear layer's extent of influence and were on the whole much smaller than the simulated ones.

Figure 4-3131 to Figure 4-3737 shows the progression of suspended sediment as it travels down the flume. Recall that the suspended sediment concentrations shown in Figure 4-1111 to Figure 4-1414 can be considered to have been sampled on average fifteen to twenty minutes after the test began. Compared to this the simulation suspended sediment took a great deal longer to travel the total length of the flume. The reason for this discrepancy is either the fact that the velocities in the physical model and the simulation could not be well correlated and/or the possibility that there are some programming errors in the logging of time values. The reason for this suspicion is that the total simulation time should be around three hours and yet the data file logs a run time of around two and a half days. The cause of this error most likely has something do to with the fact that the model adjusts the sediment time step as the simulation progresses. As such, no real observations regarding travel time can be made.

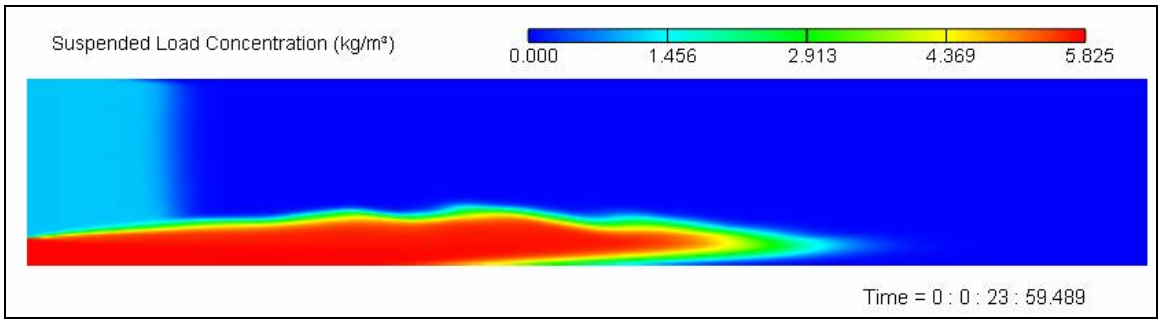

Figure 4-3131: Simulated Sediment Concentrations 1

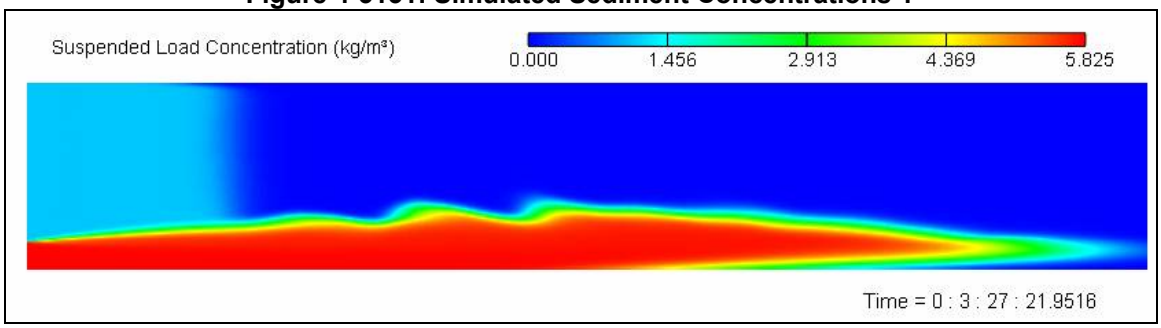

Figure 4-3232: Simulated Sediment Concentrations 2

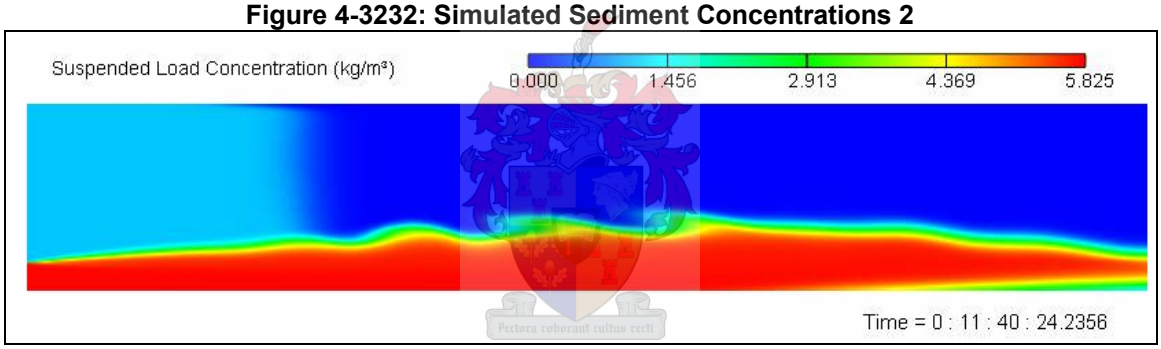

Figure 4-3333: Simulated Sediment Concentrations 3

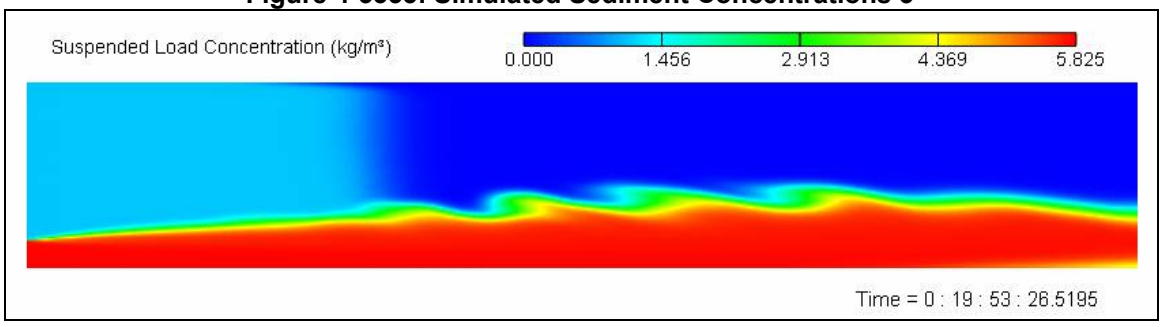

Figure 4-3434: Simulated Sediment Concentrations 4

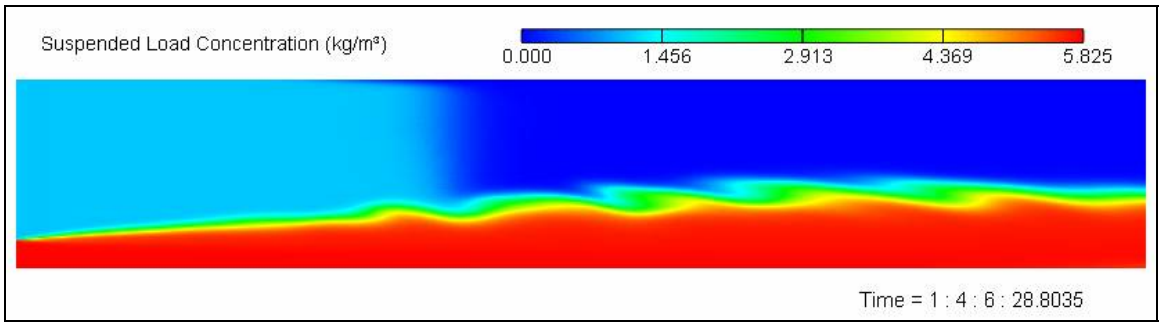

Figure 4-3535: Simulated Sediment Concentrations 5

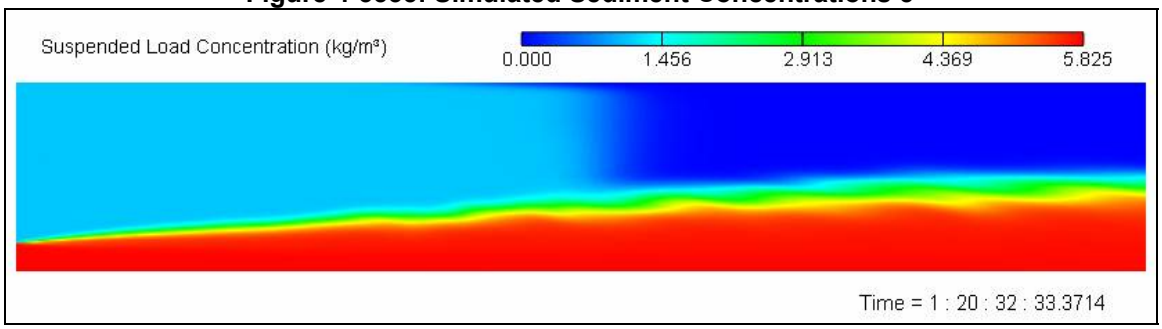

Figure 4-3636: Simulated Sediment Concentrations 6

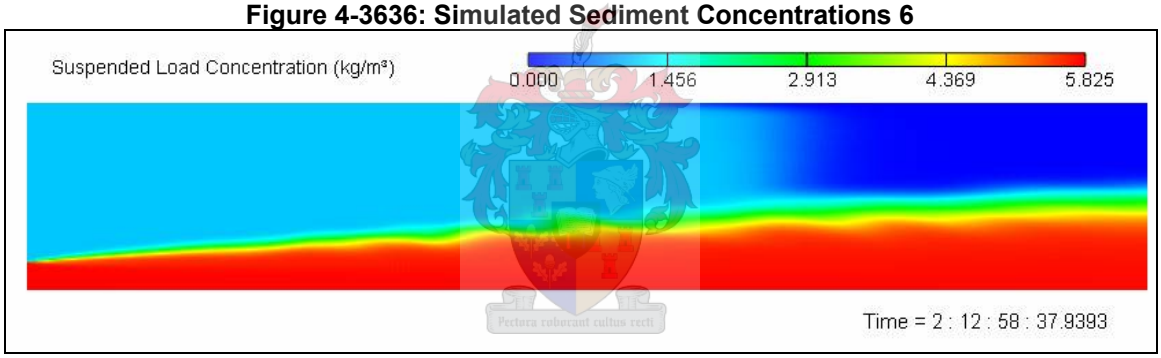

Figure 4-3737: Simulated Sediment Concentrations 7

The above sequence of images, especially Figure 4-3434 and Figure 4-3535 indicate that the vertical axis eddies play the most significant role in spreading sediment on the floodplain. These eddies were indeed observed in the physical model but were not as significant as simulated here. The literature survey that was conducted confirms that these eddies do have an effect but that the major role-player that affects transverse dispersion are the secondary currents. It therefore brings forth the question whether or not the CCHE2D model is capable of simulating or incorporating these three dimensional effects in its calculations.

Though the model is capable of modelling the bottom shear stress accurately enough it is however not entirely enabled or equipped to deal with secondary flow. As such, only limited success was achieved in obtaining similarity between the suspended sediment concentration values measured in the physical model and the mathematical one. Actual values did not correspond to one another. Figure 4-1616 in the previous section showed that the maximum

observed suspended concentration was in the order of 800 mg/ℓ whilst the maximum simulated value lies in the order of 5000 mg/ℓ (The explanation behind this discrepancy is explained later in this chapter). If however the values are standardised by viewing them relative to the maximum concentration, satisfactory spreading trends are apparent as can be seen from Figure 4-3838 to Figure 4-4141 below. Note that the simulated concentration profile data was abstracted from the timestep depicted in Figure 4-3131 (23 minutes after start), placing it at roughly the same time as when the observed concentration samples were taken.

The three first figures show that the lateral distance covered by the solute is roughly the same, but is in general greater for the observed concentration profiles. Therefore despite the much higher concentrations in the simulation and the accompanied higher concentration gradients, there was no significant increase in transverse suspended sediment transport as would be expected since the higher the gradient the higher the rate of spread would be. The last figure of the four (Figure 4-4141) together with comparing Figure 4-1212 with Figure 4-3131 also clearly indicates once again that the sediment is not travelling down the flume as fast as was observed. This is another indication concerning time logging problems in the program.

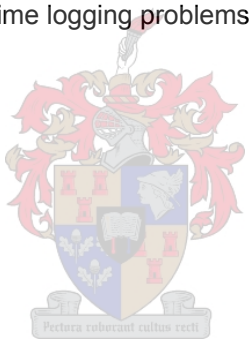

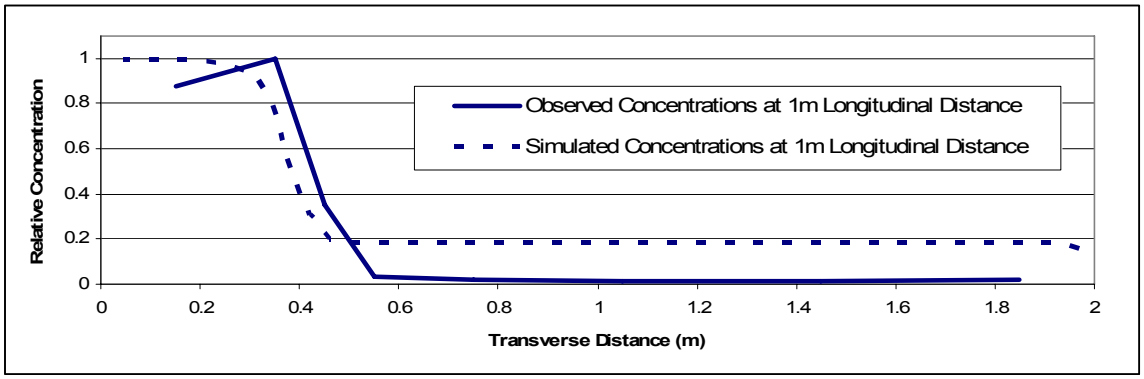

Figure 4-3838: Simulated vs Observed Relative Concentrations at 1 m

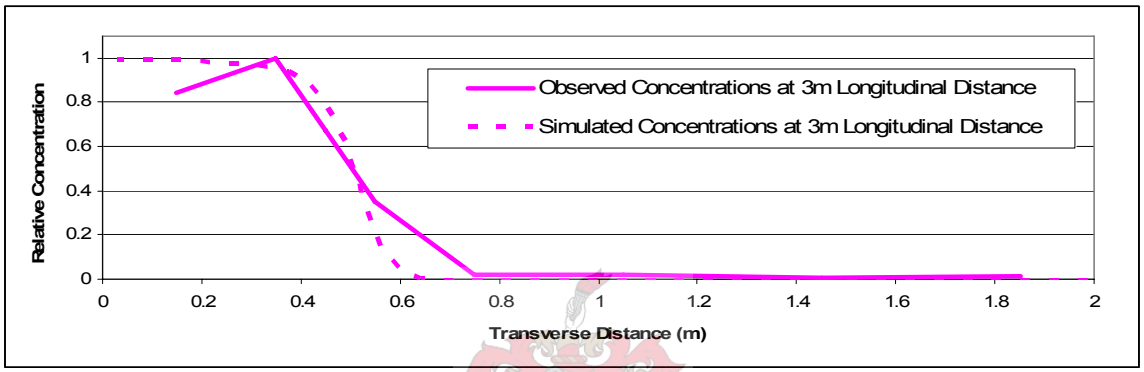

Figure 4-3939: Simulated vs Observed Relative Concentrations at 3 m

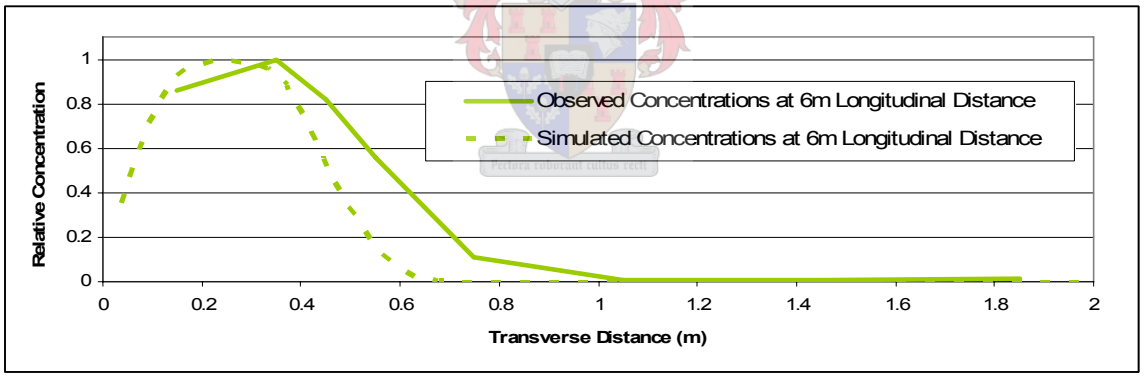

Figure 4-4040: Simulated vs Observed Relative Concentrations at 6 m

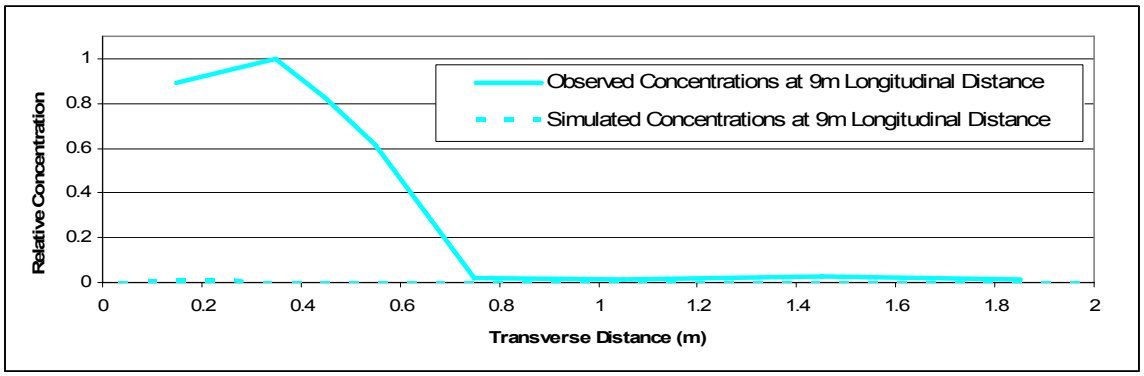

Figure 4-4141: Simulated vs Observed Relative Concentrations at 9 m

The general patterns of spread between the simulated and observed profiles are the same. Sediment first travels from the main channel through the shear layer onto the floodplain from where currents generated by the shear layer carry it further. Although not actually modelled due to the limited length of the simulated flume, the trend exists that the sediment would continue spreading until it reaches the opposite (left) boundary of the flume. It is therefore clear from the simulation that distance plays a large role in the diffusion process.

A further problem that could be a contributing factor to the discrepancies in the simulations is that the suspended sediment could not easily be inserted at the upstream boundary. The physical model used a point source in order to introduce the sediment in the flume. In the simulations this was difficult to implement so it was decided to simply add the sediment across the whole section. The majority of the sediment would then be introduced in the main channel since CCHE2D distributes the sediment at an even concentration. This means that the deeper parts of flow would receive a higher depth-averaged concentration. The even distribution of sediment is readily visible in the above figures as the light-blue region moving slowly from left to right.

This extra sediment inserted on the floodplain has no real effect on the dispersion of sediment from the main channel. Its slow progression is however an additional piece of evidence that points to problems with time logging in the model. This sediment should according to theory be travelling on average at the velocity of the water that carries it. This velocity, equal to 0.1 m/s (Figure 4-3030) should cause the sediment to reach the end of the flume in 30 seconds. Yet, in two days it has scarcely moved two meters.

Despite the problems with time logging it can be seen from the figures that the process whereby sediment travels from the main channel to the floodplain is a slow one. Even though the transverse dispersion is not reduced via the lack of secondary currents it still takes some time and distance before the sediment moves onto the floodplain. Another contributing factor may be that the flow on the floodplain is not very deep and thus not much cross sectional area is available through which the sediment can travel.

4.2.4 Simulation 3

This simulation can be regarded as the successor to the previous model run in that it runs the same parameters but at a larger cell size but with a smaller time step. The cell size was increased to 0.05 m by 0.05 m squares and the time step decreased to 0.02 seconds. The aim behind this was to attempt to increase accuracy by decreasing the timestep but at the same time

keeping the total running time manageable by increasing the cell size. The simulation was also run for a much longer time than the previous one. This was done so as to see how far the sediment would travel given ample time.

The results shown below in Figure 4-4242 to Figure 4-4444 indicate that the same trends observed in the physical modelling are maintained here in the mathematical models. This is despite the suspected shortcomings concerning secondary flow, which goes to show that secondary flow may be a deciding factor but is by no means the only factor that plays a role. The vertical axis eddies which were significant in the previous simulation again make an appearance yet they are much reduced and thus resemble the observed eddies more closely.

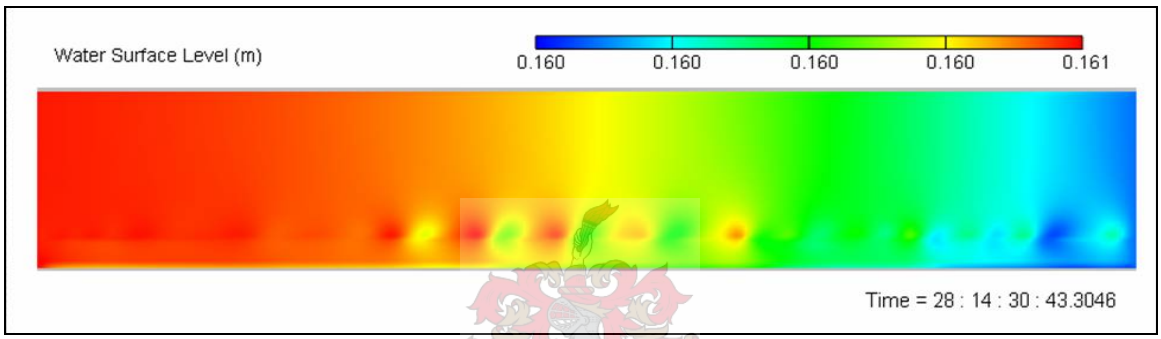

Figure 4-4242: Simulated Surface Elevation for Simulation 3

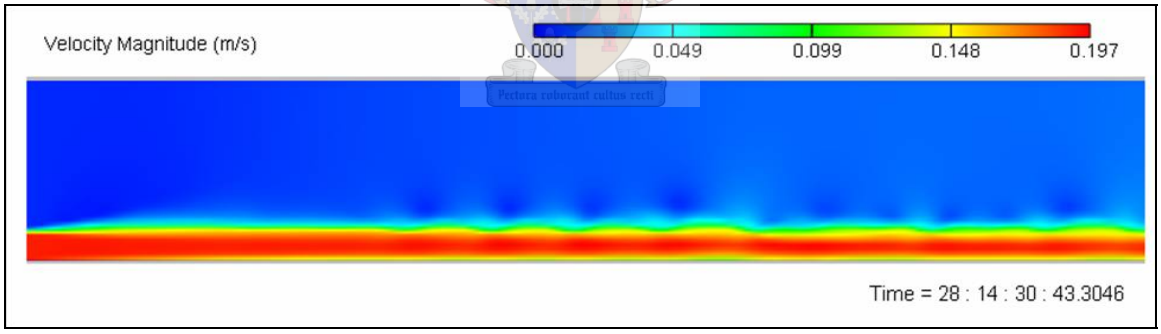

Figure 4-4343: Simulated Velocity Profile for Simulation 3

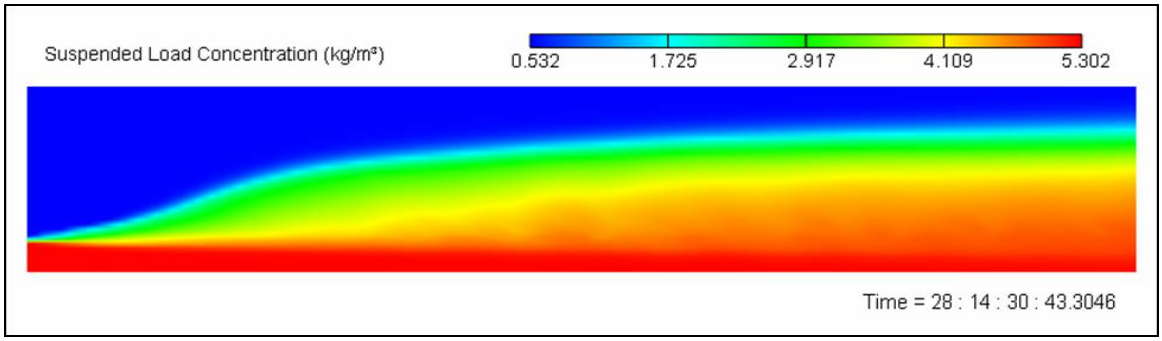

Figure 4-4444: Simulated Sediment Concentrations

The general spread of suspended sediment load seen in this simulation is closer to what would be expected and follows the trend that was observed in the experiments. Initial concentrations in the main channel are high and decrease with distance down the flume as the sediment is transferred to the floodplain. Beyond the shear layer, vertical axis eddies then mix this sediment laden flow with the clear water on the floodplain. Further away from the floodplain where these eddies are less evident the transverse transport of sediment is predominantly caused by diffusion.

Once again both time and distance play a large role in establishing trends. As Figure 4-4444 shows after some 28 days (of simulation time) and after the equilibrium condition has been established that the sediment does not reach the opposite side of the flume due to the fact that the flume is too short. It is however likely that given enough distance it would reach the floodplain boundary.

4.2.5 Enhanced CCHE2D

Despite the model's shortcomings concerning the logging of time values and secondary currents there has been a successful undertaking which aimed to enhance CCHE2D to be able to incorporate them. The research project formed part of a doctorate dissertation entitled "*Simulation of Alluvial Channel Migration Processes with a Two-dimensional Numerical Model.*" (Duan, 1998).

The specific objectives were to use the three-dimensional computational fluid dynamics (CFD) model, CCHE3D, to develop a set of characteristics of secondary flow in a meandering river and apply these in CCHE2D to convert the two dimensional flow field into a quasi three dimensional one. The resultant model aptly named the enhanced CCHE2D (enCCHE2D) was then used to model the morphological changes in a meander bend. Specific focus was given to the transverse suspended sediment transport rate and the development of the quasi-3D velocity field which controls it.

4.3 Conclusions

When performing research or any project involving hydrodynamics and sediment transport it is always a good idea to conduct both a physical and a subsequent mathematical model. The data collected from the physical model can then be used to calibrate the computer simulations. This seems a very simple statement but in practise it is a very time consuming process and is highly reliant on the quality of the tools being used.

The physical model tests conducted at the university laboratory were a success in that the desired phenomenon was observed and documented. All gathered data can be found in the Appendix. The tests, as shown later in the computer simulations, should under ideal circumstances have been run for a longer period of time. Further changes that could have improved the quality of the experiment is that the depth of flow should be increased so as to allow a greater transport of sediment onto the floodplain. Nonetheless, the model did reveal enough trends to be useful. Trends such as the importance of time and distance were evident as demonstrated in sections 4.2.3 and 4.2.4.

The model selected for the simulation runs was CCHE2D. The reason for its selection is the fact that it is freely available. Unfortunately, the part of the program which still requires a great deal of attention is the part that is key to the successful modelling of cross shear boundary suspended sediment transport. As such, the computer simulations cannot be considered as being accurate emulations of actual phenomena. They can however still reproduce the general trends observed in the physical tests.

Trends in terms of the model parameters were also observed during the simulation procedure, especially regarding their individual sensitivity. The large difference in the behaviour of transverse sediment transport between simulation 2 and 3 show that both grid cell size and time step are highly sensitive characteristics. These two factors more than any of the other parameters such as roughness values, sediment size or turbulence formulation had the largest effect in the process of calibrating the simulations to the observed phenomena. The reason for this most likely stems from the fact that particularly grid cell size plays a deciding role in the development and size of the vertical axis eddies which spread most of the sediment in the model. Thus it goes to show that the smaller the grid size, the more accurate the results will be. However, the decrease in time step which must go alongside this decrease in cell size would most likely play the deciding role. The shorter the time step the fewer errors will accumulate in the model calculations and thus the more stable and accurate the outcome.

CHAPTER 5

5 DAM IMPACTS

It has been thoroughly proven that the construction of in-channel reservoirs has a profound impact on not only the environment but also the morphological behaviour of the river downstream as well as upstream. This chapter focuses on the suspended sediment related impacts downstream of a dam.

5.1 Decrease in Flood Peaks and Frequency

One effect that a dam basin has on the floods passing through it is that the flood hydrograph is attenuated. Depending on the operating rules the dam is managed with, a flood can be reduced by as much as 50 % as is the case for the Pongolapoort dam (Table 5-11) (DWAF, 2006). The implication for the river system downstream of the reservoir is that the flood frequency characteristics are altered in such a way that large floods occur less frequently.

Table 5-11: Pongolapoort Flood Peaks (DWAF, 2006)

Recurrence interval (years)	Inflow Flood Peak – DWAF (m^3/s)	Outflow Flood Peak (m^3/s)
5	1200	800
10	1850	800
20	2550	1800
50	3700	1800
100	4750	2800
200	5900	3250
RMF	15550	8150

This in turn has the effect that the floodplain is not inundated as often as under natural conditions and that the inundations that do take place are reduced in scale. Flood waters carrying nutrients are therefore unable to recharge the furthest edges of the plain. Soil fertility in such regions is thus likely to drop.

The decrease in flow rates also has the consequence that the sediment carrying capacity of the river is reduced. A large part of the sediment entering the system downstream of the dam could therefore be deposited in or near the main river channel before it can be transported onto the wider floodplain. As the levees that are thus formed become higher, the transfer of momentum, turbulence and sediment from the main channel to the floodplain becomes less and less.

5.2 Decrease in Sediment Inflow

Probably the most major impact a dam has on a river morphologically is the fact that most if not all of the sediment is trapped in the dam basin. The water leaving the reservoir is thus devoid of sediment. This can cause large scale erosion just downstream of the dam. In terms of bed-load transport the extra erosion is usually negligible only a few kilometres downstream of the reservoir.

The effect on suspended transport is however much more pronounced. Although a river does become saturated with sediment after a while, during flood events not enough sediment is available to provide the entire floodplain with its normal load of deposition. During such floods the floodplain directly downstream of a reservoir undergoes erosion resulting in the long term effect of a decrease in fertility of a usually agriculturally rich part of land. This decrease in sediment deposition is not always very evident seeing as it takes centuries for any real changes to assert themselves. There is however the unique example of the Nile River delta which under normal circumstances not only rises by a few mm every year but also expands several centimetres out to sea. Currently without the influx of Nile sediment the delta, which naturally subsides under its own weight, is losing highly fertile land to the Mediterranean (Yamauchi, 2004).

Dams don't always cause a decrease in suspended sediment however. There have been cases where an increase in certain types of sediment has been observed. The High Aswan Dam is a prime example in that it lies in the middle of a desert. As such this large expanse of water (525 km^2) is able to intercept a great deal more aeolian sediment delivered by the desert winds than the original Nile river was able to intercept. This is particularly true for fine clay sediment such as kaolinite (Janak et al, 1996).

In the new delta forming upstream of Lake Nasser, the artificial lake created in 1964 by the closure of the High Aswan Dam, kaolinite values of around 50% of the total suspended sediment are recorded. Downstream of the dam this value increases to 70% (Janak et al, 1996). Therefore despite the fact that a great deal of sediment settles in the dam basin (some 60 to 70 Mm^3/a), the clay content of the water actually increases due to extra sediment entering the system.

This statement seems to be in conflict with the fact that the Egyptians need to use some 13 000 tons of chemical fertiliser every year. The reason for this discrepancy is that the measurements taken above are applicable to base flow conditions and not to flood flows when this extra sediment would recharge the floodplains.

5.3 Sediment Releases

Regarding the management of suspended sediment at a particular dam, river and dam managers basically have two choices. The reservoir could either be operated in such a way so as to collect the sediment which subsequently could prevent the heavily sediment laden flows like those in the Yellow River. This then has the benefit that river levees can be constructed relatively close to the river in an attempt to keep the flow confined and fast flowing so as to prevent suspended sediment from settling within the channel.

A second option would be for the upstream reservoirs to release as much sediment through the basin as is possible. As a consequence, river managers downstream must allow for wide floodplains to allow the river to move relatively freely due to the varying deposits of suspended sediment. This approach seems more favourable because the dam would have a much longer lifespan and the river would be in a much healthier state than the option of retaining all sediment. There is however the negative effect of having to sacrifice large areas of valuable land to the river. It has been postulated that a mix of the two approaches might be put in place on the Yellow River (Leung, 1996). In regions where land cannot be spared, levees would line the river. In other places large spans of floodplain are left free of permanent habitation for the purpose of temporarily storing flood waters and capturing large amounts of suspended sediment.

If the dam is managed with sediment releases forming part of the operating procedure, the question must be asked as to when these sediment releases should take place. It would be best that any storm event hydrograph entering the dam should leave the dam attenuated and also carrying some of the sediment brought into the dam. This task may however be difficult to perform in practice. Only sediment that manages to reach the dam wall or at least the outlet structure can be released from the reservoir.

Certain dams have been built with this problem in mind. A diversion canal on the upstream side of the dam can intercept the heavily laden flow and transport it around the basin and into the river downstream, thereby preventing any sediment from entering the dam basin. This of course has the effect that these sediment laden flows cannot be utilised to fill up the dam.

Another concern is that usually high flows which are required to fill a dam are also the ones which carry most sediment. A good example of this antithesis is faced by the operators of the Three Gorges Dam. In theory the dam operating rules state that during the flood season (May to September) the reservoir level would be at a low elevation. Thereby creating conditions which are favourable for allowing high sediment laden flows to pass through the dam. During this period the inflows are used for power generation. After the flood season lower flows with a lower sediment

content will be impounded (IRN, 2004). The operators are relying on the fact that in many rivers the peak inflow does not necessarily coincide with the peak in sediment transport. Generally the peak in sediment transport (Q_s) arrives a short time before the peak inflow (Q) (Figure 5-11). The trick is then to pass through sediment rich flows and then close the gates before the flow peak arrives. Experience however shows that operating such a scheme is not always successful.

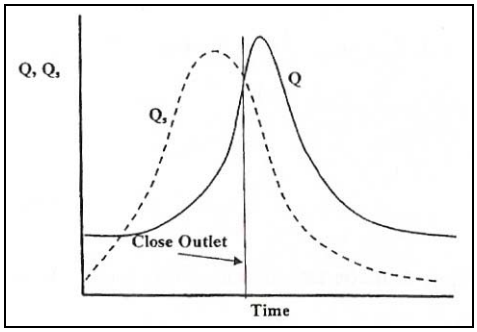

Figure 5-11: Relationship between the Flood and Sediment Peak (Shen, 2000)

As to how unnatural releases can be loaded with sediment many of the proposed solutions are impractical. The option of installing so-called silt fans which can resuspend material in the basin prior to a release looks good on paper. But once sediment, especially fine sediment, has settled it is notoriously difficult to resuspend it. As such these silt fans would have to cause large scale and intense turbulence in the reservoir in order for them to be effective.

Another option includes dredging the material and pumping the material out together with the release. Though this option seems more feasible than the previous one dredging is in general a very expensive exercise plus there is the added complication that the amount of water that is released may or may not be able to carry the sediment that has been thrown into it. Therefore there is the possibility that the sediment could just deposit just downstream of the outlet.

A related topic is that of sediment flushing. Water in the dam or reservoir is drawn down during a flood for the sole purpose of removing settled sediment from the basin via retrogressive erosion. This process has varying degrees of success depending mainly on the design of the outlet as well as the type of sediment involved. What is of concern here is the very large concentrations of suspended sediment being released. Flows discharged by flushing rarely exceed the bankfull stage and so the majority of this sediment is deposited in the main channel. This would then be resuspended during the next overbank flood and so transported onto the floodplain. However, the probability of such a flood is largely decreased because of the now empty dam upstream. The sediment therefore does not get transported to the floodplain as it normally would but gradually gets removed by the baseflow further downstream.

5.4 Artificial Floods

Artificial floods can refer to several things, such as the releases of constant flow for irrigators or the attenuated floods during storm events or the release of freshets for environmental purposes.

5.4.1 Increase in Base Flow

Increasing the base flow above the natural norm is practised in several rivers in order to supply water to irrigators alongside the watercourse. The problem that arises is that this water usually originates from a reservoir and is thus devoid of sediment. Not only that, but an increase in flow is generally accompanied by an increase in turbulence and thus sediment carrying capacity. Sediment is scoured from the river bed for the first few kilometres downstream of the dam or pipeline outlet until the sediment load reaches capacity.

Then when floods occur the river which would normally scour away smaller sediment and deposit them on the floodplain can no longer do so because that sediment has already been transported and only the coarser fractions remain.

5.4.2 Attenuated flow

A dam should be managed to release natural floods in accordance with the river's hydrological record. Although this is not always possible, efforts should be made to make release hydrographs look as natural as possible not only in magnitude but also in timing. One of the Environmental Flow Requirements for the Berg River Dam includes the operational release of a hydrograph which fits entirely within the hydrograph entering the dam. In other words there must be no lag in time between the "supposed" natural hydrograph at the dam site and the one actually released.

The reason for this is that during any storm event rain will not only fall in the Berg River Dam's catchment but also in adjacent catchments. As such these will then also produce runoff hydrographs which would then superimpose on the Berg Dam's release hydrograph further downstream. Thus, in order for the hydrograph downstream of the confluence of these various rivers to remain natural in shape no lag at the dam site is allowed.

In practise this means that the dam operator must know exactly what is happening in the dam's catchment on a continuous basis, especially during a storm event. This is so that preparations can be made for the release of water in time with the inflow hydrograph. Care must also be taken

that no more water is released than actually enters the dam, both in terms of total volume and flow rate. The reason for this operating rule is not only to satisfy the environmental requirements but also to ensure that even though water is being released from the reservoir there is still an increase in storage.

The shape of a release hydrograph when not coinciding with a natural event should if possible mimic the natural hydrograph at the dam location for a given recurrence interval. This will ensure that the floodplains of the river are not inundated for longer or shorter periods than is naturally the case.

Longer periods than natural could cause an increase in total sedimentation and as such lead to problems regarding the removal of this sediment from important infrastructure. A further consequence is that a far greater volume of sediment has been mobilised thereby speeding up the naturally occurring morphological processes that move the river both laterally and vertically.

However, for example the Pongola system, which requires a peak flow of at least a day that is then followed by a long tail of decreasing flow. It has been found that this near-natural hydrograph is the most ideal to keep the downstream floodplains healthy. Computer simulations (DWAF, 2006) have revealed that a release of a relatively low peak flow of several days followed by an immediate cut-off is insufficient to recharge the many pans on the floodplain.

As can be seen from Figure 5-22 there is a great deal of attenuation that takes place on the Pongola floodplain. The “New Pongola Bridge” is some 100 km downstream from the dam wall and the “Ndumu” game reserve a further 60 km (see Figure 5-33 and Figure 2-1414). It takes the flood approximately two days to travel the distance to the bridge and in this time it has lost 200 m^3/s off its peak due to large volumes being temporarily stored on the floodplain and its pans. If say, the flood that is released at the dam only peaks at around 600 m^3/s then it will have decreased to 400 m^3/s at the bridge which is not large enough to cause the rise in flood levels necessary to overtop some of the levees cutting of the pans.

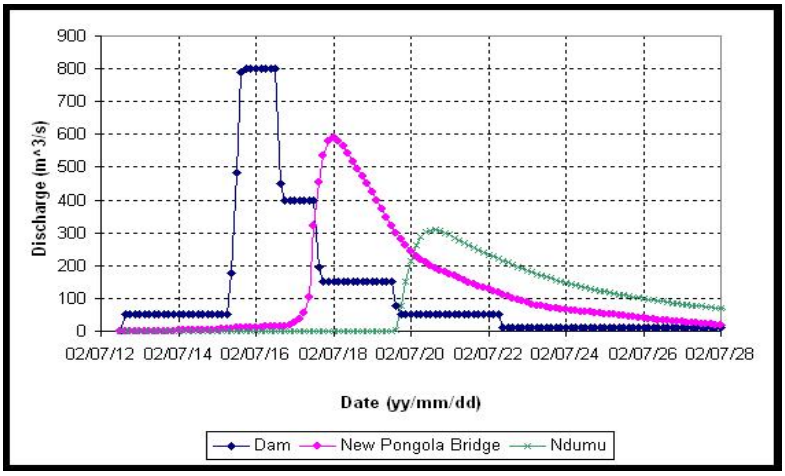

Figure 5-22: Attenuation of Pongolapoort flood release (DWAF, 2006)

It is thus evident from the study that if the peak flows are not sufficiently large enough (in the order of 800m^3/s) or do not vary enough from year to year the system downstream of the Pongolapoort Dam will suffer as not enough inundation for sufficient periods of time takes place.

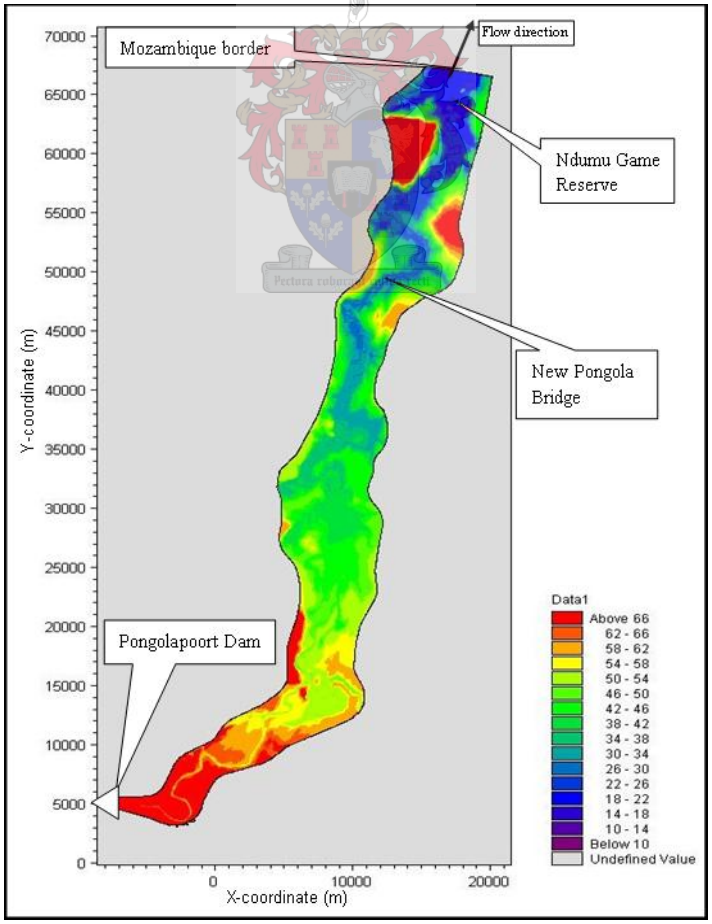

Figure 5-33: Bathymetry of Pongola Study (DWAF, 2006)

5.5 Dam Removal

5.5.1 Planned Dam Removal

A developing science that has recently been called into service is that of dam removal. Once a dam is beyond its service lifetime and cannot be rehabilitated its removal must be investigated. Morphological consequences of such an action are severe. A vast amount of sediment has under normal conditions accumulated in the reservoir since its construction. Once the dam wall is demolished this sediment once again becomes eroded and is deposited in great quantities downstream. Depending on the sediment size and the method of removal, different magnitudes of deposition occur.

If the sediment is mainly coarse gravel sediment, deposition will not propagate far downstream of the dam and may be limited to reaches where transport capacity is low. When the reservoir deposit is primarily fine sediment there may be more extensive sediment deposition (both larger area and higher quantities) downstream following dam removal.

Dredging part of the sediment prior to removal reduces the downstream impact due to reduced volumes as well as the extra distance allowing for increased attenuation. Costs of such an exercise may however be excessive.

Staged dam removals are only minimally beneficial for coarse sediments but can be effective in the case of fine sediments. In such a case the sediment concentrations downstream are lower and thus less deposition will likely occur in the main channel and the floodplain (Cui et al, 2003).

A recent well documented dam removal study is that of the Matilija Dam in California, USA. The dam has lost nearly all of its storage capacity due to sedimentation and as such had lost all purpose for its existence. Its inability to store floods, and the fact that it is a barrier to both sediment moving downstream and spawning fish moving upstream prompted calls for the dam to be removed. The final decision was however most likely made because of the fact that even old inefficient dams require costly repairs, especially considering the fact that there are practically no returns on money spent.

As can be seen from Figure 5-44 the dam still has considerable surface area most of which is however very shallow as is evident in Figure 5-55. Several monitoring factors were identified and alternatives were considered which would minimise the cost of the undertaking in terms of economic cost, aesthetics, beach nourishment, fish movement and restored habitat. The most

critical parameter that was identified was in fact the sediment dynamics and as such this had a large role to play in the decision process (Matilija Coalition, 2002).

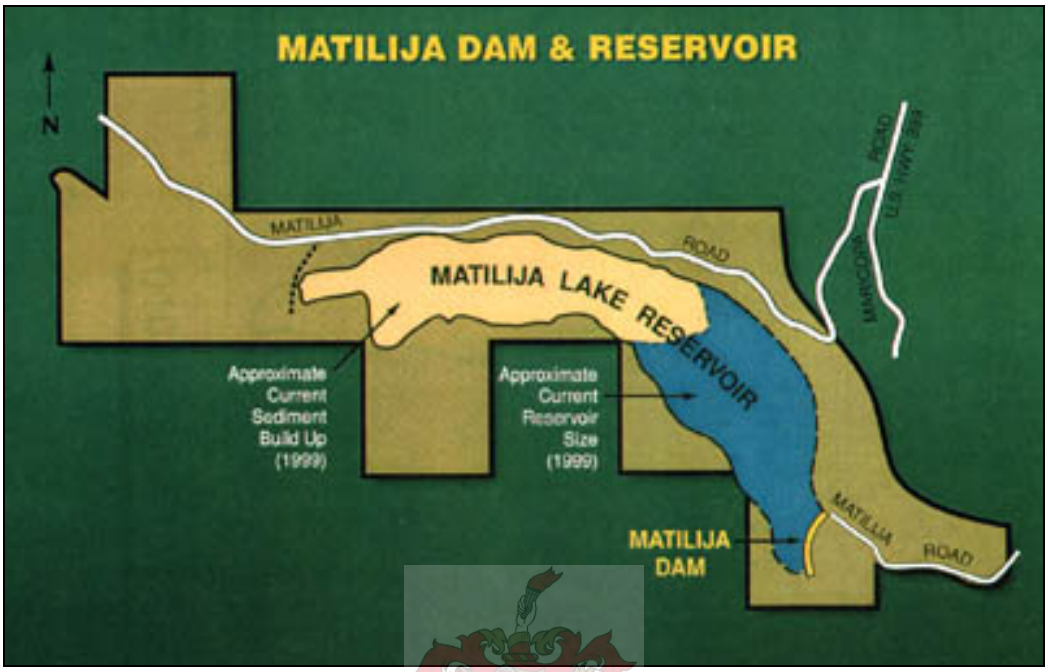

Figure 5-44: Matilija Dam (Matilija Coalition, 2002)

Figure 5-55: Matilija dam wall and sediment deposits, (Matilija Coalition, 2002)

The list below shows the top four alternatives which were determined to be most successful in terms of the project outcomes:

- **Full dam removal with natural sediment transport:**
  The dam is completely removed all at once and the majority of the sediment is left in place for natural transport downstream.
- **Full dam removal with sediment stabilisation:**
  The dam is completely removed whilst some sediment is stabilised in place and the remainder is placed in upland areas. The stream channel is re-established using natural topographical gradients.
- **Full dam removal and mechanical sediment removal:**
  Both the dam and sediment are removed in one phase. Sediment is displaced using trucks to disposal sites such as beaches and landfills.
- **Incremental dam removal and natural sediment transport:**
  Dam will be removed in phases with horizontal notches whilst sediment is allowed to erode naturally over the notch.

Other alternatives that were looked at included a full-scale fish ladder, a diversion channel as well as a pool and riffle system. The chosen alternative is the one shown below in Figure 5-66. The channel would be re-established so as to provide immediate passage for native trout and large amounts of sediment would be temporarily stabilised and released over time so as to gradually restore the natural riverine processes that nourish coastal beaches.

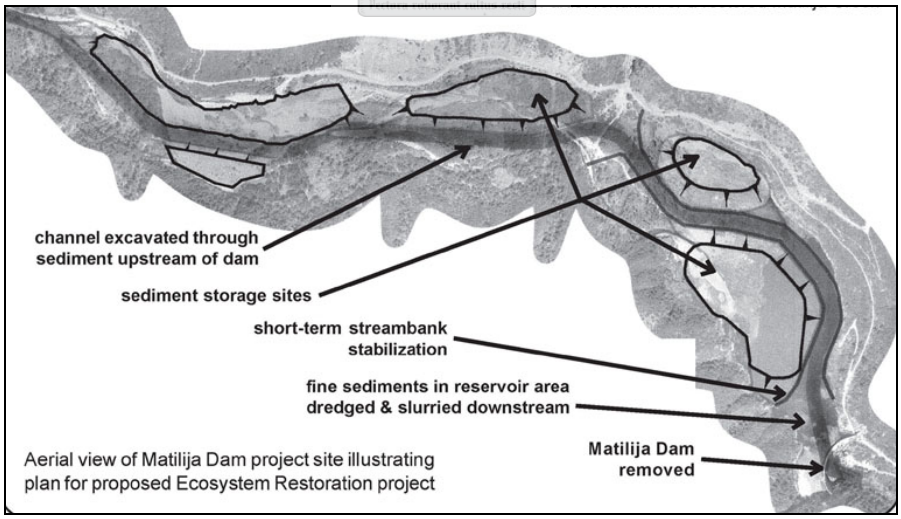

Figure 5-66: Matilija ecosystem restoration project (Matilija Coalition, 2002)

5.5.2 Unplanned Dam Removal

Another related topic is that of unplanned dam breaches or failures. Although the flood wave which would result from such an occurrence would be far more damaging than any sediment related damage, it is still of interest to look into some morphological consequences.

As can be expected from such an immense flood the nett sediment movement would be away from the floodplain and into the main channel as erosion would be the dominant process. Subsequent to the flood however, large amounts of sediment would enter the system from the deposits in the previous dam basin. Under normal circumstances such an increased influx of sediment can be dealt with by simply cleaning up any large accumulations around important infrastructure. However, if the sediment influx contains poisons the problem is that the cleanup has to be widespread and may thus never reach completion.

Take for example the threat posed by the Dnieper reservoirs in the Ukraine (Wikipedia). The Dnieper River has a set of five hydroelectric dams which not only boosts local industry but also provides for a navigable channel. The concern arises that even though each dam individually is specified to be safe from failure (either from natural events such as earthquakes, meteors or floods or from unnatural events such as aircraft collisions), the five dams form a cascade with an atypically short distance between them. As such, a failure of one of the topmost dams will cause hyperflooding at the other dams within hours, possibly causing these to fail as well. A similar disaster occurred with the Banqiao Dam in China resulting in a total of 62 dam failures.

What makes the Dnieper system unique however is that its catchment area was one of the main regions affected by the Chernobyl Nuclear Disaster and as such contaminated sediment from this region has been collected in the reservoir. As can be seen in Figure 5-77 much of the contaminated area is drained by the Dnieper River upon which lies the Kiev reservoir. The concern thereby is that should the Kiev Reservoir fail or accidentally release flows it would effectively blanket the entire downstream area and the Black Sea with radioactive material (Wikipedia).

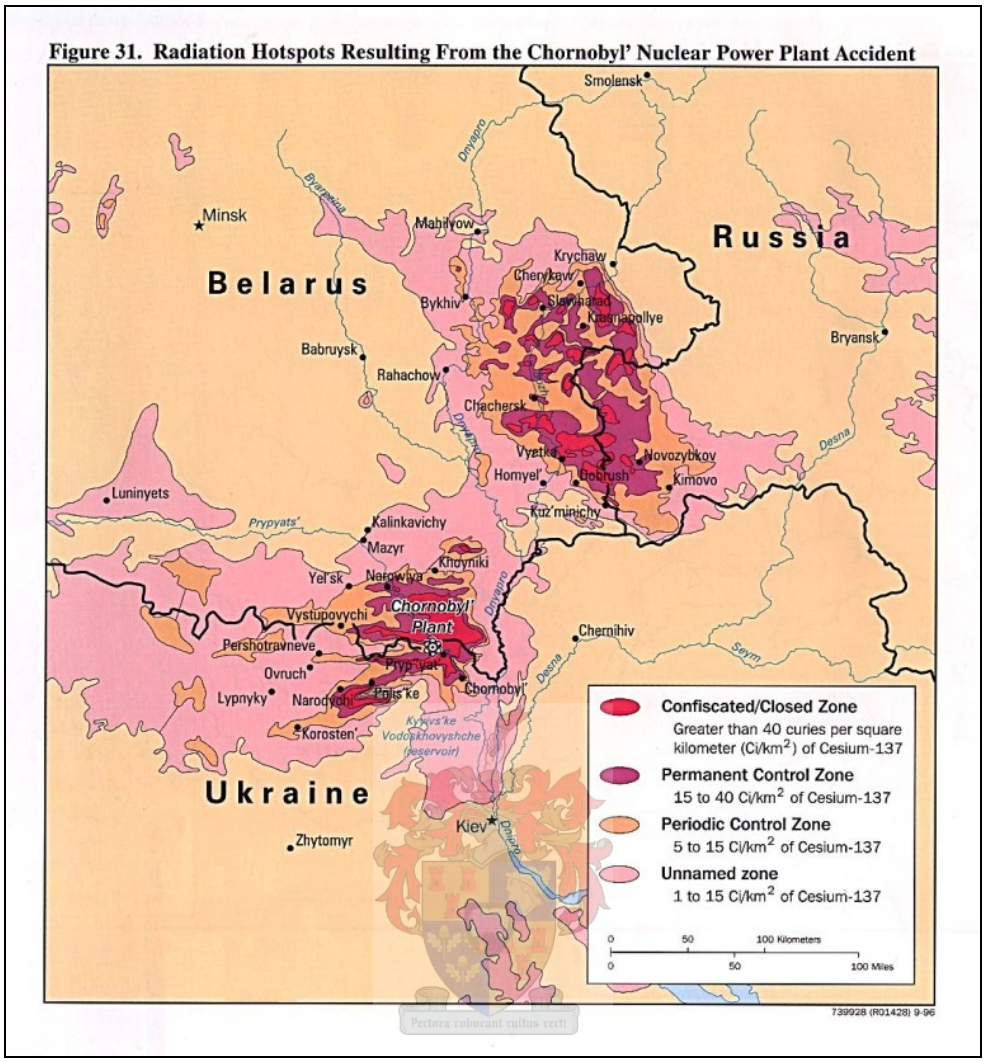

Figure 5-77: Radiation hotspots resulting fromthe Chernobyl Nuclear Accident (Wikipedia)

A further potential hazard is that the floodplain near Kiev and Dnipropetrovsk is not only the site for a current nuclear power plant but also the location of several nuclear and toxic dump sites left there by the Soviet government.

A researcher recently labelled the area “the most dangerous place on the planet”; also stating that after such a disaster the Ukraine would “never revive again”. There is unfortunately little that can currently be done to halt the possible damage but mitigation measures can be put in place. It is therefore of paramount importance that the system is modelled as a unit and that both the large scale deposition patterns of the radioactive sediment as well as the local spreading from the dump sites be determined (Wikipedia).

CHAPTER 6

6 CONCLUSIONS

Suspended sediment has a profound effect not only on the river which carries it but also on the floodplain alongside the main channel. It was shown that the sediment carried to the floodplain from the main channel is the cause of many of the landforms witnessed there. The most profound of these is the presence of levees which border the main channel of rivers which carries large amounts of suspended sediment.

The suspended sediment remains in suspension in the main channel due to the occurrence of high turbulence there. This has the result that the main channel has a high transport capacity. This characteristic is however not shared by the flow on the floodplain and so sediment transported there tends to settle out quickly. The rate at which this suspended sediment settles out is mostly dependent on the settling velocity of the sediment particle which in turn is dependent on the sediment size.

Another factor which plays a major role is the strength of the shear layer between the main channel and floodplain flows. This layer of high turbulent mixing is the result of the transfer of momentum from the main channel to the floodplain. It not only has unique vertical mixing characteristics but also a strong influence on the flow structure around it. It was shown that it is responsible for the establishment of secondary currents or vortices such as those shown in Figure 6-11 which affect the transverse diffusion of suspended sediment.

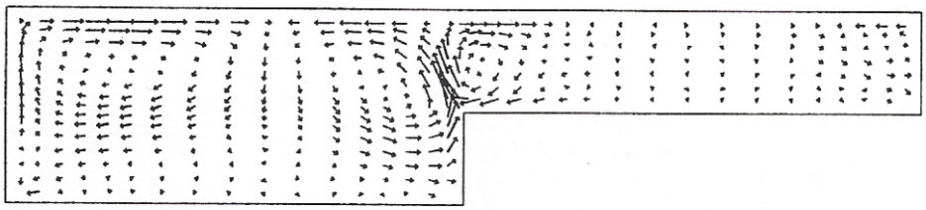

Figure 6-11: Secondary currents driven by shear layer

Under normal turbulent flow conditions there are no strong secondary currents and so the factor most responsible for the transverse mixing of sediment is turbulence. For this reason transverse mixing can be directly related to shear velocity and it is this variable which determines the amount of turbulence dispersion. This relationship fails however, in the vicinity of the shear layer where the relationship describing transverse dispersion is defined by equation (5555) which is reproduced below.

$$\frac{D_z}{(U_C - U_P)} = \frac{0.3\left(\frac{H_C}{H_P} - 1\right)^3}{\left(\frac{U_C - U_P}{u_{*\infty}}\right)^2} \cdot A(\eta)$$

As is evident from this equation transverse dispersion is dependent on the strength of the shear layer and as such is dependent upon the difference in flow velocity between the main channel and the floodplain. Besides this it is also reliant upon the relative depth of the channel versus that of the floodplain as well as the undisturbed shear velocity on the floodplain. The A(η) term at the right hand side of the equation incorporates a distance related function which decreases the amount of dispersion as the distance from the interface increases.

A physical laboratory model was set up for this study for the purpose of investigating and subsequently calibrating a series of computer simulations. The basic premise consisted of a straight rectangular channel alongside a wide floodplain. Sediment would be inserted in the main channel only and would then be allowed to spread across the shear boundary onto the floodplain. Suspended sediment samples would be taken at fixed control points to assess the distribution of the sediment under various flow conditions.

The end result of the experiments was that there was a clear indication that the tests were not run for a long enough period of time. The conducted experiments were limited in scope due to the constraints imposed by a finite supply in sediment. Despite this, general trends involving the transport of the solute from the main channel to the floodplain could be made. The most profound of these is the observation that as depth increases the rate of transport toward the floodplain decreases. Figure 6-22 and Figure 6-33 below show this trend clearly since the sediment in Figure 6-22 has spread farther in the transverse direction than in Figure 6-33. The topmost figure represents experiment 1 which had an inflow of 10 ℓ/s and a water level of 0.135 m. The second figure, which represents test 3, also had an inflow of 10 ℓ/s but had a main channel depth of 0.15 m.

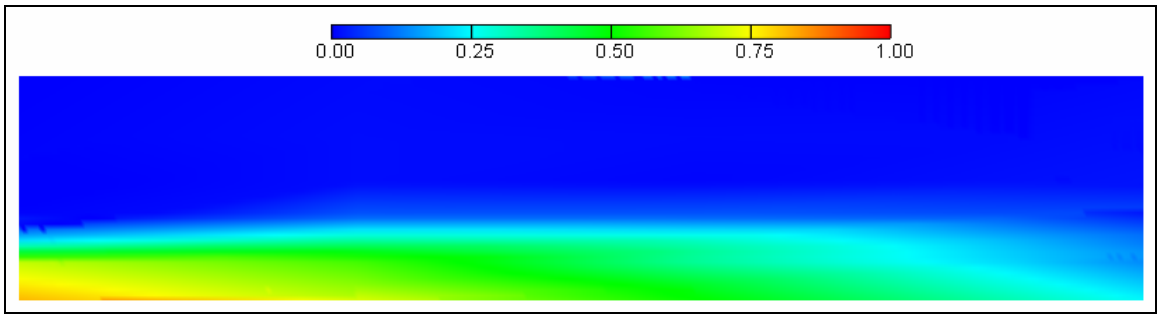

Figure 6-22: Plan View of Observed Physical Model Suspended Sediment Concentration (g/ℓ) (H=0.135)

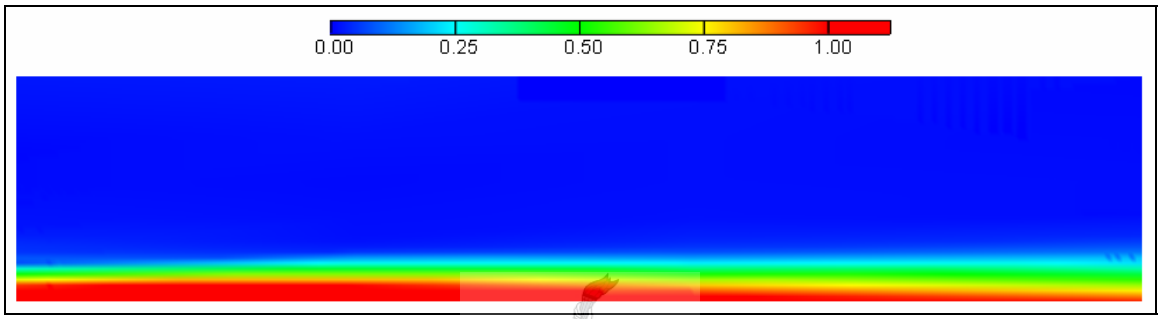

Figure 6-33: Plan View of Observed Physical Model Suspended Sediment Concentration (g/ℓ) (H=0.15)

One would expect that a deeper flow would correlate to a greater cross sectional area through which sediment can traverse. This is however not what was observed, but by considering section 3.6 the behaviour can be explained. This section highlights the fact that a deeper flow corresponds with a higher velocity on the floodplain and that the difference in velocity between the main channel and the floodplain decreases as depth increases. The smaller this difference between these velocities the smaller or weaker the shear layer between the two flows becomes, and the weaker the shear layer the less transfer of transverse momentum and sediment takes place.

This behaviour was also expected in the subsequent computer simulations that were run, but because there were problems with the computer model these expectations could not be confirmed. The selected computer model, CCHE2D, though capable of modelling the horizontal flow field was not able to predict the secondary currents required to accurately model trans-shear boundary sediment transport. As such, the computer simulations cannot be considered as being accurate emulations of actual phenomena. They can however still reproduce the general trends observed in the physical tests.

Trends in terms of the model parameters were also observed during the simulation procedure, especially regarding their individual sensitivity. The large difference in the behaviour of transverse

sediment transport between simulation 2 and 3 show that both grid cell size and time step are highly sensitive characteristics. These two factors more than any of the other parameters had the largest effect in the process of calibrating the simulations to the observed phenomena. The reason for this most likely stems from the fact that particularly grid cell size plays a deciding role in the development and size of the vertical axis eddies which spread most of the sediment in the model.

The question that then has to be put forth is whether or not this theory is valuable in practical terms, if general trends of spread are achieved. The theory is indeed required to increase the accuracy of computer models and to establish what the data requirements are, but in terms of simulating real (i.e. less than ideal) bathymetries, does it play a role? It is evident from the literature that local aspects on the floodplain will have a far larger effect on the spreading of sediment than do the secondary currents. It is also doubtful that these secondary currents will be able to establish themselves in any case within the context of an actual floodplain. Therefore, though the theory is required to set up and establish the requirements for simulations and to increase the accuracy of these model predictions, it is considered most likely that in actual circumstances, local bathymetry will play the decisive role in the spread of sediment onto the floodplain.

CHAPTER 7

7 RECOMMENDATIONS

It is recommended that the physical experiments that were conducted as part of this thesis be repeated and adjusted so as to minimise the effect of a limited supply in sediment inflow at the upstream boundary. This can be achieved either by pre-preparing a larger batch of suspended sediment or decreasing the rate at which this sediment is fed into the system. The latter would however have the consequence that observed concentrations would be lower and thus the rate of transverse spreading would be smaller and therefore be more difficult to sample.

A set of simulations should be run prior to such a physical experiment. The aim of such would be to determine optimal testing parameters for a successful experiment. Care should however be exercised in selecting the computer model to be used to do this. As was shown in the thesis, not every model is fully capable of modelling the required flow fields, such as secondary currents. Computational Fluid Dynamics programs do however exist that were specifically designed to tackle this cross-shear boundary sediment transport and one of these should be used to simulate the physical model for calibration or verification purposes of the computer models.

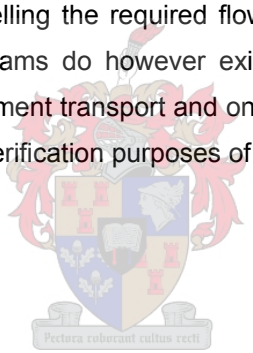

CHAPTER 8

8 REFERENCES

1. Armitage M and McGahey C, 2003. *A unit stream power model for the prediction of local scour in rivers.* WRC Report No. 1098/1/03

2. Bagnold RA, 1966. *An approach to the sediment transport from general physics geological survey*. Prof paper 422-I, Washington.

3. Beck JS, Basson GR, 2003. Water Research Commission Report No. 1102/1/03: The Hydraulics of the Impacts of Dam Development on the River Morphology

4. Berendsen HJA, Makaske B, Smith DG, 2002. *Avulsions, channel evolution and floodplain sedimentation rates of the anastomising upper Columbia River, British Columbia, Canada*. Sedimentology (2002) 49, 1049-1071

5. Bousmar D & Zech Y, 2001. *Periodic turbulent structures modelling in a symmetric compound channel*. XXIX IAHR Congress Proceedings.

6. Bowie GL, Mills WB, Porcella DB, Campbell CL, Pagenkopf JR, Rupp GL, Johnson KM, Chan PWH, Gherini SA, Chamberlin CE & Barnwell TO, 1985. *Rates, constants and kinetics formulations in surface water quality modelling (Second Edition)*

7. Carrera J, 1993. *An overview of uncertainties in modelling groundwater solute transport.* Journal of contaminant hydrology 13, 23-48, Elsevier Science, 1993

8. Cellino M and Graf WH, 2002. *Suspension flows in open channels; experimental study*. Journal of Hydraulic Research Vol. 40, No. 4.

9. Cui Y, Dietrich WE, Brauderick C, Cluer B, Parker G, 2003. *Dam Removal Express Assessment Models (DREAM) part 2: Sample runs/sensitivity tests*. Journal of Hydraulic Research

10. DHI (2003) Mike21C

11. Duan G, 1998. Simulation of Alluvial Channel Migration Processes with a Two-dimensional Numerical Model. *PhD thesis*, University of Mississippi, Oxford, Mississippi

12. DWAF (1987) Mathematics model of the hydraulics of the Pongola river flood plain

13. DWAF (2006). Pongolapoort Dam Flood Release Operational Analysis – Socio-Hydrological Investigation, Historical Flood Releases and Mathematical Modelling. Compiled by ASP Technology (Pty) Ltd, Basson GR, Beck JS & Denys FJM.

14. Elder JW, 1959. *The dispersion of marked fluid in turbulent shear flow*. Journal of Fluid Mechanics. Vol. 5, p 544-560

15. Engelund and Fredsøe, 1976. *A sediment transport model for straight alluvial channels*. Nordic hydrology ,7 ,1976.

16. Fisher HB, List EJ, Koh RCY, Imberger J, Brooks NH, 1979. *Mixing in inland and coastal waters.*

17. Graf WH, 2003. *Fluvial Hydraulics: Flow and transport processes in channels of simple geometry*. Wiley & Sons, New York.

18. http://earth.google.com/

19. http://en.wikipedia.org/wiki/Main_Page

20. Matilija Coalition, 2002. http://pages.sbcglobal.net/pjenkin/matilija/how_to.htm

21. Yamauchi, 2004. http://www.cabnr.unr.edu/swwf/presentations/yamauchi.pdf

22. Leung, 1996. http://www.cis.umassd.edu/%7Egleung/

23. International River Network. http://www.irn.org/programs/threeg/leopold.html

24. World Bank, 1993. http://www.worldbank.org.cn/English/content/loess.shtml

25. Cowen R, 2000. *Exploiting the Earth.* http://www-geology.ucdavis.edu/~cowen/~GEL115/115CHXXYellow.html

26. James CS, 1985. *Sediment transfer to overbank sections.* Journal of Hydraulic Research Vol. 23, No. 5, p 435-452.

27. Janak M, O'Brien PJ, Hurai V, Reutel C, Stanley DJ, Wingerath JG, 1996. *Nile sediment dispersal altered by the High Aswan Dam: The kaolinite trace*. Marine Geology.

28. Jia Y and Wang S, 2001. *CCHE2D Technical Report*. (http://www.ncche.olemiss.edu/)

29. Krom MD, Stanley JD, Cliff RA, Woodward JC, 2002. *Nile river sediment fluctuations over the past 7000 years and their key role in sapropel development*. Geology Vol. 30 No. 1 p 71-74.

30. Lau YL and Krishnappan BG, 1977. *Transverse Dispersion in Rectangular Channels*. Journal of the Hydraulics Division, ASCE, Vol. 103, No. HY10, October 1977, p 1173-1189.

31. Lin B and Shiono K, 1995. *Numerical modelling of solute transport in compound channel flows*. Journal of Hydraulic Research Vol. 33, No. 6.

32. Martin JL & McCutcheon SC, 1999. *Hydrodynamics and transport for water quality modelling.*

33. Microsoft Encarta, 1993-2004 Microsoft Corporation

34. Naot D, Nezu I, Nakagawa H, 1993. *Hydrodynamic behaviour of compound rectangular open channels*. Journal of Hydraulic Engineering Vol. 119, No. 3.

35. Rajaratnam N and Ahmadi R, 1981. *Hydraulics of channels with floodplains*. Journal of Hydraulic Research Vol. 19, No. 1.

36. Raudkivi AJ 1990. Loose Boundary Hydraulics. Pegram Press, Oxford, GB.

37. Shen HW, 2000. *Flushing sediment through reservoirs*. Journal of Hydraulic Research Vol. 37, No. 6.

38. Toda Y, Ikeda S, Kumagai K, Asano T, 2005. *Effects of flood flow on flood plain soil and riparian vegetation in a gravel river*. Journal of Hydraulic Engineering, ASCE Vol. 131 No. 11 p 950-960.

39. van Rijn LC, 1993. *Principles of Sediment Transport in Rivers Estuaries and coastal seas.*

40. Walling DE and Owens PN, 2003. *The role of overbank sedimentation in catchment contaminant budgets*. Hydrobiologia 494: p 83-91.

41. Walling DE, Quine TA and He Q, 1992. *Investigating Contemporary Rates of Floodplain Sedimentation*. Lowland floodplain river, geomorphological perspectives, Edited by Carling PA and Petts GE. Wiley & Sons.

APPENDIXES

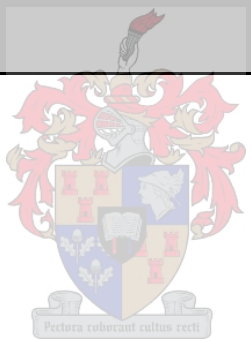

EXPERIMENT DATA

As was described in the thesis the bottle samples from the physical experiment were analysed, from which the following results were obtained. Take note that the mass of a single empty bottle was equal to 19.892 grams.

Table A - 11: Data from experiment 1

Test	Distance (m)	Width (m)	Bottle weight (g)	Volume (ml)	Filter mass before (g)	Filter mass after (g)	Sediment mass (g)	concentration (mg/ℓ)
I	1	0.15	530.3	510.4	0.2262	0.5951	0.3689	722.8
I	1	0.35	464.9	445.0	0.2238	0.5124	0.2886	648.5
I	1	0.45	521.8	501.9	0.2255	0.4438	0.2183	434.9
I	1	0.55	507.9	488.0	0.226	0.3415	0.1155	236.7
I	1	0.75	491.8	471.9	0.2218	0.2265	0.0047	10.0
I	1	1.05	502.4	482.5	0.2242	0.2256	0.0014	2.9
I	1	1.45	480.3	460.4	0.2227	0.2259	0.0032	7.0
I	1	1.85	503.3	483.4	0.2242	0.2266	0.0024	5.0
I	3	0.15	544.8	524.9	0.2243	0.5581	0.3338	635.9
I	3	0.35	473.5	453.6	0.2232	0.48	0.2568	566.1
I	3	0.45	508.7	488.8	0.2261	0.4528	0.2267	463.8
I	3	0.55	478.5	458.6	0.2236	0.3713	0.1477	322.1
I	3	0.75	488.6	468.7	0.2246	0.2663	0.0417	89.0
I	3	1.05	495.1	475.2	0.2236	0.23	0.0064	13.5
I	3	1.45	541.0	521.1	0.2217	0.2287	0.007	13.4
I	3	1.85	413.9	394.0	0.2251	0.2295	0.0044	11.2
I	6	0.15	498.0	478.1	0.2274	0.4465	0.2191	458.3
I	6	0.35	466.7	446.8	0.2261	0.3806	0.1545	345.8
I	6	0.45	518.1	498.2	0.2249	0.4009	0.176	353.3
I	6	0.55	484.7	464.8	0.2237	0.3631	0.1394	299.9
I	6	0.75	512.2	492.3	0.226	0.2702	0.0442	89.8
I	6	1.05	485.2	465.3	0.2249	0.228	0.0031	6.7
I	6	1.45	472.7	452.8	0.2263	0.2312	0.0049	10.8
I	6	1.85	451.0	431.1	0.2255	0.2281	0.0026	6.0
I	9	0.15	466.0	446.1	0.2254	0.344	0.1186	265.9
I	9	0.35	504.0	484.1	0.2235	0.321	0.0975	201.4
I	9	0.45	488.4	468.5	0.2268	0.3172	0.0904	193.0
I	9	0.55	505.2	485.3	0.2264	0.3092	0.0828	170.6
I	9	0.75	459.6	439.7	0.2266	0.2623	0.0357	81.2
I	9	1.05	522.6	502.7	0.2246	0.2332	0.0086	17.1
I	9	1.45	536.6	516.7	0.224	0.2302	0.0062	12.0
I	9	1.85	383.1	363.2	0.2234	0.2262	0.0028	7.7

Table A - 22: Data from experiment 2

Test	Distance (m)	Width (m)	Bottle weight (g)	Volume (ml)	Filter mass before (g)	Filter mass after (g)	Sediment mass (g)	concentration (mg/ℓ)
II	1	0.15	493.8	473.9	0.2249	0.5682	0.3433	724.4
II	1	0.35	492.8	472.9	0.2266	0.6028	0.3762	795.5
II	1	0.45	517.3	497.4	0.2254	0.3655	0.1401	281.7
II	1	0.55	543.8	523.9	0.2232	0.2376	0.0144	27.5
II	1	0.75	497.6	477.7	0.223	0.23	0.007	14.7
II	1	1.05	485.0	465.1	0.2235	0.2279	0.0044	9.5
II	1	1.45	513.8	493.9	0.2242	0.2296	0.0054	10.9
II	1	1.85	543.0	523.1	0.2237	0.2309	0.0072	13.8
II	3	0.15	533.1	513.2	0.2245	0.5691	0.3446	671.5
II	3	0.35	480.5	460.6	0.224	0.5781	0.3541	768.8
II	3	0.45	497.1	477.2	0.2261	0.4745	0.2484	520.5
II	3	0.55	498.8	478.9	0.2235	0.3516	0.1281	267.5
II	3	0.75	503.1	483.2	0.2245	0.2326	0.0081	16.8
II	3	1.05	502.7	482.8	0.222	0.2288	0.0068	14.1
II	3	1.45	515.2	495.3	0.223	0.2253	0.0023	4.6
II	3	1.85	543.9	524.0	0.2244	0.2299	0.0055	10.5
II	6	0.15	517.5	497.6	0.2222	0.5119	0.2897	582.2
II	6	0.35	491.6	471.7	0.2227	0.5311	0.3084	653.8
II	6	0.45	502.2	482.3	0.2231	0.4819	0.2588	536.6
II	6	0.55	496.1	476.2	0.221	0.3946	0.1736	364.5
II	6	0.75	518.9	499.0	0.2239	0.2594	0.0355	71.1
II	6	1.05	365.2	345.3	0.221	0.2225	0.0015	4.3
II	6	1.45	516.1	496.2	0.2235	0.2263	0.0028	5.6
II	6	1.85	526.5	506.6	0.226	0.2303	0.0043	8.5
II	9	0.15	506.3	486.4	0.2252	0.4637	0.2385	490.3
II	9	0.35	511.3	491.4	0.2242	0.4845	0.2603	529.7
II	9	0.45	476.5	456.6	0.2244	0.4244	0.2	438.0
II	9	0.55	498.5	478.6	0.2247	0.3819	0.1572	328.5
II	9	0.75	5232.6	5212.7	0.2256	0.2765	0.0509	9.8
II	9	1.05	511.4	491.5	0.224	0.2277	0.0037	7.5
II	9	1.45	494.6	474.7	0.2228	0.2297	0.0069	14.5
II	9	1.85	511.8	491.9	0.2249	0.2292	0.0043	8.7

Table A - 33: Data from experiment 3

Test	Distance (m)	Width (m)	Bottle weight (g)	Volume (ml)	Filter mass before (g)	Filter mass after (g)	Sediment mass (g)	concentration (mg/ℓ)
III	1	0.15	505.7	485.8	0.2286	0.7127	0.4841	996.5
III	1	0.35	499.5	479.6	0.2254	0.2759	0.0505	105.3
III	1	0.45	486.2	466.3	0.2248	0.2458	0.021	45.0
III	1	0.55	482.3	462.4	0.2255	0.2397	0.0142	30.7
III	1	0.75	501.2	481.3	0.2242	0.2323	0.0081	16.8
III	1	1.05	514.3	494.4	0.2253	0.2317	0.0064	12.9
III	1	1.45	501.5	481.6	0.2227	0.2288	0.0061	12.7
III	1	1.85	498.3	478.4	0.2216	0.2322	0.0106	22.2
III	3	0.15	512.1	492.2	0.224	0.7091	0.4851	985.6
III	3	0.35	483.1	463.2	0.2223	0.33	0.1077	232.5
III	3	0.45	452.6	432.7	0.2219	0.2366	0.0147	34.0
III	3	0.55	471.7	451.8	0.222	0.2293	0.0073	16.2
III	3	0.75	469.5	449.6	0.226	0.2323	0.0063	14.0
III	3	1.05	471.8	451.9	0.2266	0.2317	0.0051	11.3
III	3	1.45	508.7	488.8	0.2255	0.2331	0.0076	15.5
III	3	1.85	429.8	409.9	0.223	0.2328	0.0098	23.9
III	6	0.15	519.0	499.1	0.2245	0.621	0.3965	794.4
III	6	0.35	396.1	376.2	0.2261	0.3065	0.0804	213.7
III	6	0.45	423.5	403.6	0.2264	0.2519	0.0255	63.2
III	6	0.55	497.4	477.5	0.2245	0.2406	0.0161	33.7
III	6	0.75	496.9	477.0	0.2282	0.2358	0.0076	15.9
III	6	1.05	393.9	374.0	0.2265	0.2322	0.0057	15.2
III	6	1.45	500.7	480.8	0.2227	0.2299	0.0072	15.0
III	6	1.85	438.6	418.7	0.2247	0.2312	0.0065	15.5
III	9	0.15	450.2	430.3	0.2266	0.5207	0.2941	683.5
III	9	0.35	469.9	450.0	0.2238	0.3321	0.1083	240.7
III	9	0.45	449.7	429.8	0.2218	0.2622	0.0404	94.0
III	9	0.55	436.9	417.0	0.2216	0.2385	0.0169	40.5
III	9	0.75	461.6	441.7	0.223	0.2292	0.0062	14.0
III	9	1.05	345.7	325.8	0.2239	0.2286	0.0047	14.4
III	9	1.45	485.4	465.5	0.2232	0.2288	0.0056	12.0
III	9	1.85	403.1	383.2	0.227	0.2344	0.0074	19.3

Table A - 44: Data from experiment 4

Test	Distance (m)	Width (m)	Bottle weight (g)	Volume (ml)	Filter mass before (g)	Filter mass after (g)	Sediment mass (g)	concentration (mg/ℓ)
IV	1	0.15	481.8	461.9	0.2234	0.7739	0.5505	1191.8
IV	1	0.35	494.2	474.3	0.2228	0.2686	0.0458	96.6
IV	1	0.45	482.4	462.5	0.2224	0.239	0.0166	35.9
IV	1	0.55	499.8	479.9	0.2209	0.2551	0.0342	71.3
IV	1	0.75	557.6	537.7	0.2234	0.2479	0.0245	45.6
IV	1	1.05	432.7	412.8	0.2239	0.266	0.0421	102.0
IV	1	1.45	487.2	467.3	0.2241	0.2336	0.0095	20.3
IV	1	1.85	492.9	473.0	0.2236	0.2337	0.0101	21.4
IV	3	0.15	448.7	428.8	0.2237	0.6765	0.4528	1055.9
IV	3	0.35	456.5	436.6	0.2239	0.3357	0.1118	256.1
IV	3	0.45	488.5	468.6	0.2238	0.247	0.0232	49.5
IV	3	0.55	479.2	459.3	0.223	0.2338	0.0108	23.5
IV	3	0.75	473.9	454.0	0.221	0.2307	0.0097	21.4
IV	3	1.05	489.0	469.1	0.2255	0.2348	0.0093	19.8
IV	3	1.45	499.5	479.6	0.2223	0.2332	0.0109	22.7
IV	3	1.85	498.6	478.7	0.2247	0.2345	0.0098	20.5
IV	6	0.15	502.4	482.5	0.2247	0.5975	0.3728	772.6
IV	6	0.35	452.0	432.1	0.224	0.3231	0.0991	229.3
IV	6	0.45	458.9	439.0	0.2208	0.2462	0.0254	57.9
IV	6	0.55	480.7	460.8	0.2214	0.2308	0.0094	20.4
IV	6	0.75	477.8	457.9	0.2222	0.2303	0.0081	17.7
IV	6	1.05	481.7	461.8	0.2216	0.2287	0.0071	15.4
IV	6	1.45	503.4	483.5	0.2235	0.2312	0.0077	15.9
IV	6	1.85	496.6	476.7	0.2236	0.2312	0.0076	15.9
IV	9	0.15	518.6	498.7	0.2237	0.5571	0.3334	668.5
IV	9	0.35	479.6	459.7	0.2245	0.2974	0.0729	158.6
IV	9	0.45	461.6	441.7	0.2254	0.2522	0.0268	60.7
IV	9	0.55	488.4	468.5	0.2241	0.2689	0.0448	95.6
IV	9	0.75	317.1	297.2	0.2224	0.28	0.0576	193.8
IV	9	1.05	479.2	459.3	0.2241	0.28	0.0559	121.7
IV	9	1.45	485.3	465.4	0.2243	0.3075	0.0832	178.8
IV	9	1.85	502.5	482.6	0.2236	0.2788	0.0552	114.4

SEDIMENT DATA

The following section presents the characteristics of the sediment used in the physical experiment. The sediment used is a very fine light brown powder called Western Province Ball Clay. A sieve analysis showed that all the particles were smaller than 0.075 mm thus the ASTM hydrometer method was used to determine the particle size distribution.

This method entails taking 60 g of the sample (smaller than 2.63 mm) and mixing it with a 120 ml of Sodium hexametaphosphate solution (at 40 g/ℓ) and left for 16 hours. Thereafter it is transferred to a 1 litre sedimentation cylinder which is then topped up with distilled water and placed in a constant temperature bath until it reaches a temperature of 20˚C. The cylinder is then remixed for a period off 60 seconds and returned to the temperature bath. Measurements were then taken with an ASTM 152H hydrometer at increasing time intervals. The temperature of the suspension was also measured at every interval.

As time progressed and more sediment settled out of suspension, so the liquid became less and less dense. These density readings together with the time intervals and temperature information were then used to establish a particle distribution. First the time interval was linked to the largest particle still in suspension via the following formula:

$$D = (Temperature\ constant) \sqrt{\frac{Effective\ depth\ (cm)}{Time\ (\min)}}$$

Table A - 55: Particle sizes remaining over time

Particle	Temp (°C)	Temp. const.	Eff. Depth (cm)	Time (min)	D (mm)
D_2	20	0.01365	7.7	2	0.0268
D_5	20	0.01365	7.9	5	0.0172
D_{15}	19.7	0.01365	8.3	15	0.0102
D_{30}	19.7	0.01365	8.5	30	0.0073
D_{60}	19.5	0.01365	8.8	60	0.0052
D_{250}	21	0.01348	9.1	250	0.0026
D_{1440}	19.5	0.01365	9.65	1440	0.0011

Then using the hydrometer measurements shown in Table A - 66 below the concentration of the particles versus time can be determined. The results can be seen in Table A - 77 and Figure A - 11.

Table A - 66: Hydrometer readings

Time (min)	Reading (g/ℓ)	*Corrected reading (g/ℓ)	Temp (°C)
2	57.5	52.5	20
5	56	51	20
15	54	49	19.7
30	52.5	47.5	19.7
60	51	46	19.5
250	49	44	21
1440	45.5	40.5	19.5

* A correction factor is applied to account of the density of the distilled water and Sodium hexametaphosphate

Table A - 77: Concentration of particles

Particle	D (mm)	P (% of Conc.)
D_0	0.0750	100
D_2	0.0268	87.50
D_5	0.0172	85.00
D_{15}	0.0102	81.67
D_{30}	0.0073	79.17
D_{60}	0.0052	76.67
D_{250}	0.0026	73.33
D_{1440}	0.0011	67.50

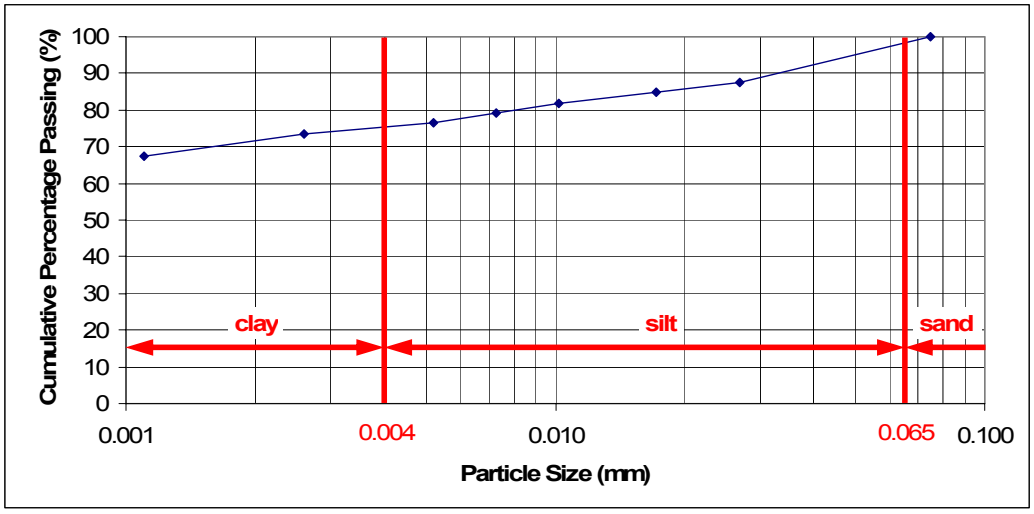

Figure A - 11: Particle Size Distribution of Sediment used in Physical Model

This data, when extrapolated backwards, defines the median particle size as 0.00014 mm (or 0.14 μm) making the material a fine clay. Then using Stokes's equation (equation(3333)) the average settling velocity of the material is 0.00002 mm/s.